Investigating the Function of Single-pass Leucine-Rich Repeat Transmembrane Proteins in Cell Signalling and Early Neural Development

Shaun Murray Gaskin, B.Sc. (Hons)

Thesis submitted for the degree of

Master of Philosophy

Department of Molecular and Cellular Biology
School of Biological Sciences
Faculty of Sciences
University of Adelaide

April 2018

THE UNIVERSITY of ADELAIDE

Contents

Declaration

I certify that this work contains no material which has been accepted for the award of any other degree or diploma in my name in any university or other tertiary institution and, to the best of my knowledge and belief, contains no material previously published or written by another person, except where due reference has been made in the text. In addition, I certify that no part of this work will, in the future, be used in a submission in my name for any other degree or diploma in any university or other tertiary institution without the prior approval of the University of Adelaide and where applicable, any partner institution responsible for the joint award of this degree.

I give consent to this copy of my thesis, when deposited in the University Library, being made available for loan and photocopying, subject to the provisions of the Copyright Act 1968.
I also give permission for the digital version of my thesis to be made available on the web, via the University's digital research repository, the Library Search and also through web search engines, unless permission has been granted by the University to restrict access for a period of time.

.....

Shaun M Gaskin

Developmental Biology Laboratory
Department of Molecular and Cellular Biology
School of Biological Sciences
Faculty of Science
University of Adelaide
Adelaide, Australia 5005

Acknowledgements

This thesis has been compiled on the back of some good and some hard times, but through it all, there have been people around me who have helped me through it.

First up, this work wouldn't have been possible without the help, guidance and advice of my supervisor, Dr Bryan Haines, and my co-supervisor, Prof. Paul Thomas. I am very grateful for the time, resources, effort and ideas that you contributed towards my learning as a part of my project. You have both had busy schedules and always made time to meet with me, speak with me, and look over my work.

To the members of the Thomas Lab, and extended to the people of the Biochemistry department, thanks for the support and memories. Events such as weekly Friday night drinks and footy tips, lab lunches and Christmas parties, and the pub crawls and wine tours were highlights of my time in the department. It was great being part of fun!

My family has supported me through this process from day 1 and been there always showing interest, even if they didn't really know what I was doing! To my mum and dad, thanks for all of your support and love, through all the cranky times and the happy ones, and the times where you know I had to focus on what I was doing.

To my partner, Tatiana, there are not enough words or phrases to express how thankful of you I am. You are my number 1 supporter, have helped me through the good times and the bad, always managed to put a smile on my face, and motivated me to finish this thesis. You have made this process so much easier; from the mulling over of ideas and structure of sentences and paragraphs, to the quick feedback you give me on my drafts, and the time you allowed me to hide away and get stuck into what I needed to do. I couldn't have done this without your love and support, and I cannot thank you enough!

To everyone who I have mentioned above, and to those I have unfortunately missed, thank you for fostering my interest in science and driving me to be the best I can. Bigger and better things are on the horizon!

Abstract

Single-pass leucine-rich (LRR) repeat transmembrane proteins contain a diverse number of repeating motifs of approximately 24 amino acid residues with a large number being conserved leucines. Flrt expression is observed in the developing embryo in important developmental regions such as the central nervous system and developing skeletal muscle. Knockout of *Flrt3* during embryogenesis results in early embryonic lethality making *in vivo* analysis of endogenous Flrt3 function difficult. No cell based model exists for studying Flrt function. Flrt family members have previously been shown to interact with FgfR1 and 2, with the Flrt1 FgfR1 interaction resulting in an increase in FgfR1 signalling activity. Immunofluorescent microscopy reveals that Flrt3 from mouse (*Mus musculus*) co-localises with FgfR1 both intracellularly and at the plasma membrane, with the interaction resulting in a trend of increased FgfR1 signalling being observed, and phosphorylation of tyrosine residues within Flrt3. An attempt was made to identify domains of the protein important in the trend of increased FgfR1 signalling, but no domains could be identified as contributing to this outcome.

To study endogenous Flrt3 function, the P19 embryonic carcinoma retinoic acid-induced neural differentiation model was used, and the results showed a rapid and robust induction of *Flrt3* mRNA and protein expression. A region of the promoter between 4 kb and 6 kb upstream of the *Flrt3* start site was found to be partially responsible for the induction of *Flrt3*. Interestingly, this response element was not within a region of promoter that showed conservation among higher-order mammals. An effect of increased Flrt3 expression during neural differentiation was observed, resulting in decreased MAPK pathway activation. Induction of *Flrt3* is found to occur prior to that of *Sox1*, accepted to be one of the first genes up-regulated in early neurectoderm differentiation, yet was found to be not solely responsible for the induction of *Sox1*. The individual cell expression of Flrt3 and Sox1 was analysed by immunofluorescence, although it did not reveal details regarding induction of Sox1 in cells with increased Flrt3 expression.

The potential for a common feature of single-pass LRR transmembrane proteins to function as modulators of receptor signalling during embryonic development was investigated, using Lrrtm3 and FgfR1 as an example. Lrrtm3 was investigated as a modulator of FgfR1 signalling due to overlapping region of expression with FgfR1 in the developing embryo. Lrrtm3 was found to co-localise and form an interaction with FgfR1, with this interaction resulting in an increase in FgfR1 signalling.

The data obtained in this thesis provides further insight into not only the role of the Flrt protein family as FgfR1 modulators, but potentially identifies a role for similar, if not all single-pass LRR transmembrane proteins as regulators of receptor signalling during embryonic development. While the results of Chapter 3 and 5 were obtained using a protein over-expression system, the first model for studying endogenous Flrt3 was identified and characterised in Chapter 4, providing the opportunity to study Flrt3 function during development with protein expression levels closely resembling those that are found in the embryo.

Abbreviations

αMEM	minimum essential media alpha
aa	amino acids
AER	apical ectodermal ridge
Amp	ampicillin
BME	2-mercaptoethanol
BMPR	bone morphogenic protein receptor
$Ca_3(PO4)_2$	calcium phosphate
CHO	Chinese hampster ovary
CIP	calf intestinal alkaline protease
CNS	central nervous system
DMEM	Dulbecco's modified eagle media
dpc	day post-coitum
DRG	dorsal root ganglia
EBM	modified embryoid bodies
EC	embryonic carcinoma
EGTA	ethylene glycol tetra-acetic acid
EPL EB	early primitive ectoderm-like embryoid bodies
Fgf	fibroblast growth factor
FgfR	fibroblast growth factor receptor
Flrt	fibronectin-like, leucine-rich repeat transmembrane
GAPDH	glyceralhdehyde-3-phosphate dehydrogenase
GM	growth media
GTS	glycine Tris SDS
HEPES	4-(2-hydroxyethyl)-1-piperazineethanesulfonic acid
HI-FCS	heat inactivated foetal calf serum
HRP	horse radish peroxidase
h	hours
IP	immunoprecipitation
KHB	Krebs HEPES buffer
LIF	leukemic inhibitory factor
LRR	leucine-rich repeat

Lrrtm	leucine-rich repeat transmembrane
MHB	mid-hindbrain boundary
min	minutes
ORF	open reading frame
PBS	phosphate buffered saline
PBST	PBS plus 0.1% (v/v) Tween-20
PCR	polymerase chain reaction
P/S	penicillin and streptomycin
pY	phosphorylated tyrosine
qRT-PCR	quantitative real time polymerase chain reaction
RO	reverse osmosis
RQ	relative quantity
RT	room temperature (25^{o}C)
SDS	sodium dodecyl sulphate
Secs	seconds
TBS	Tris buffered saline
TBST	TBS plus 0.1% (v/v) Tween-20
TCL	total cell lysate

1. Introduction

1.1 Leucine-rich Repeat Proteins

Throughout the mammalian genome, a large number of protein families exist that are defined by specific protein modules encoded within their sequence. The leucine-rich repeat (LRR) family contains a motif consisting of approximately 24 amino acids (aa), with a high percentage of conserved leucine residues arranged in the general consensus sequence **L** X X **L** X X **L** X **L** X X **N** X **L** X X **L** p X X **o** F X X where L is leucine, X is any amino acid, N is asparagine, o is a non-polar residue and lower case letters indicate more than 30% conservation [1]. This motif typically occurs as a repeat structure that can vary in number. Despite the varying number of repeats, this structure produces a hydrophobic concave surface that favours protein-protein interactions [2] [3] (Figure 1).

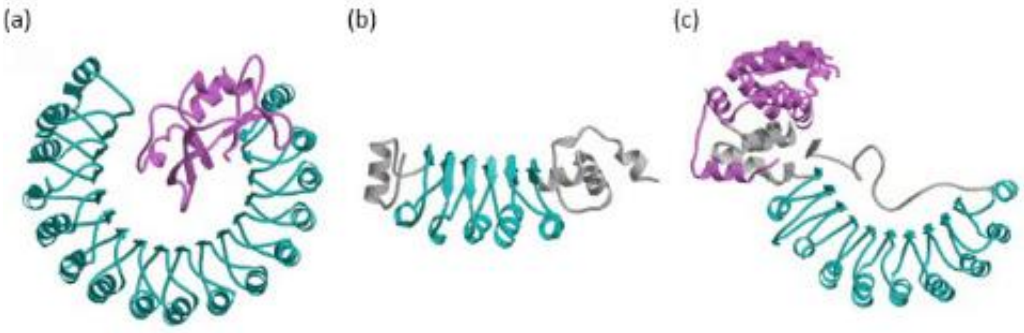

Figure 1: 3D crystal structures of LRR proteins. The LRR domains are shown in blue, with flanking regions that are an integral part of the LRR domain but do not correspond to LRR motifs shown in grey, and other structures shown in magenta. (a) RI, (b) TAP and (c) dynein LC1. Adapted from [3].

LRR proteins perform a wide variety of functions and occur in many different cellular locations, with proteins containing the motif present within the cell including the cytoplasm, at the cell membrane or secreted into the extracellular space. Structural and functional diversity within the LRR family is caused by a different number of motif repeats (Figure 1) and the inclusion of various other domains within the protein that can affect its localisation and/or function. Extracellular, membrane-bound LRR proteins can be GPI-anchored or transmembrane proteins with the majority of transmembrane proteins occurring in single pass transmembrane subfamilies.

The LRR single pass transmembrane proteins contain an N-terminal extracellular LRR motif surrounded by N- and C-terminal cysteine-rich flanking sequences, a hydrophobic transmembrane sequence and a short cytoplasmic C-terminal tail (Figure 2).

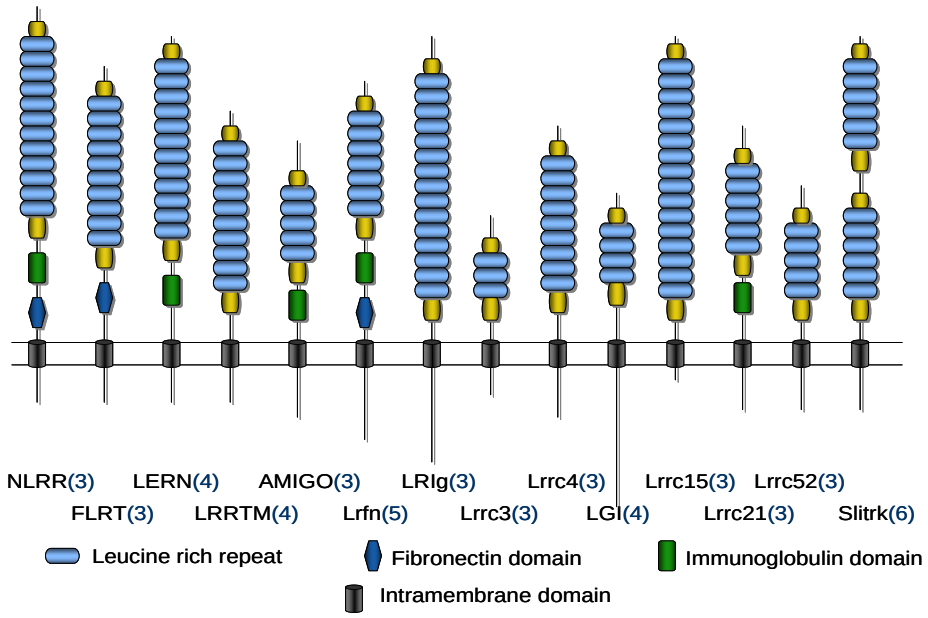

Figure 2. Single-pass transmembrane protein families: Schematic diagram showing the secondary structure of the mouse single pass leucine-rich repeat (LRR) transmembrane protein families. Numbers indicate number of family members.

Variation between families occurs by different numbers of LRR repeats and the inclusion of other additional domains such as fibronectin-like domains and immunoglobulin-like domains, situated between the transmembrane domain and the LRRs. The extracellular positioning and LRR hydrophobic concave surface gives the single pass transmembrane LRR proteins a probable role in cell-cell adhesion and/or cell signalling [4].

1.1.1 Flrt family

The molecular function of LRR membrane proteins in not well understood. One of the best studied LRR membrane families is the Flrt family. It contains three members; Flrt1, 2 and 3, which share a conserved secondary structure of a short intracellular tail, a single transmembrane domain, a fibronectin-like domain and ten LRRs surrounded by C and N-terminal cysteine flanking regions [5]. Flrt proteins are glycosylated type I transmembrane proteins expressed at cell membranes [5]. No complete crystal structures are available for any of the Flrt members, but the structure of the LRR domain of Flrt3 has been solved [6]. All Flrts show highly specific expression during mouse embryonic development, with expression of *Flrt1* present at the compartmental boundaries of the brain from days 9 to 11 *dpc*, and *Flrt2* expressed in the developing sclerotome [5]. From day 6 *dpc, Flrt3* shows a highly-regulated pattern of expression in mid-gestation mouse embryos, with specific domains of expression localised to the midbrain/hindbrain boundary, apical ectodermal ridge (AER) and the developing somites [5] (Figure 3).

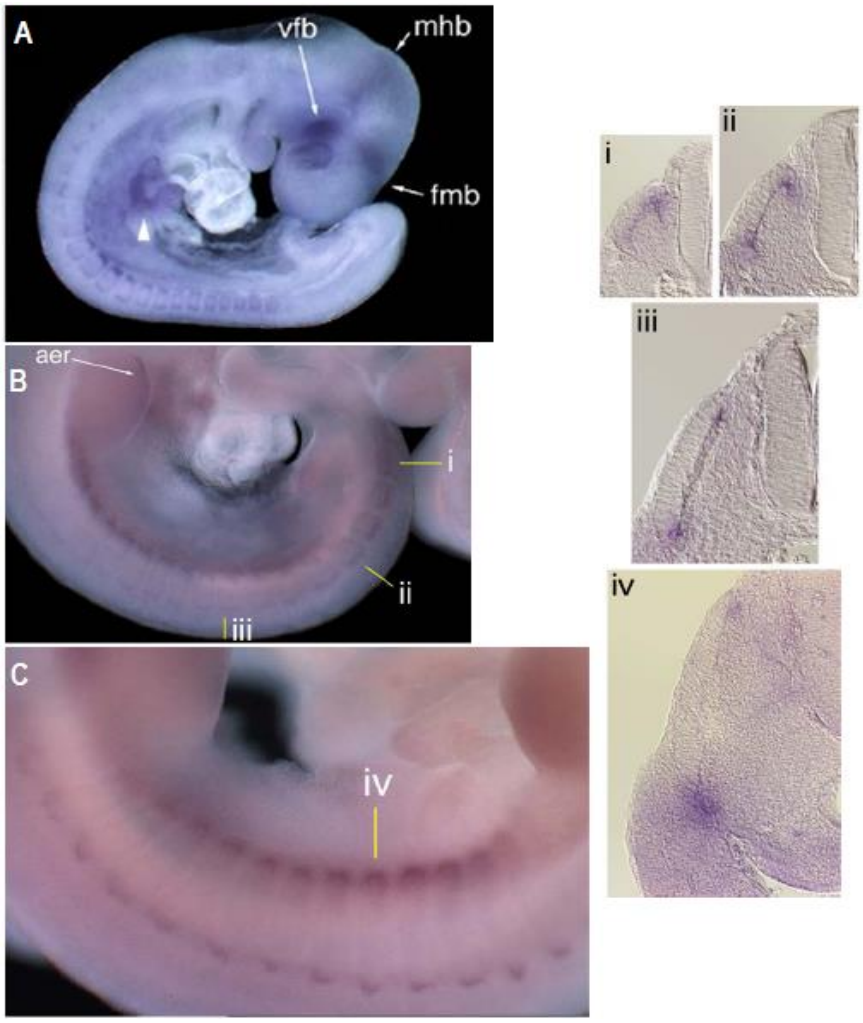

Figure 3. Expression of *Flrt3* during somite development: *In situ* hybridisations of 9.5 dpc (A) and higher magnification of the developing somites from *in situ* hybridisations of 10.5 dpc (B) and 11 dpc (C) mouse embryos with a riboprobe for *Flrt3*. i–iii are sections of the embryo in panel B and iv of the embryo in panel C with the approximate planes of section shown by yellow lines. vfb - hypothalamic region of the ventral forebrain; mhb - midbrain/hindbrain boundary; fmb - forebrain/midbrain boundary; aer - apical ectodermal ridge [5].

Neural expression analysis in mouse embryos at 9.5 *dpc* and 10.5 *dpc* showed *Flrt3* expression at the midbrain/hindbrain (MHB) boundary and the forebrain/midbrain boundary. Mesodermal expression of *Flrt3* from 8 *dpc* to 11 *dpc* in newly formed somites occurs throughout the inner edge of the somitic epithelium but is stronger dorsally, with more mature somites showing decreased epithelial expression and an increase in expression at the somitic lips. Strong expression occurs in the dermomyotome and myotome in the ventral lip at the interlimb level at 11 *dpc*. The AER on the developing limb bud displays *Flrt3* expression from 10.5 *dpc* [5]. This expression pattern is also seen in E12 rat [7]. Post-natal expression of *Flrt3* is present in the adult hippocampus [7]. Initial expression studies of *Xenopus Flrt3* showed expression at the midbrain/hindbrain boundary in gastrulae, matching expression in the mouse in this region [8].

Protein function can vary depending on where the protein is localised. Being transmembrane proteins, the Flrt family are possibly present within the plasma membrane, exposed to the extracellular environment, or within an intracellular membrane, where its function could be vastly different. Flrt3 is found not only at the plasma membrane in over-expression and endogenous assays, but also in intracellular vesicular membranes as a result of various post-translational modifications occurring to the protein, such as glycosylation. This is evident by the different sized proteins detected in Western blots. These differ from the predicted molecular weight of 72.9 kDa (http://www.ncbi.nlm.nih.gov/protein/AAH52043.1) [7, 9] (Figure 4).

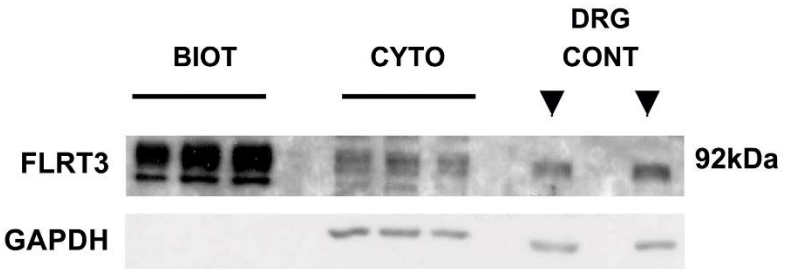

Figure 4. Flrt3 is localised to the plasma and intracellular membranes in dorsal root ganglion (DRG): The E15 rat cortical neuron cell surface proteins were biotinylated *in vitro*. Both biotinylated (BIOT) and cytosolic (CYTO) protein samples were analysed by Western blot. A sample DRG lysate (DRG CONT) was included as a control for immunostaining. Loading control of GAPDH was used. n=3 Adapted from [7].

Several LRR proteins, including chaoptin and tartan, function in intercellular adhesion or the formation of tissue boundaries, exhibiting homotypic cell adhesion properties. As Flrt3 is expressed at the plasma membrane, and at brain compartmental boundaries, a role in cell adhesion was investigated [10-13]. Binding of *Xenopus laevis* Flrt3 (xFlrt3) to other xFlrt3 proteins was observed by Karaulanov *et al.* (2006), and interestingly, xFlrt3 was shown to also bind human Flrt1 (hFlrt1) and Flrt2 (hFlrt2). Flrt self-interactions were also shown to result in a homotypic cell sorting phenotype using cells co-over-expressing eGFP and xFlrt3. This cell sorting phenotype was also observed with Flrt2 [10] (Figure 5).

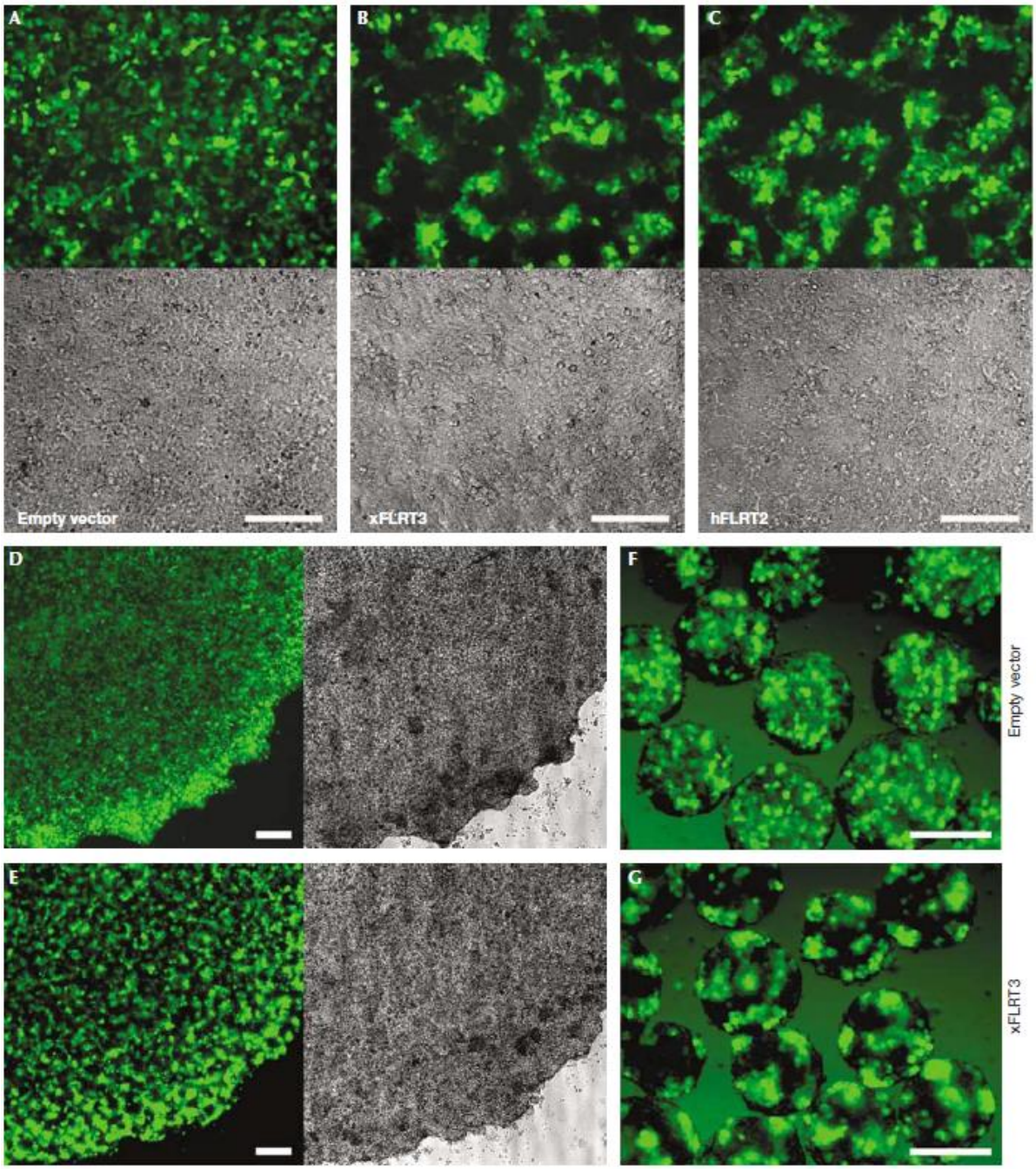

Figure 5: Over-expression of Flrt proteins causes cell sorting. (A–C) HEK-293T cells were co-transfected with enhanced green fluorescent protein (EGFP) and Xenopus FLRT3 (xFLRT3) or human FLRT2 (hFLRT2) expression plasmids. Fluorescence and bright-field images of confluent monolayers were taken 60 h after transfection. (D–G) FLRT-mediated cell sorting does not require substrate adhesion. 24 h after transfection with Xenopus FLRT3 and EGFP, HEK-293T cells were dissociated, mixed 1:1 with non-transfected cells, re-plated on agarose and photographed after 20 h (D,E) or aggregated in suspension and photographed after 48 h (F,G). Empty vector transfections served as sorting controls (A,D,F). Scale bars, 200 µm [10].

Cells co-over-expressing eGFP and xFlrt3, or hFlrt2, grown in either monolayer, aggregation or on agar gave rise to a homotypic cell sorting phenotype. It was observed that cells in the centre of the clusters were the brightest, indicating Flrt dose-dependent changes in cell-cell adhesion [10].

The role of Flrt3 in mature neural cells has been investigated by a number of groups [7, 9, 14, 15]. Documented cases of its involvement in both neural growth and repair exist, with Tanabe *et al*. being the first group to provide evidence of a role for *Flrt3* as a nerve regeneration-associated gene [14]. Using a microarray comparing gene profiles of dorsal root ganglia (DRG) 7-days post-transection to healthy adult DRG, *Flrt3* showed a 9.5-fold up-regulation, confirmed by Northern blot and *in situ* hybridisation analysis [14] (Figure 6).

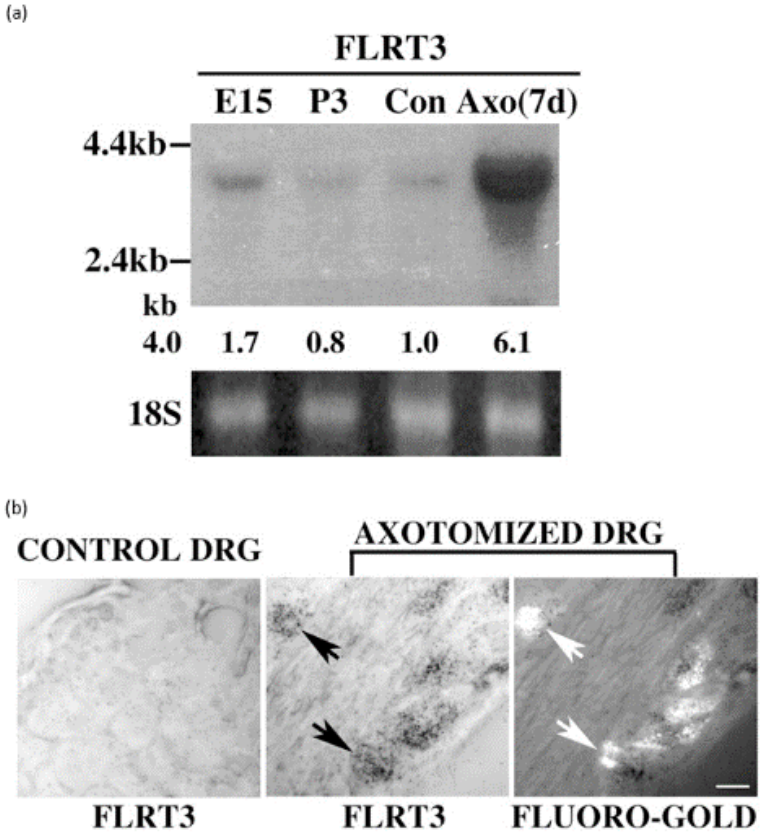

Figure 6. The Flrt3 gene is induced in DRG neurons by axotomy: a) Northern blot analysis shows mRNA expression of Flrt3 in uninjured embryonic day 15 (E15), uninjured post-natal day 3 (P3), adult contralateral (Con) and adult axotomized (Axo) L4-6 mouse dorsal root ganglion (DRG) neurons. Samples were collected 7 days after axotomy. Relative signal intensity for indicated bands is reported at the bottom of each lane. The ethidium bromide staining pattern of the 18S ribosomal RNA is shown to demonstrate the quantity of RNA loaded, and size markers are shown on the left. b) *In situ* hybridisation shows the localisation of *Flrt3* transcripts in the fluoro-gold-labelled axotomized DRG (arrowheads) and little mRNA expression in control DRG sections. Scale bar, 50 µm. Adapted from [14].

This is the second largest change in gene expression observed, only 0.1-fold smaller than the gene with the largest change in expression (9.5-fold vs 9.6-fold for fibroblast growth factor inducible-14) [14].

Robinson *et al*. went on to show that the increase in *Flrt3* mRNA was not caused by inflammation, but specifically axotomy. They confirmed the results of Tanabe *et al*. and discovered that

levels of *Flrt3* mRNA were drastically increased to their maximal levels after just 24 h post-injury, with these levels maintained over the 7-day period investigated (Figure 7) [7].

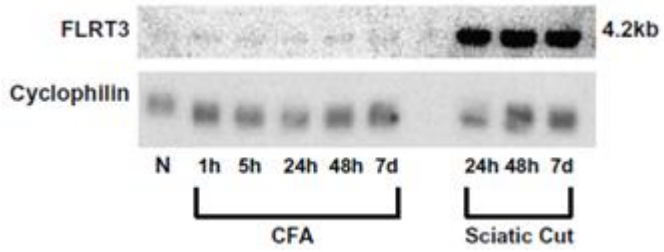

Figure 7. *Flrt3* mRNA is up-regulated in DRG neurons by axotomy and not by inflammation: Northern blot analysis showed that *Flrt3* mRNA was up-regulated in adult rat L4–L5 DRG after peripheral inflammation and sciatic nerve lesion. L4–L5 DRGs were taken over a time course (h = hour; d = day) after peripheral inflammation (by CFA injection into the hind paw) and after sciatic nerve lesion [7].

While Figure 6 shows that *Flrt3* levels increase upon nerve injury, it also shows the levels of *Flrt3* in both embryonic and neonatal mice compared to adult mice. It can be seen that the DRG of a E15 mouse shows a 1.7-fold increase in *Flrt3* expression by Northern blot compared to neonatal and adult mice, which show very similar expression. This adds to the *Flrt3* expression seen by Haines *et al*. observed in Figure 3 [5]. While we do see an increase in mRNA levels, this doesn't appear to lead to an increase in Flrt3 protein levels [7].

Given previous data, including that from Figure 6 and 7, experiments to analyse the role of Flrt3 protein function in neurite outgrowth were undertaken [7, 9, 14]. By growing cerebellar granular cells from post-natal day 8 (P8) rat pups on a confluent layer of Flrt3-expressing or control CHO cells in a neurite outgrowth assay, differences were observed [9] (Figure 8).

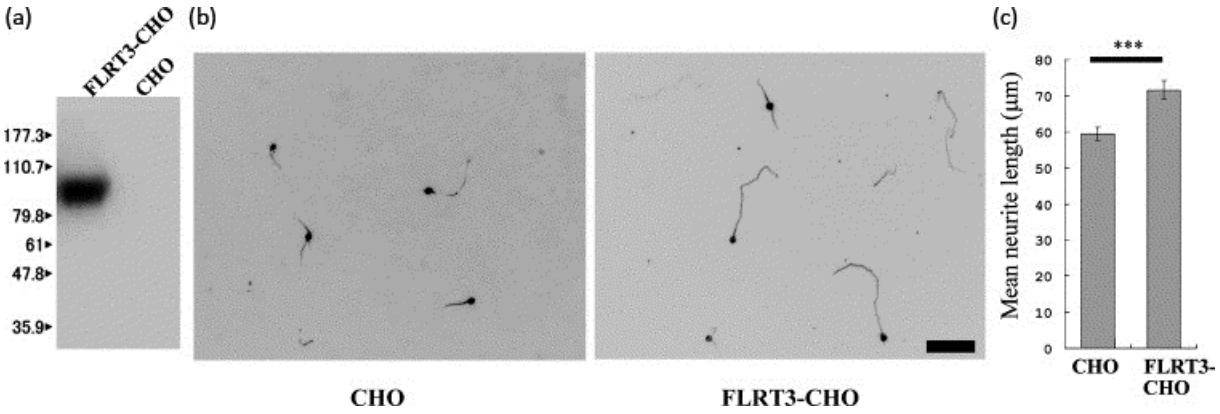

Figure 8. FLRT3 promotes neurite outgrowth from primary cultured cerebellar granule neurons: (a) Expression of HA-FLRT3 in Flp-in CHO cells. (b) Representative image of cerebellar granule neurons of P8 rat pups plated on control CHO and FLRT3-CHO cells. The images are reversed to enhance contrast. (c) Neurite length of at least 150 neurons per each condition in three independent experiments is presented as the mean neurite length. ***p < 0:001; one-way ANOVA. Scale bar, 50 μm [9].

When grown on CHO cells over-expressing Flrt3 (Figure 8. a, b FLRT3-CHO), neurite outgrowth of the cerebellar granular neurons is increased compared to the control (CHO) after 24 h. Mean neurite length of neurons grown on the control CHO cells was 59.1 ± 1.9 µm, which is significantly less than neurons grown on Flrt3 over-expressing CHO cells, which had a mean neurite length of 72 ± 2.6 µm [9].

It appears that Flrt3 within the neuron is also important for neurite outgrowth. Using antisense knockdown of Flrt3 protein in *in vitro* assays on dorsal root ganglia, Robinson *et al*. showed a 44% decrease in neurite outgrowth length and a 43% decrease in the number of neurite outgrowths compared to sense oligonucleotide control cells [7] (Figure 9).

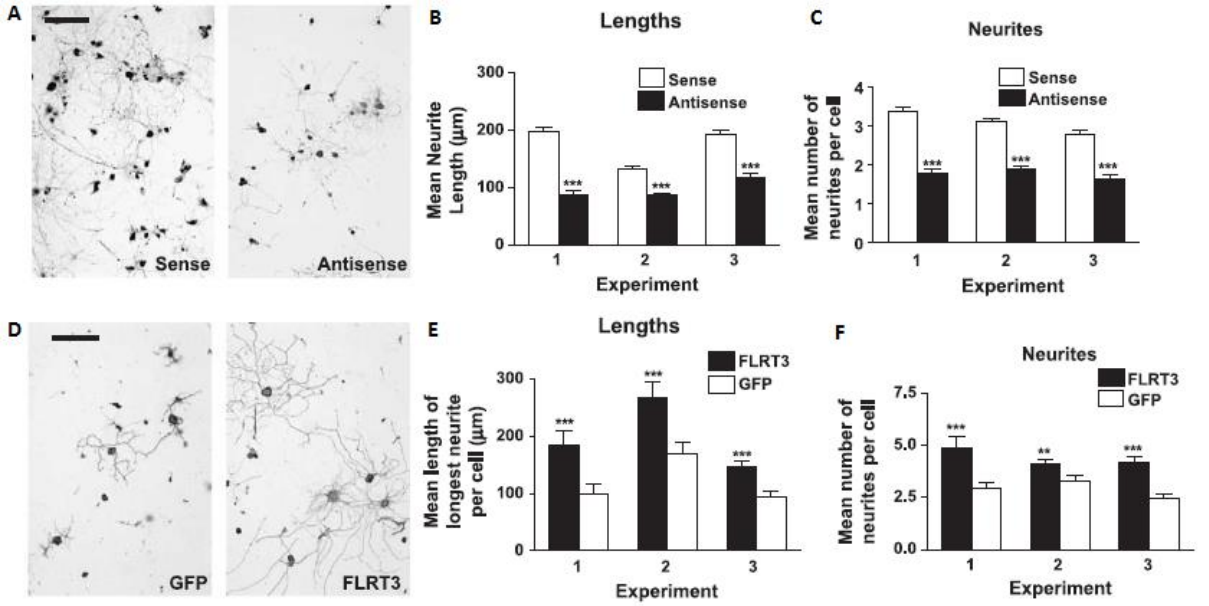

Figure 9. Flrt3 promotes neurite outgrowth: (A) Fixed dorsal root ganglion neuronal cells in vitro 24 h after application of sense or antisense oligonucleotides and immunostained for the pan-neuronal marker PGP9.5. Scale bar = 250 µm. (B + C) Antisense knockdown of FLRT3 protein in dorsal root ganglion neuronal cells in culture resulted in a significant reduction in both maximum neurite length (B) and number (C) (mean values ± SEM are shown). *** P < 0.001, two-way ANOVA. (D) Fixed dorsal root ganglion neuronal cells in vitro 24 h after application of GFP- or FLRT3 over-expressing HSV-1 virus and immunostained for the pan-neuronal marker PGP9.5. Scale bar = 250 µm. (E + F) Over-expression of FLRT3 by HSV-1 in dorsal root ganglion neuronal cells in vitro resulted in a significant increase in both maximum neurite length (E) and number (F) (mean values ± SEM are shown). *** P < 0.001, ** P < 0.01—two-tailed Mann–Whitney test. Adapted from [7].

The key role of Flrt3 in neurite length and number was confirmed by the over-expression of Flrt3 in DRG (Figure 9 D – F). With the over-expression of Flrt3, maximum neurite length increased by 51% and the number of neurites increased by 65% compared to control cells [7].

Not only does Flrt3 increase maximum neurite length and the number of neurites, it also appears to be important in the direction of neurite extension. Evidence of a cleavage event adjacent to the transmembrane domain of the Flrt in over-expression systems was first seen by Haines *et al*.,

resulting in the discovery of a short C-terminal sequence species and confirmed by Yamagashi, *et al.* (data not shown) [5, 15]. Extracellular domains (ECDs) of each Flrt protein were found in the total cell lysate (TCL) and shed in the cell culture media of over-expressing HEK-293T cells, while the presence of short C-terminal species in the TCL was also shown (data not shown) [15]. This cleavage even was also observed in dissociated embryonic cortical neurons isolated from E16.5 embryos and grown for 6 days *in vitro*, which express endogenous Flrt proteins [15] (Figure 10).

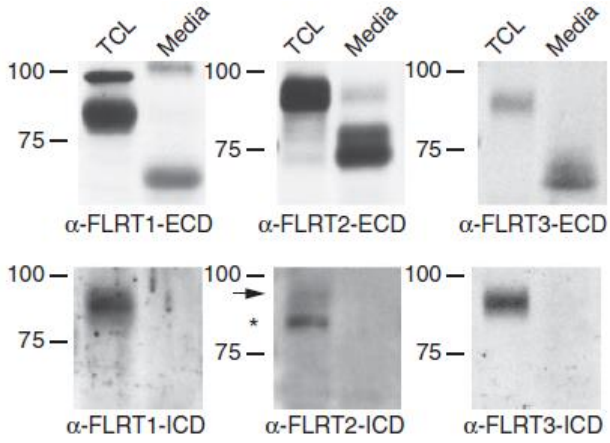

Figure 10: Detection of shed FLRT1–3 ECDs in 6 DIV conditioned media of E16.5 cortical neurons. FLRT1–3 ECDs are visible in blots probed with anti-ECD antibodies (upper panels) but not with anti-ICD antibodies (lower panels). The positions of full-length FLRT2 (arrow) and of a non-specific band (asterisk) are indicated. Adapted from [15].

Using alkaline phosphatase fused soluble Flrt ECDs, binding assays in HEK-293T cells revealed that the ECDs of Flrt3 could bind to full-length Flrt3 as well as Netrin receptor Unc5B, which had both been shown to previously interact with full-length Flrt3 (data not shown) [10, 11]. Together with the data shown above by Karaulanov *et al.* (2006), strongly suggests that the homotypic cell sorting phenotype observed here is facilitated by the Flrt3 ECD. It had been previously found that Netrin-1 binds to and acts as repulsive guidance cue for path-finding axons [16]. Therefore, using stripe assays and E15.5 hippocampal neurons, the effect of Flrt3 binding to Unc5B-positive extending axons was investigated. This found that Flrt3, like Netrin-1, act as repulsive guidance cue for path-finding axons [15] (Figure 11).

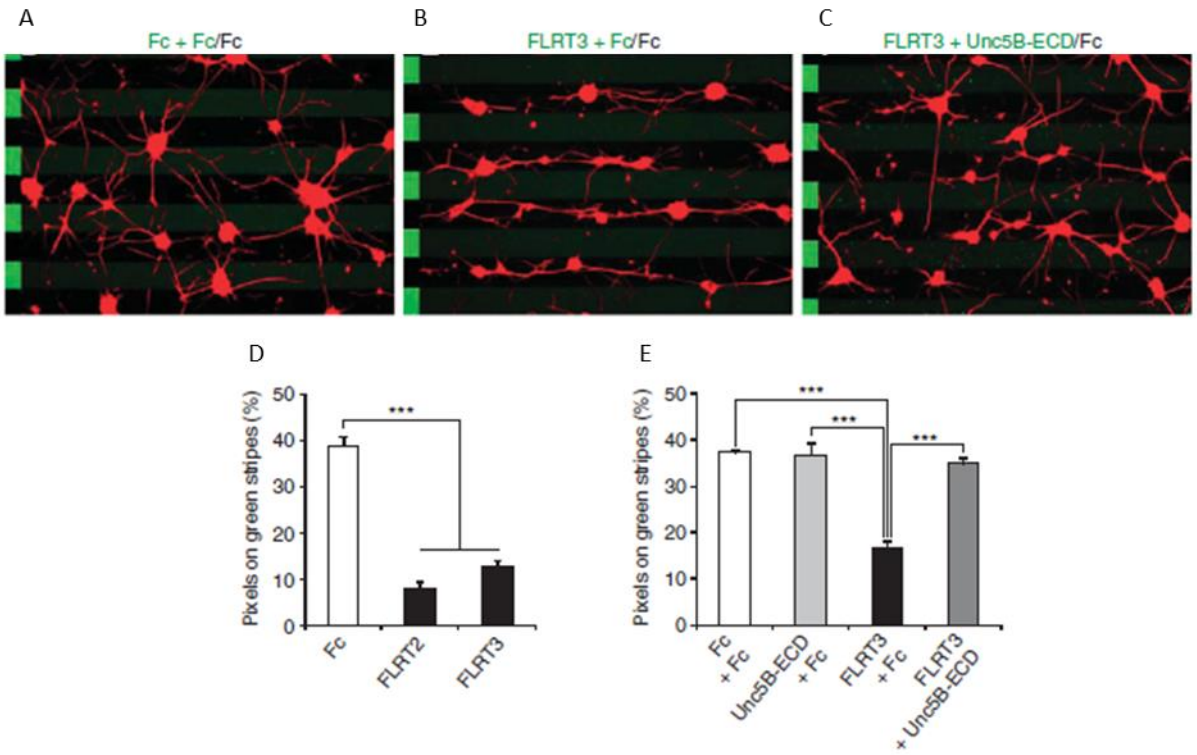

Figure 11: Stripe assays with FLRT2/3 ECDs and hippocampal neurons. (A–C) E15.5 hippocampal neurons were grown on stripes containing (A) control Fc preincubated with control Fc (green) against control Fc (black), (B) FLRT3-Fc preincubated with control Fc (green) against control Fc (black), (C) FLRT3-Fc preincubated with Unc5B-ECD-Fc (green) against control Fc (black). Cells were stained with anti-Tau1 antibodies to visualize axons (red). The location of the faintly stained green stripes is indicated by alternating stripes on the left side of each image. FLRT2/3-Fc had repulsive effects on both axons and soma (see Supplementary Figure S5). Scale bar: 100 mm. (D, E) Images were digitalized and the percentage of Tau1þ pixels on green stripes was quantified. (D) Maximal repulsion by FLRT2-Fc and FLRT3-Fc without dilution with control Fc. (E) Inhibition of FLRT3-induced repulsion by preincubation with the respective Unc5-ECD-Fc proteins (n=3 independent experiments, **P<0.01, ***P<0.001, t-test). Adapted from [15].

This data provided the first direct evidence of a role for Flrt3 in spatial arrangement of neurons in the developing embryonic brain through neurite extension.

Further evidence exists that Flrt3 is a key protein in neuron function. Latrophilin3 (LPHN3) is a member of the G-coupled protein receptor latrophilin family. LPHN3 is expressed predominantly in the CNS, and is known to mediate the exocytotic effect of black widow spider venom on synaptic terminals [17]. Evidence is gathering for a role of latrophilins in the function of neural circuits, with *LPHN3* mutations linked to attention deficit hyperactive disorder [18]. Investigation of potential ligands of LPHN3 revealed that Flrt3 can interact directly and in *trans* as a post-synaptic protein. Using post-natal hippocampal cells, knockdown of Flrt3 by shRNA resulted in a 34% reduction in synapse density and a 17% reduction in synapse area by immunofluorescence, while shRNA-resistant Flrt3 transfected cells rescued these reductions [19] (Figure 12).

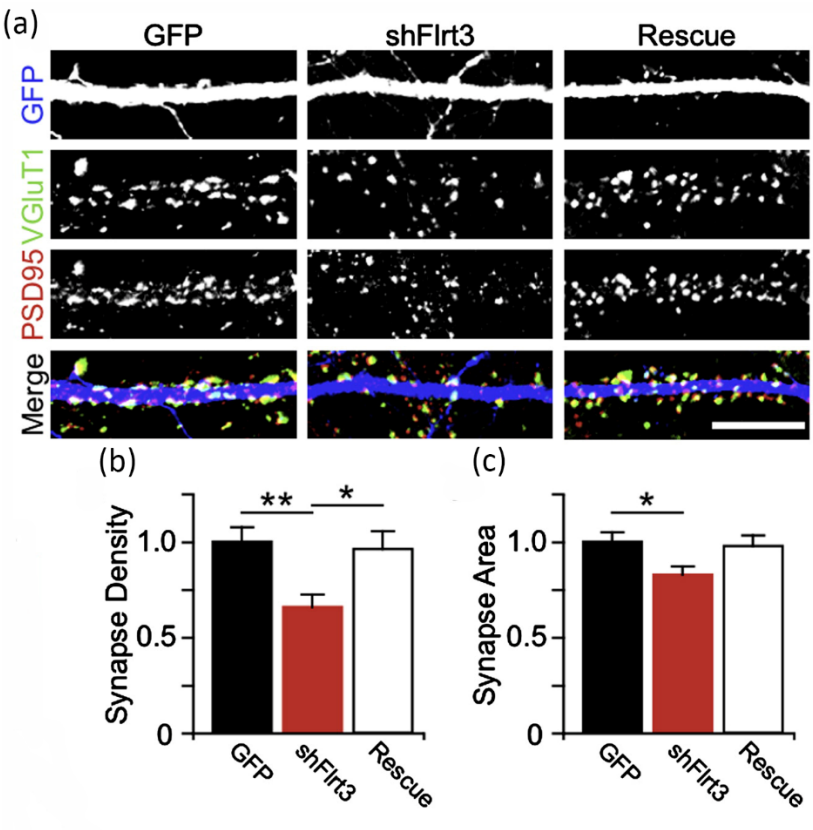

Figure 12: Flrt3 regulates glutamatergic synapse number. (a) Hippocampal neuron cultures were electroporated with GFP control plasmid (GFP), a plasmid encoding shFlrt3 and GFP (shFlrt3), or the shFlrt3 plasmid plus an shFlrt3-resistant Flrt3-myc expression construct (Rescue) and were fixed and immunostained for VGlut1 (green), PSD95 (red), and GFP (blue) at 14 days *in vitro*. (b) Synapse density was reduced by shFlrt3 and returned to control levels in the rescue condition (GFP 1.00 ± 0.08, n=35; shFlrt3 0.66 ± 0.06, n=33; rescue 0.96 ± 0.09, n=34; analysis of variance [ANOVA] $p < 0.01$, significant *post hoc* comparisons shown on graph). (c) Synapse area was slightly reduced by shFlrt3 (GFP 1.00 ± 0.05, n=35; shFlrt3 0.83 ± 0.04, n=33; rescue 0.98 ± 0.06, n=34; ANOVA $p < 0.05$, significant *post hoc* comparisons shown on graph). Adapted from [19].

Knockdown of Flrt3 also resulted in the reduction of dendritic spines in granule cells and consequently negatively regulated synapse formation onto these cells [19]. It is thought that a possible explanation for the interaction between Flrt3 and LPHN3 is to stabilise LPHN3 and allow signal transduction within the pre-synaptic neuron [20].

The role of *Flrt3* in earlier stages of development is yet to be elucidated. Flrt3 expression is first seen at E9.5, yet the above studies use much later time-points (E15.5). Such highly regulated and distinct expression patterns imply an important role, yet this question has been poorly addressed. The regions of expression of *Flrt3* in the developing embryo are reliant on proper signalling function to allow for viable development. Fgf signalling is a critical signalling pathway involved in the formation and patterning of the midbrain and hindbrain by the organising centre and the boundary, while facilitating the tissue patterning of the developing limb bud in the proximodistal axis from the AER. Expression of *Flrt3*

in *Xenopus* in various species at the MHB and AER, paired with *Lrrtm3* expression at the AER, suggested a role for particular LRR proteins in the regulation of Fgf signalling.

1.2 Fibroblast Growth Factor Receptors

Fibroblast growth factor receptor 1 (FgfR1) is a member of the fibroblast growth factor receptor (FgfR) family that contains four members and seven isoforms. FgfRs are involved in proliferation, migration, differentiation and survival of cells, especially in the CNS [21], and play an important role in somitogenesis [22]. FgfR1 contains three extracellular immunoglobulin-like domains and a cytoplasmic tyrosine kinase domain. The receptor binds 15 of the 23 Fgf ligands [23] in a complex with heparin sulphate (HS), resulting in dimerisation of two FgfR molecules. This leads to autophosphorylation of intracellular tyrosine residues and activation of the intracellular tyrosine kinase domain, resulting in the activation of downstream signalling through the MAPK (predominantly, associated with proliferation and differentiation [24]), PI3K (associated with cell survival [24]) and phospholipase C (PLC, associated with cell morphology and migration [24]) activation through a series of adapter proteins [25] (Figure 13).

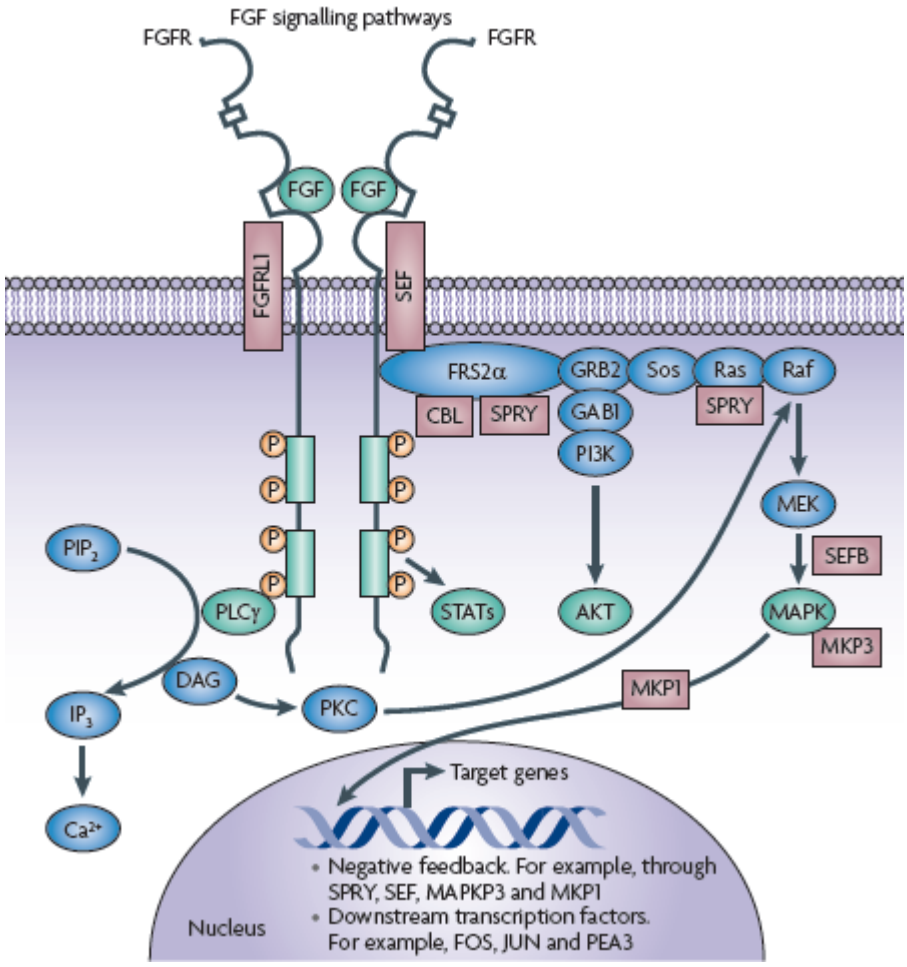

Figure 13. Schematic diagram showing the FGFR signalling network: The signal transduction network downstream of fibroblast growth factor (FGF) receptors (FGFRs), along with negative regulators. Following ligand binding and receptor dimerization, the kinase domains transphosphorylate each other, leading to the docking of adaptor proteins and the activation of four key downstream pathways: RAS-RAF-MAPK, PI3K-AKT, signal transducer and activator of transcription (STAT) and phospholipase Cγ (PLCγ) (green). Signalling can be negatively regulated at several levels by receptor internalisation or the induction of negative regulators, including FGFR-like 1 (FGFRL1), SEF, Sprouty (SPRY), CBL, MAPK phosphatase 1 (MKP1) and MKP3 (brown). These regulators may modulate ligand binding (FGFRL1 and SEF) or interfere with intracellular signalling, principally through modulation of the MAPK pathway. DAG, diacylglycerol; FRS2α, FGFR substrate 2α; GRB2, growth factor receptor-bound 2; IP_3, inositol triphosphate; P, phosphorylation; PIP_2, phosphatidylinositol-4,5-biphosphate; PKC, protein kinase C; Sos, son of sevenless [25].

With control over so many important cellular decisions via a number of pathways, regulation of Fgf signalling is vital for the proper cell growth and function during development. Two key components regulating Fgf signalling are FRS2α and Sprouty. FRS2α plays a dual role in Fgf signalling; in the presence of Fgf ligand, FRS2α initially activates downstream signalling, but later represses the signalling in a feedback loop. During stimulation, FRS2α undergoes tyrosine phosphorylation, followed by tyrosine phosphorylation of Shp2, causing complex formation with Grb2. This complex interacts with Sos and propagates Fgf signalling within the cell through the MAPK pathway. It has also been shown to allow phosphorylation of docking protein Gab1, which binds constitutively with Grb2 in complex with FRS2α, leading to the recruitment of PI-3K and activation of the Akt pathway. In FRS2α's role to

negatively regulate Fgf signalling, Grb2 bound to tyrosine phosphorylated FRS2α forms a complex with Cbl, a ubiquitin ligase, and results in ubiquitination of FgfR and FRS2α. Also, through threonine phosphorylation of FRS2α, recruitment of Grb2 is decreased and MAPK signalling is attenuated. Threonine phosphorylation of FRS2α can be a result of EGF, insulin or PDGF stimulation, and growth factors or hormones that do not result in tyrosine phosphorylation of FRS2α [26] (Figure 14).

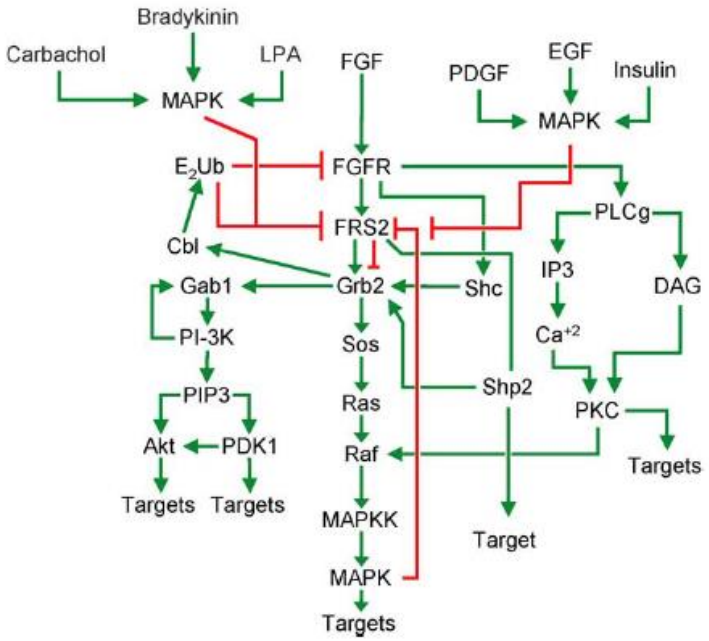

Figure 14. FGF signaling pathway: A wiring diagram depicting signaling pathways downstream of FGFR including the pathways that are dependent upon tyrosine phosphorylation of FRS2α following FGF-stimulation (green arrows). The negative signals that are mediated by or impinge upon FRS2α are marked by red arrows. Also shown, heterologous control of FGF signaling by growth factors (i.e. insulin, EGF) or G-protein coupled agonists (i.e. LPA, carbachol) that stimulate threonine phosphorylation of FRS2α [26].

Sprouty is an antagonist of Fgf signalling and binds to FRS2α (Figure 13), inhibiting the propagation of Fgf signalling via the MAPK pathway. Fgf stimulation causes an increase in expression of Sprouty in an ERK-dependent manner and Y55 phosphorylation [27, 28]. Upon phosphorylation, Sprouty translocates to the plasma membrane and co-localises with Grb2, where it inhibits the interaction between Grb2 with FRS2, and Shp2, resulting in the down-regulating Fgf signalling [29].

1.3 Fgf Signalling and Development

1.3.1 Limb development

Fgf signalling plays a critical role in limb bud formation, with signalling vital for the function of the AER. The AER is a specialised tissue formed on the distal tip of the vertebrate limb bud, essential for limb proximodistal patterning and functions by producing signalling molecules that act on the adjacent mesenchyme tissue [30]. Ligands Fgf2, Fgf4, Fgf8 and Fgf9 are expressed in the AER, with

receptors FgfR1 and FgfR2 expressed in the adjacent nascent limb bud mesenchyme [30]. To demonstrate the importance of Fgf signalling in the function of the AER in limb bud development, removal of the AER and replacement with heparin beads soaked in recombinant Fgf protein, such as Fgf4, leads to the normal formation of a functional limb [31]. Knockout of individual Fgf ligands and FgfR in the AER result in malformation of the limb and showed some functional redundancy between Fgfs and FgfRs [32].

1.3.2 Central nervous system development

The midbrain-hindbrain organiser (MHO), also known as the isthmus, located at the boundary between the midbrain and hindbrain, controls the development and patterning of these 2 parts of the brain. Conditional knockout of *Fgf8* results in the midbrain and anterior hindbrain not forming, demonstrating the importance of Fgf signalling in the MHO [33]. Fgf8 is thought to act through FgfR1, with expression of FgfR1 identified throughout the entire neural tube; overlapping with Fgf8 expression, the ventral midbrain and floor plate, and the ventral hindbrain in the formation of the MHB [34, 35] (Figure 15).

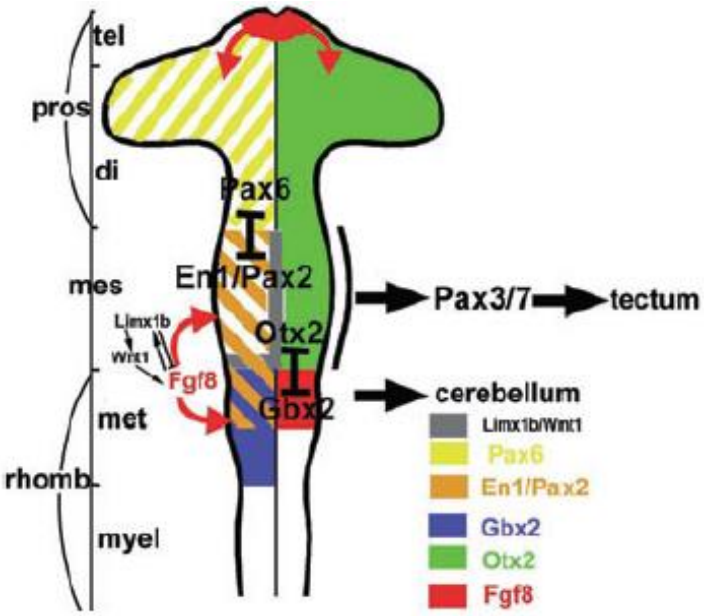

Figure 15. Schematic drawing of brain vesicles: Patterning of the vertebrate brain occurs immediately after the closure of the neural tube. Fgf8 signal from the isthmus and signals to the midbrain (mes) and hindbrain (met) through FgfR1, resulting in specific tissue fate by the expression of specific transcription factors within different neural compartments. tel=telencephalon, di=diencephalon, mes=mesencephalon, met=metencephalon, mye=myelencephalon, pros=prosencephalon, rhomb=rhombomeres, [35].

In situ analysis has confirmed the presence of *FgfR1* in the blastocyst (both the inner cell mass and telecephalon), *FgfR1* and *FgfR2* during gastrulation (day 6.5-8 *p.c.* mouse embryos), and *FgfR1* is expressed in the ectoderm and mesoderm during organogenesis (day 9.5-14.5 *p.c.* mouse embryos)

[36], where FGF signalling is important in the formation of the central nervous system (CNS) and peripheral nervous system (PNS) [23]. Mice lacking *FgfR1* and/or *FgfR2* die early *in utero* prior to or at gastrulation due to severe growth retardation [37].

Fgf signalling through FgfRs has been shown to be important in the development of the limb bud and midbrain/hindbrain and Flrts are specifically expressed in these regions.

1.4 Influential Interactions Between Proteins and LRR Proteins

In situ hybridisation analysis of *Xenopus* FGF8 (XFGF8) and XFLRT3 expression patterns showed very similar expression in early embryonic development and the mid-hind brain (MHB) boundary [8] (Figure 16).

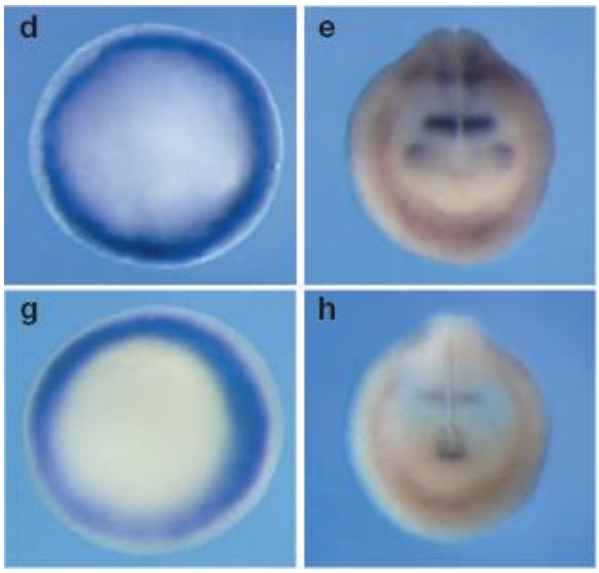

Figure 16. XFLRT3 and XFGF8 expression patterns: Expression pattern of XFLRT3 (d, e) and XFGF8 (g, h) in Xenopus gastrulae (d, g, vegetal view), neurulae, (e, h, anterior view). Adapted from [8].

Mouse studies show expression of FLRT3 in regions where FGF signalling is vital for embryonic development such as the MHB boundary, the somites and the apical ectodermal ridge (AER) [5] (Figure 17).

Figure 17. Expression of FLRT3 during mouse development: *In situ* hybridisation of 10.5 dpc mouse embryos with a RNA probe for FLRT3. vfb—hypothalamic region of the ventral forebrain; mhb—midbrain/hindbrain boundary; aer—apical ectodermal ridge [5].

Due to the distinct and precise expression of *Flrt3* that overlaps with *Fgf* and *FgfR* expression the hypothesis of a potential relationship between FgfRs and Flrts was explored.

HEK-293T cells were stimulated with Fgf-2, and using semi-quantitative PCR, it was found that transcription of all Flrt members was increased as a result of the stimulation [5] (Figure 18).

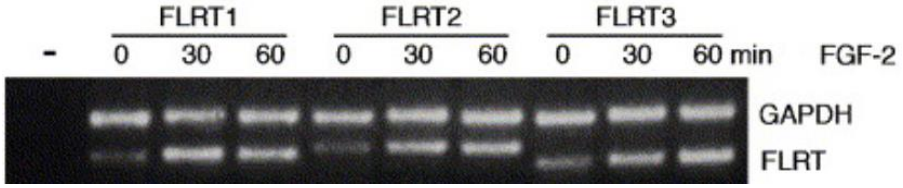

Figure 18. Fgf signalling up-regulates *Flrt* mRNA levels: HEK-293T cells were stimulated with FGF-2 and RNA subjected to semi-quantitative PCR to examine Flrt expression. Samples were taken before stimulation (0) and after stimulation for 30 and 60 min. GAPDH is shown as a control. Adapted from [5].

This data suggest Flrts may regulate Fgf signalling *in vivo*.

With Fgf signalling shown to up-regulate *Flrt* expression, it was investigated if *Flrt3* expression could regulate Fgf signalling. Over-expression analysis of XFLRT3 was shown to induce phosphorylation of ERK in the MAP-kinase signalling pathway in HEK-293T cells; a pathway used by FGF signalling. A unique role for Fgf signalling within *Xenopus* embryos is to induce expression of the strong mesodermal marker, *Xbra*. Introducing XFLRT3 mRNA into animal caps revealed an increase in diphosph-ERK levels, and a dose-dependent increase in *Xbra* expression [8] (Figure 19).

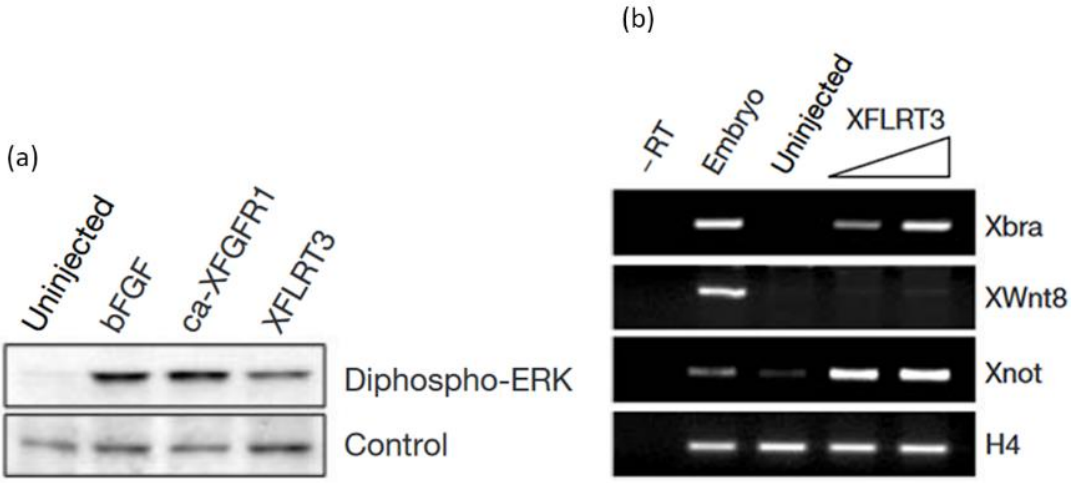

Figure 19. XFLRT3 functions in the FGF signalling pathway: a) Animal caps injected with XFLRT3 (0.5 ng per blastomere), ca-XFGFR1 (50 pg per blastomere), or bFGF-treated caps (100 ng per ml), as well as uninjected control caps, were isolated at blastula stages and cultured for 1.5 h at room temperature. Cell lysates were analysed by Western blotting for diphosphorylated (activated) ERK and the nucleolar protein NO38 as a loading control. b) Eight-cell embryos were microinjected into all four animal blastomeres with the indicated mRNAs. Animal caps were excised from blastula embryos, cultivated until stage 10 and analysed by RT–PCR. XFLRT3 (0.5, 0.75 ng per blastomere) induces *Xbra*. Adapted from [8].

Given that Fgf signalling is required for *Xbra* expression, and that an increase in XFLRT3 results in and increase in both pERK levels and *Xbra* expression, this was the first evidence that the presence of XFLRT3 causes a difference in the output of FgfR signalling. The increase in pERK levels appears not to be corrected intracellularly, which results in an increase in target gene transcription. This may occur as a part of a feedback loop, as the expression of the *Flrt* family can be regulated by Fgf stimulation.

Investigation of an interaction between XFLRT3 and FgfR1, causing the increase in *Xbra* transcription, was performed using co-transfection and co-immunoprecipitation in HEK-293T cells. XFLRT3 was shown to interact with XFGFR1 but not XBMPR1 [8] (Figure 20).

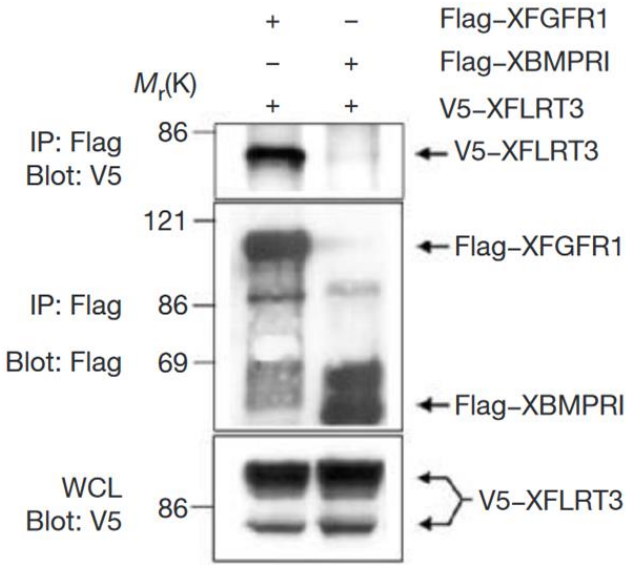

Figure 20. Interaction of XFLRT3 and Xenopus FGFRs: XFGFR1 interacts with XFLRT3. HEK-293T cells were transfected with the indicated constructs and analysed by co-immunoprecipitation. WCL= whole-cell lysate. V5, Flag = epitope tag. Adapted from [8].

The interaction between XFLRT3 and XFGFR1 was confirmed *in vivo* by luciferase reporter assay and bioluminescence resonance energy transfer (BRET), which also determined that the fibronectin and transmembrane domains were vital for this interaction [8]. This provides a mechanism for the regulation of FGF signalling by FLRT3, while also showing the interaction with FgfR1 is selective.

Regulation of receptor signalling may be able to explain how a variety of cell decisions be made in multiple tissues by a common receptor. With over-lapping Flrt3 and FgfR1 expression in the AER, which goes on to form the limb (mesoderm), and the MHB, which patterns the developing brain (neurectoderm), this may be a perfect example of this idea. Modulation of cell signalling due to binding of a single-pass LRR transmembrane protein is not unheard of, with two examples of LRR transmembrane proteins interacting with receptors to influence cell signalling having been published in the literature; LINGO-1 and the p75NTR/NgR1 complex, and FLRTs with FGFR1 [5, 38, 39].

The LINGO family of LRR proteins contains four members; LINGO-1, -2, -3, and LINGO-4. The LINGO-1 protein consists of an extracellular N-terminal sequence containing a secretory signal sequence, 12 LRRs flanked by cysteine-rich sequences, an immunoglobulin domain, a single transmembrane domain and a short C-terminal cytoplasmic sequence which contains an epidermal growth factor receptor-like tyrosine phosphorylation site with expression predominantly in the central nervous system (CNS) [38]. Analysis of whole rat brain cDNA of LINGO-1 showed expression rose steadily to its peak at post-natal day 1 after which it declined into adulthood. qRT-PCR and

immunohistochemistry revealed a 5-fold increase in LINGO-1 expression in injured rat spinal cord tracts that peaks at day 14 post injury occurrence. This results suggests that LINGO-1 is an important protein in CNS neuronal development and repair [38].

The p75 neurotrophin receptor (NTR) and Nogo-66 receptor (NgR1) are localised to the neuron surface and form a complex able to bind components of myelin and inhibit neurite outgrowth [39]. This inhibition is regulated by RhoA which is not found in neurons that do not express both p75NTR and NgR1 [39, 40]. It has been demonstrated that LINGO-1 effectively binds to p75NTR and to NgR1. With the co-transfection of the LINGO-1 gene with p75NTR or NgR1, RhoA could not be induced. But when all three constructs were co-transfected, a complex was shown to exist using co-immunoprecipitation and ELISA [38, 39] (Figure 21).

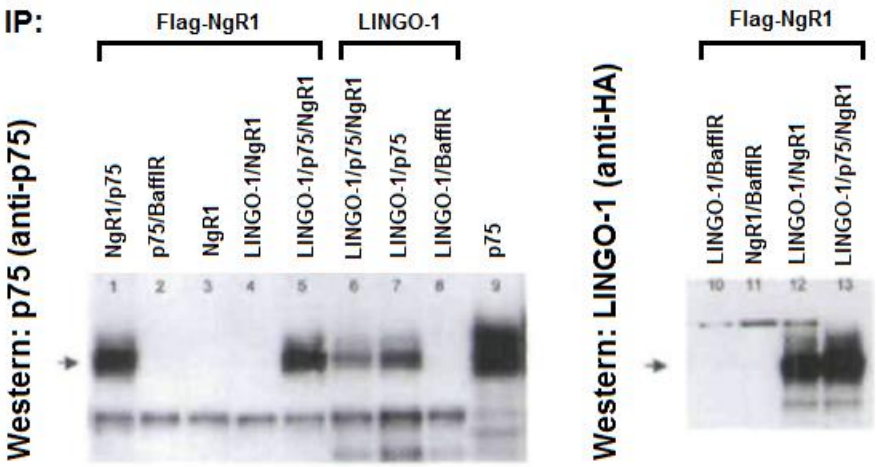

Figure 21. Co-immunoprecipitation of LINGO-1, p75 and NgRI: Utilising anti-Flag tag or rabbit anti-LINGO-1 from COS-7 cells co-expressing combinations of Flag-NgRI. p75, HA-LINGO-1 or Flag-BaffR. BaffR was used as a specificity control. Lane 9, total cell lysate, no IP. Adapted from [38].

Co-transfection of LINGO-1, p75NTR and NgR1 induced an increase in RhoA-GTP levels, restoring the ability to inhibit neurite outgrowth [38] (Figure 22).

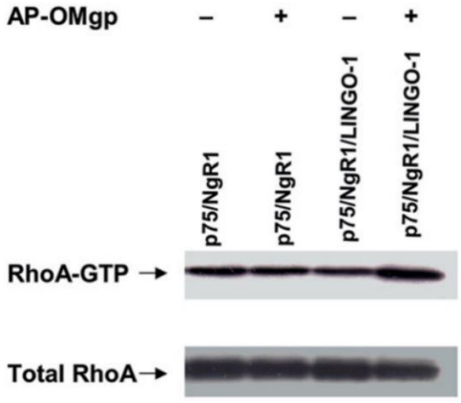

Figure 22. NgR1, p75 and LINGO-1 expression activates RhoA and transduces an inhibitory signal for neurite outgrowth: RhoA-GTP levels in COS-7 cells co-expressing NgR1/p75 or NgR1/p75/LINGO-1, in the presence or absence of AP-OMgp. Adapted from [38].

Therefore, the interaction of the LINGO-1 protein in the p75NTR/NgR1 complex is important for signal transduction.

Mouse FLRT family members were assessed for interaction with FGFR1. Expression of Flrt proteins and FgfR1 in the same or adjacent vesicular membrane is necessary for an interaction between FGFR1 and FLRT proteins to occur. Wheldon, *et al.* (2010) showed that FLRT1-HA and FGFR1 are expressed at common membranes [41] (Figure 23).

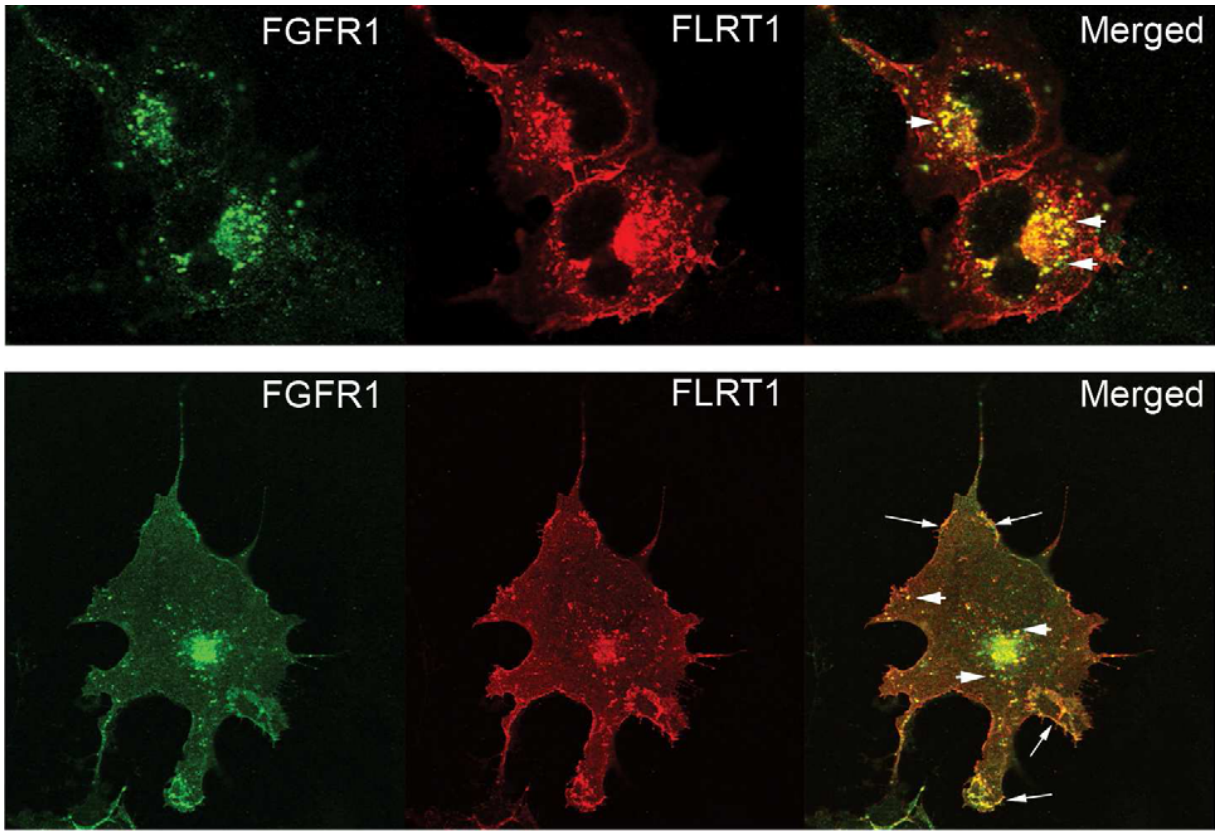

Figure 23. Co-localisation of FLRT1 and FGFR1: Immunofluorescent staining of Cos-7 cells co-transfected with plasmids encoding FGFR1 and 3'HA-tagged FLRT1. Cells stained with anti-FGFR1 (green) and anti-HA (FLRT1- red). Merged images show areas of co-localisation in yellow. Arrows highlight examples of co-localisation on the cell surface, arrowheads highlight examples of co-localisation in intracellular vesicle.s. Images (in section) taken with a confocal microscope and are representative cells from 11 total fields of cells. Adapted from [41].

FLRT1-HA and FGFR1 co-localise within membranes of intracellular vesicles (arrowheads) and at the cytoplasmic membrane (arrows). This shows that FLRT1 is present at locations within the cell to interact with and alter the output of FgfR1. Co-immunoprecipitation of cells co-transfected with FGFR1 and FLRT proteins showed that all FLRT family members bound to FGFR1 independent of FGF stimulation [5] (Figure 24).

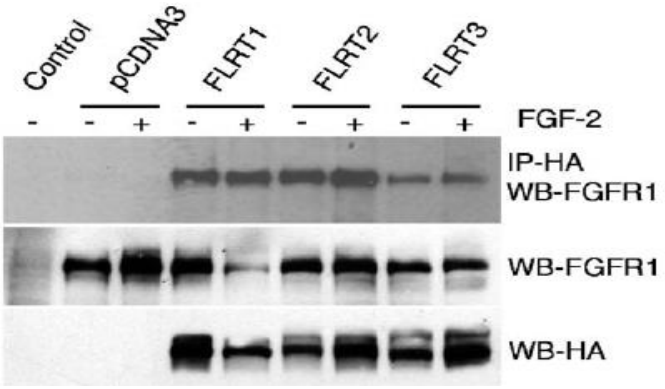

Figure 24. FLRT proteins interact with FGFR1: HEK-293T cells were co-transfected with 3'HA-tagged FLRT cDNAs and FGFR1 cDNA and analysed by immunoprecipitation with anti-HA antibody and Western blotted with anti-FGFR1, with (+) or without (−) stimulation using FGF-2. Western blots using anti-FGFR1 (WB-FGFR1) and anti-HA (WB-HA) antibodies confirm expression of FGFR1 and FLRT proteins in the IP input samples. Control is untransfected cells [5].

The interaction between Flrt3 and FgfR1 mediated by both the fibronectin III domain and transmembrane domains [5, 8]. All FLRT proteins have also been shown to interact with FGFR2 [41].

Tyrosine kinase domains located in the intracellular domain allow FgfR-mediated tyrosine phosphorylation of interacting proteins. An interaction between FgfR1 and Flrt1 means that it is possible that Flrt1 intracellular tyrosines could be phosphorylated dependent on ligand binding to FgfR1. Immunoprecipitation of HA-tagged Flrt1 from HEK-293T cells over-expressing Flrt1-HA and FgfR1 reveal that tyrosine residues are phosphorylated independent of Fgf stimulation [41] (Figure 25).

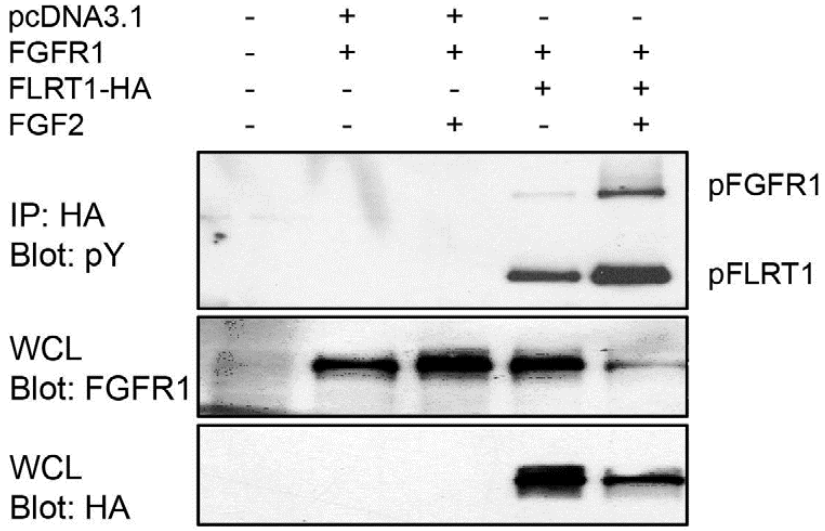

Figure 25: HEK-293T cells were co-transfected with FGFR1 and either control vector (pcDNA31) or FLRT1 (FLRT-HA). Cells were treated with or without stimulation with FGF2 (20ng/ml) in the presence of heparin (10mg/ml) for 30 min. Anti-HA immunoprecipitation was performed on whole cell lysate which was subjected to Western blot analysis with anti-phosphotyrosine (IP: HA, Blot: pY) to identify phosphorylated FLRT1 (pFLRT1). Phosphorylated FGFR1 (pFGFR1) was co-immunoprecipitated with FLRT1. The whole cell lysate (WCL) was probed for both FGFR1 (Blot: anti-FGFR1) and FLRT1 (Blot: anti-HA) expression. Data is representative of at least 4 independent experiments [41].

This also shows the phosphorylation of tyrosine residues on Flrt1 increases with FGF stimulation. It is thought that the phosphorylation of tyrosines in the unstimulated sample is due to the large number of FgfR1 molecules being expressed, resulting in auto-activation of signalling pathways [41]. Three tyrosine residues have been identified by computational analysis as having a high probability of being phosphorylated; Y^{600}, Y^{633} and Y^{671}. The FLRT1 tyrosine phosphorylation observed is dependent on FGFR1 activity, shown by the loss of FLRT1 phosphorylation in the presence of FGFR1 kinase inhibitor SU5402, while point mutation analysis showed that FLRT1 has reduced phosphorylation if any one or two of the identified tyrosine residues is mutated, and almost no phosphorylation if all three tyrosines are mutated [11, 41] (Figure 26).

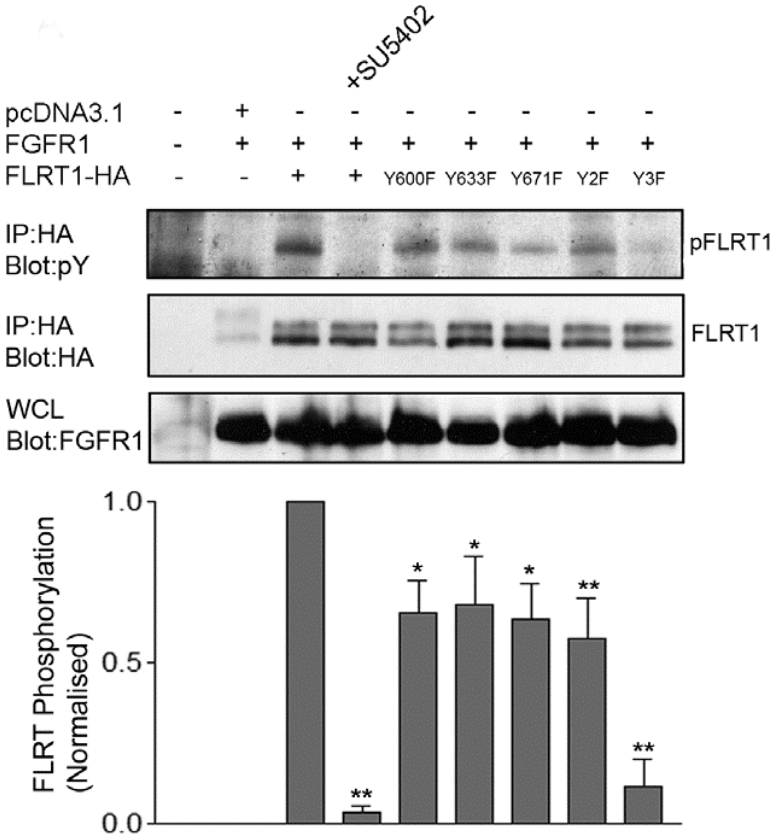

Figure 26. FLRT1 tyrosine phosphorylation: HEK-293T cells were transfected with control (pcDNA3.1) or FGFR1 and a panel of either full-length FLRT1-HA or tyrosine substitution constructs as indicated (Y600F, Y633F, Y671F, Y2F, Y3F). One sample was pre-treated with FGFR kinase inhibitor (SU5402, 50 μM, 1 hr) where indicated. Cell lysates were immunoprecipitated with anti-HA and subsequently blotted with anti-phosphotyrosine (IP: HA, Blot: pY) or anti-HA (IP: HA, Blot: HA) to examine phosphorylated FLRT1-HA levels (pFLRT1) or total immunoprecipitated FLRT1-HA levels (FLRT1), respectively. Whole cell lysate (WCL) fractions were probed with anti-FGFR1 (Blot: FGFR) to control for protein expression. Data is representative of 3 independent experiments. Densometric analysis (mean±sem, n=3) in the ration of pFLRT1:FLRT1 and normalised to FLRT1 phosphorylation in the absence of inhibitor (**p<0.01, *p<0.05, non-parametric one way ANOVA). Adapted from [41].

Haines. *et al.* showed that Flrt proteins interact with FgfR1 and 2, and with the overlap in expression of Flrt1 and FgfR and Fgf ligands, the effect of Flrt1 expression on FGFR signalling was investigated [5]. Wheldon, *et al.* used over-expression of FLRT1 in HEK-293T cells to reveal an increase

in FGF signalling pathway activation when FLRT1 transfected cells were stimulated with FGF-2 in a time-course assay, indicated by an increase in ERK phosphorylation [41] (Figure 27).

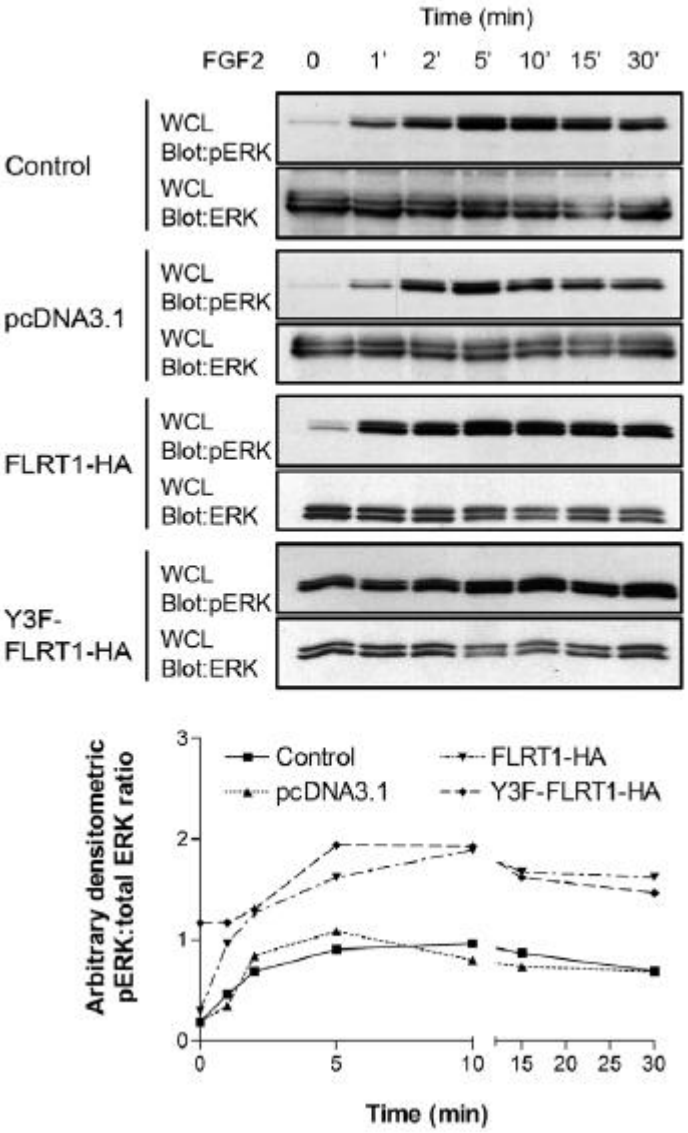

Figure 27: HEK-293T cells were transfected with either pcDNA31 vector, FLRT1-HA or Y3F-FLRT1-HA constructs Cells were co-stimulated with FGF2 (20ng/ml) and heparin (10mg/ml) for the indicated times Cell lysates were blotted for anti-phospho-ERK (WCL IB: pERK), membranes were stripped and re-probed for anti-ERK (WCL IB: ERK). Densitometric analysis has been adjusted for ERK loading and expressed as an arbitrary pERK:ERK ratio Data are representative of at least 4 independent experiments. Adapted from [41].

From time-point 0, it can already be seen that Flrt1 over-expression increases pERK levels in comparison to the control and pcDNA3.1+. Upon Fgf stimulation, the level of pERK in Flrt1 over-expressing cells increases more rapidly, and remains more robust than that of the control and pcDNA3.1+ over the 30 minute time-course. By mutating the 3 tyrosine residues found to be phosphorylated by FgfR1 activity, it was shown that pERK is constitutively active [41]. This provides evidence that Flrt1 expression alters levels of FgfR1 signalling activity.

Two transmembrane protein families interact with and regulate cell signalling. The developmentally regulated expression of many of these LRR family genes and the importance of cell signalling in development leads to the hypothesis that interactions between LRR proteins and cell receptors may be important for the regulation of signal transduction during development.

As previously mentioned, animal cap studies of *Xenopus* embryos over-expressing Flrt3 showed an increase in FgfR activity; by increased levels of pERK, and increased transcription of *Xbra*[8]. Along with the overlapped expression and FgfR interaction data, an obvious relationship exists, with the results of this relationship unknown. *Lrrtm3* is expressed in the developing neural tissue at a time when Fgf signalling is vital and has a similar structure to the Flrt family. With Flrt1 known to increase Fgf signalling intracellularly in a higher order mammal, the effect of Flrt3 and Lrrtm3 over-expression on Fgf signalling in the same system will be investigated in Chapter 3.

1.5 Identification of a Cellular System for the Study of Endogenous *Flrt3* Function

While *in-vitro* over-expression experiments can easily identify effects and/or actions of Flrt proteins in regulating Fgf signalling, it cannot confirm that these effects occur *in vivo*. Preliminary studies on *Flrt3*$^{-/-}$ mouse knockouts have thus far failed to identify the functions of Flrt3 due to early embryo lethality by what appears to be a complex phenotype, not obviously associated with Fgf signalling.

Flrt3$^{-/-}$ embryos show phenotypical malformations such as epiblast cells protruding through holes in the anterior visceral endoderm (AVE). These embryos die at mid-gestation with malformations such as asymmetric development of headfolds, *cardia bifida* and anterior neural tube closure defects [42]. These embryonic defects correspond with the timing of *Flrt3* expression in the early embryo. *Flrt3* is initially expressed at E6.75-7.0*dpc* in the anterior visceral endoderm (AVE), with later *Flrt3* expression on E7.25 present in the definitive endoderm (DE) and the posterior neuroectoderm. In E7.75 embryos, FLRT3 is still expressed in the DE and posterior neuroectoderm, with expression now seen in the head-fold and posterior mesoderm [42] (Figure 28).

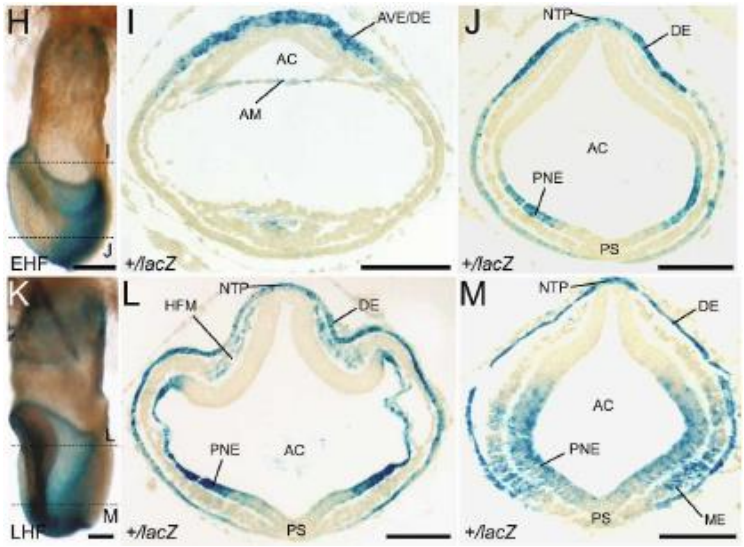

Figure 28. FLRT3 expression in the developing mouse embryo: (H–J) XGal-stained EHF stage (E7.25) and (K–M) LHF stage (E7.75) FLRT3+/lacZ embryos. Positions of the cross-sections (I,J,L,M) are indicated by dotted lines in H and K. FLRT3 is expressed in AVE and DE, amnion, posterior neuroectoderm, headfold, and posterior mesoderm. FLRT3 expression is absent or low in ectoderm underlying headfolds and in the PS. (AC) Amniotic cavity; (AM) amnion; (AVE) anterior visceral endoderm; (DE) definitive endoderm; (EHF) early head fold; (EMB) embryonic region; (EP) epiblast; (EXT) extraembryonic region; (HFM) headfold mesoderm; (LHF) late head fold; (ME) mesoderm; (MS) mid-streak; (NTP) notochordal plate; (PAC) proamniotic cavity; (PE) parietal endoderm; (PNE) posterior neuroectoderm; (PrS) pre-streak; (PS) primitive streak; (VE) visceral endoderm. Bars: H–M, 100 µm [42].

These effects could be due to the homotypic cell sorting phenotype in Flrt3-expressing cells explained above [10].

Due to the early expression of *Flrt3* and early embryonic lethality of *Flrt3* KO, analysis of Flrt3 function in the mouse embryo may be problematic. Therefore, a cell model is required to study the function of *Flrt3* in neural differentiation. The identification and characterisation of a system to study the function of *Flrt3* in neural differentiation will be addressed in Chapter 4.

1.6 Aims of the study

Based on the literature referenced above, knowledge gaps in the role of Flrt3 and Lrrtm3 are evident. I have presented data that shows Flrt1 interacts with FgfR1 and increases the levels of pERK as a result of this interaction upon Fgf stimulation. In Chapter 3, I will investigate if Flrt3 interact with FgfR1 *in vitro*, and if so, I will elucidate the effect of the over-expression of Flrt3 has on FgfR signalling. I will also address the importance of particular domains on any change to FgfR signalling using mutants and truncations of Flrt3. Addressing this aim will help establish the role of the interaction of Flrt3 with FgfR1 and subsequent intracellular signalling.

I have presented data that shows *Flrt3* is expressed early in embryonic and studies of Flrt3 KOs result in early embryonic lethality by a complex phenotype. As such, the role of *Flrt3* in the developing neural tissue, such as the MHB, is difficult to determine. In Chapter 4, I will identify a cell model system to investigate the function of endogenous *Flrt3* in the differentiation of neural tissue. Addressing this aim will help understand its role in expression in the developing nervous system.

In Chapter 5, I will investigate if other similar single-pass transmembrane LRR proteins interact with FgfR1 *in vitro*. If they do, I will elucidate the effect of the over-expression of these has on FgfR signalling.

Completion of the aims in this Masters project will allow further characterisation of Flrt3 function, and will further the broader understanding of single-pass LRR transmembrane proteins. The effect of the interaction between LRR proteins Flrt3 and Lrrtm3, with FgfR1, on the output of the FgfR1 signalling pathway will be assessed, with a cell system where the function of *Flrt3* can begin to be elucidated in respect to neural differentiation will be investigated to determine the role of endogenous *Flrt3* in this context. The desired outcomes of this project will give a deeper understanding into the regulation of FgfR signalling during embryonic development, providing a detailed insight into mechanisms that allow fine control of FgfR signalling output. This fine control differentiates development of a healthy embryo from one that is unviable.

2. Materials and Methods

2.1 Materials

Solutions

Phosphate Buffered Solution (PBS), 1x

136 mM NaCl

2.6 mM KCl

1.5 mM KH_2PO_4

8 mM $NaHPO_4$

pH to 7.4 with HCl

Tris Buffered Solution (TBS), 1x

150 mM NaCl

25 mM Tris

pH to 7.5 with HCl

Western blot transfer buffer

192 mM glycine

25 mM Tris

15% MeOH

3.6 L RO H_2O

HEK-293T cell medium

1x DMEM + HEPES (Gibco, cat: 12430)

10% (v/v) HI-FCS

100 I.U./mL pencillin

100 µg/mL streptomycin

P19 EC growth media

1x α-MEM (Gibco, cat: 12571-063)

10% (v/v) HI-FCS

100 I.U./mL pencillin

100 µg/mL streptomycin

100 mM L-glutamine

P19 EC induction media

1x α-MEM (Gibco, cat: 12571-063)

5% (v/v) HI-FCS

100 mM L-glutamine

RIPA lysis buffer

25 mM Tris-HCl, pH = 8.0

150 mM NaCl

1% (v/v) NP-40

0.01% (w/v) Na-deoxycholate

Cell lysis buffer

1x RIPA lysis buffer

1 mM Na_3VO_4

50 mM NaF

25 mM β-glycerophosphate

1x tablet of cOmplete protease inhibitor cocktail (Roche, cat: 11697498001)

Agarose gel electrophoresis buffer

0.001% EtBr

5% 20x TBE

RO H_2O

Lennox broth

1% (w/v) bacto-tryptone

0.5% (w/v) bacto-yeast extract

0.25% (w/v) NaCl

pH to 7.0 with NaOH

Blocking Solution (BS)

1x PBT-0.25%

10% heat inactivated horse serum

Krebs-HEPES buffer (KHB)

10 mM HEPES

4.2 mM $NaHCO_3$

11.7mM Glucose

1.18 mM $MgSO_4.7H_2O$

1.18 mM KH_2PO_4

4.69 mM KCl

118 mM NaCl

1.29 mM $CaCl_2.2H_2O$

pH to 7.4 with NaOH at 37^oC

BES, 2x

50 mM N,N-bis(2-hdroxyethyl)-2-aminoethanesulfonic acid (BES)

280 mM NaCl

1.5 mM Na_2HPO_4

PBT-1%, 1x

1% (v/v) Tween-20

1x PBS

PBT-0.25%, 1x

0.25% Tween-20

1x PBS

Protein load buffer (PLB), 6x

60% (v/v) Glycerol

300 mM Tris (pH 6.8)

12 mM EDTA

12% (w/v) SDS

864 mM 2-mercaptoethanol

0.05% (w/v) bromophenol blue

Oligonucleotides

Table 1. Oligonucleotide primers used to amplify sequences for *Flrt3* promoter luciferase analysis and effect of Flrt3 OE on neural differentiation: 2 kb, 4 kb, 6 kb and 10 kb bound to complimentary sequence the respective number of base pairs 5' of the *Flrt3* transcriptional start site (forward primer). These primers were used in conjunction with either the + start site or – start site primer (reverse primer), which contain the *Flrt3* transcription start site, or not, to amplify sequences to be analysed by luciferase assay. Flrt3 ORF primers used to amplify the Flrt3 ORF from the RP23-111A1 BAC clone. Primers were designed using Primer3 (http://primer3.ut.ee/).

Amplicon	Forward primer (5' -> 3')	Reverse primer (3' -> 5')	Amplicon size (bp)
RARE*	CAGTCTCAGGAGCACAGCAC	GGGCACATGCCAAAGAAAATGG	632
2 kb	ATTGAGTTTGGCAGGAATGG	+start site and –start site	2154 and 2187
4 kb	AGAGCCTGGAAAACCTGGAT	+start site and –start site	4024 and 4057
6 kb	TTTGGGTTGGCCACTTGTAT	+start site and –start site	6251 and 6284
10 kb	TACACAGGAGCCACAGGTGA	+start site and –start site	9983 and 10016
+start site (+pr)	N/A	TTCCATTGCCTGTGAGTTGA	N/A
-start site (-pr)	N/A	GCTGAGATGCCATTTGGTTT	N/A
Flrt3 ORF	TAGGATCCTGCTGACCATGATCAGC	TACTCGAGTCAGGTTATCTGAATGGT	1949

* sequence containing the conserved retinoic acid response element identified in Figure 4.2.

Table 2. Oligonucleotide primers used to in qRT-PCR experiments: Primers were designed using Primer-BLAST (https://www.ncbi.nlm.nih.gov/tools/primer-blast/index.cgi?ORGANISM=10090&INPUT_SEQUENCE=NM_009504.4&LINK_LOC=nuccore) based on the NCBI nucleotide accession number. Restrictions placed on primer design restricted amplicon size to between 75 and 150 bp, primer annealing temperature between 56^{o}C and 62^{o}C, and primers must cross an exon-intron boundary.

Gene	Accession number	Forward (5' -> 3')	Reverse (3' -> 5')
Flrt3	NM_001172160.1	TCCCGTAACCACCTTAGCAC	GATGGGGAAGAGATCGTTGA
Sox1	NM_009233.3	CCTCTCAGACGGTGGAGTTATATT	GACTTGCAGGCTATGTACAACATC
Pax6	NM_001244200.2	AGAATTTGTGTGCAAATGAAGG	GTATTTGAATGGGCAATGAGC
Oct4	NM_001252452.1	CCCAGGCCGACGTGG	GATGGTGGTCTGGCTGAACAC
GAPDH	NM_001289726.1	ATGCCAGTGAGCTTCCCGTTCAG	AACCAGAAGACTGTGGATGG
FgfR1	NM_010206.3	AGCGCAAGACACAGACACC	ATGGATATTCCACCGTGAGC
FgfR2	NM_010207.2	GGATCAAGCACGTGGAAAAG	AGAGCCAGCACTTCTGCATT
FgfR3	NM_008010.5	GCCAGCTGCACACATGCAC	TGAGGATGCGGTCTAAATCC
FgfR4	NM_008011.2	TTGAGGCCTCTGAGGAAATG	GTCAACACCTGCTCTTGCTG

Antibodies

Table 3. Primary antibodies used for western blot, immunoprecipitation and/or immunofluorescence assays: Specific details of the antibodies mentioned in the Methods and/or Results that were used to obtain my results.

Name	Clonal Type	Raised in	Supplier	Catalogue #
4G10® Platinum Anti-phosphotyrosine (pY)	Monoclonal	Mouse	Millipore	05-1050
HA-Tag (6E2)	Monoclonal	Mouse	Cell Signalling	2367
HA.11	Monoclonal	Mouse	Jomar	MMS-101R
Anti-FLAG M2	Monoclonal	Mouse	Sigma	F3165
Flg (C-15)	Polyclonal	Rabbit	Santa Cruz	sc-121
ERK1 (K-23)	Polyclonal	Rabbit	Santa Cruz	sc-94
p-ERK (E-4)	Monoclonal	Mouse	Santa Cruz	sc-7383
Anti-human FLRT3	Polyclonal	Goat	R&D Systems	AF2795
Human FLRT3	Monoclonal	Mouse	R&D Systems	MAB2795
Sox1	Polyclonal	Goat	R&D Systems	AF3369

Table 4. Secondary antibodies used for western blot and/or immunofluorescence assays: Specific details of the antibodies mentioned in the Methods and/or Results that were used to obtain my results.

Name	Raised in	Supplier	Catalogue #
anti-mouse HRP	Donkey	Rockland	610-703-124
anti-rabbit HRP	Donkey	Rockland	611-703-127
anti-goat HRP	Donkey	Rockland	605-703-002
anti-mouse Alexa 488	Donkey	Jackson IR Labs	715-485-151
anti-goat Alexa 488	Donkey	Invitrogen	913911
anti-rabbit Alexa 488	Donkey	Jackson IR Labs	711-545-152
anti-rabbit Alexa 594	Donkey	Molecular Probes	A21207
anti-mouse Alexa 594	Donkey	Molecular Probes	A21203
anti-mouse Cy2	Donkey	Jackson IR Labs	715-225-020
anti-goat Cy3	Donkey	Jackson IR Labs	705-165-147
anti-goat Cy5	Donkey	Rockland	605-710-125
anti-rabbit Cy5	Donkey	Jackson IR Labs	711-175-152

Enzymes

Table 5. List of enzymes utilised to perform molecular cloning.

Name	Catalogue #	Supplier	Function
Native Poly Pfu	600136-81	Aligent	DNA polymerase
Advantage 2	639201	Clontech	DNA polymerase
T4 DNA ligase	M0202S	New England Biolabs	DNA ligase
*Sac*I	R0156S	New England Biolabs	Restriction enzyme
*Sma*I	R0141S	New England Biolabs	Restriction enzyme
*Xho*I	R0146S	New England Biolabs	Restriction enzyme
*BamH*I	R0136S	New England Biolabs	Restriction enzyme
DNAse I	M0303S	New England Biolabs	DNAse

2.2 Methods

2.2.1 Molecular cloning

The target sequence (2 kb ± pr, 4 kb ± pr, 6 kb ± pr, 10 kb ± pr, and Flrt3) was amplified from the RP23-111A1 BAC clone using the oligonucleotide primers from Table 1, allowing the polymerase 30 secs of extension time per 500 bp of target. Amplicons were purified using gel electrophoresis and obtained using the QIAquick Gel Extraction kit (Qiagen, catalogue #: 28706) as per manufacturer's instructions. Purified fragments were ligated into pGEMT-Easy using T4 DNA ligase (New England Biolabs, catalogue #: M0202S) overnight at 4^{o}C as per manufacturer's instructions. Ligation mixture underwent heat-shock transformation into competent DH5α *E. coli* cells by mixing 5 µL of ligation mixture with 45 µL of the competent cells, incubating on ice for 20 min, heat-shocking at 42^{o}C for 75 sec, incubating on ice for 10 min, then adding 450 µL of Luria broth and incubating mixture at 37^{o}C with shaking for 45 min. Transformed bacteria was plated onto Luria broth agar plates containing 100 µg/mL ampicillin and grown overnight at 37^{o}C (30^{o}C for 6 kb ± pr). Colonies were chosen and grown in Luria broth plus 100 µg/mL ampicillin 1.5 mL bacterial cultures overnight at 37^{o}C (30^{o}C for 6 kb ± pr) with rotation. Subsequent bacterial culture underwent plasmid extraction using the QIAprep Spin Miniprep kit (Qiagen, catalogue #: 27106) as per manufacturer's instructions, and check-digest with appropriate restriction enzymes to confirm insertion of amplicon. Clones containing what appeared to be the correct digestion pattern were sequenced using Big Dye® Terminator Cycle Sequencing kit (Applied Biosystems, catalogue #: 4337455) as per manufacturer's instructions, with products sent to the Australian Genome Research Facility (AGRF) for sequence analysis. Clones returning the correct sequence were digested with appropriate restriction enzymes. Digestion products were separated by

agarose gel electrophoresis and target sequence purified using the QIAquick Gel Extraction kit, as per manufacturer's instructions. Purified fragments were ligated into appropriately digested expression vectors (see Table 6) using T4 DNA ligase overnight at 4^{o}C as per manufacturer's instructions. Ligations of digested expression vector alone were set-up as negative controls. Reactions underwent heat-shock transformation into DH5α *E. coli* cells (as outlined above) and were plated onto Luria broth agar plates containing 100 µg/mL ampicillin and grown overnight at 37^{o}C (30^{o}C for 6 kb ± pr). Colonies were chosen and grown in Luria broth plus 100 µg/mL ampicillin 1.5 mL bacterial cultures overnight at 37^{o}C* with rotation. Subsequent bacterial culture underwent plasmid extraction using the QIAprep Spin Miniprep kit (Qiagen, catalogue #: 27106), as per manufacturer's instructions, and check-digest with appropriate restriction enzymes to confirm presence of insert. Results were run on an agarose DNA gel electrophoresis and cultures containing clones that displayed correct digestion pattern were grown in 100mL overnight cultures while shaking at 37^{o}C containing 100 µg/mL ampicillin (30^{o}C for 6 kb ± pr). Subsequent bacterial cultures underwent plasmid extraction using the QIAfilter Plasmid Midi kit (Qiagen, catalogue #: 12243) as per manufacturer's instructions. Purified plasmid was stored at -20^{o}C.

Table 6. Molecular cloning strategy for *Flrt3* promoter analysis luciferase constructs and Flrt3 OE on neural differentiation: Amplicons were amplified using the primers in Table 1 from the templates listed here. Sequence analysis was undertaking utilising the T7 and SP6 primers on the pGEMT-Easy plasmid (intermediate vector). Once confirmed, amplicon was sub-cloned into the specific destination plasmid (expression vector) for assay use.

Plasmid name	Template DNA source	Cloned via plasmid (intermediate vector)	Destination plasmid (expression vector)
RARE, 2kb-pr, 4kb-pr, 6kb-pr	RP23-111A1 BAC clone (Murdoch Children's Research, Melbourne)	pGEMT-Easy (Promega, cat. #: A3600)	pGL3 Promoter (Promega, cat. #: E1751)
2kb+pr, 4kb+pr, 6kb+pr	RP23-111A1 BAC clone	pGEMT-Easy	pGL3 Basic (Promega, cat. #: E1761)
Flrt3 untagged	RP23-111A1 BAC clone	pGEMT-Easy	pcDNA3.1+ (Life Technologies, cat. #: V790-20)

2.2.2 Tissue culture

Cell growth conditions

Table 7. Cell culture media used for growth of HEK-293T, Cos-7 and P19 EC cells: Mammalian cell lines HEK-293T, Cos-7 and P19 EC were grown in and experiments undertaken using the following medium + supplement combinations.

Media Name	Cell Type	Base Media	Supplements
DMEM	HEK-293T, Cos-7	DMEM (Gibco, cat. #: 12430-054)	10% (v/v) HI-FCS, 100 I.U./mL pencillin, 100 µg/mL streptomycin
P19 GM	P19	α-MEM (Gibco, cat. #: 12571-063)	10% (v/v) HI-FCS, 100 I.U./mL pencillin, 100 µg/mL streptomycin, 100 mM L-glutamine
P19 IM	P19	α-MEM (Gibco, cat. #: 12571-063)	5% (v/v) HI-FCS, 100 I.U./mL pencillin, 100 µg/mL streptomycin, 100 mM L-glutamine

All cells were passaged in 75 cm^2 U-shaped tissue culture flasks (Sigma Aldrich, cat. #: CLS430461U) prior to experiment set-up, and incubated in humidified air at 37°C, 5% CO_2.

Thawing of cells

Vials of cells taken from liquid nitrogen storage were thawed in a 37°C water bath until just defrosted. HEK-293T and Cos-7 cells were resuspended in the freezing medium and added to a flask containing approximately 30 mL of DMEM. P19 cells were resuspended and washed twice with P19 GM, before being added to a T75 tissue culture flask containing approximately 30 mL of P19 GM.

Passaging of cells

Cells were grown until approximately 85% confluency. Old medium was removed and cells washed with 1x PBS three times. Cells were trypsinised for 5 min with 1 mL of 10 mM trypsin. For HEK-293T and Cos-7 cells, a 1:10 dilution of the cells was added to approximately 30 mL of DMEM. For P19 cells, $7x10^5$ cells were added to approximately 30 mL of P19 GM.

Cell transfection

24 hrs prior to transfection, 10 cm tissue culture plates were seeded with $1x10^6$ HEK-293T cells and incubated overnight. Cells were transfected by $Ca_3(PO_4)_2$ in 10 cm tissue culture plates using the following protocol:

5 µg expression vector was added to 50 µL 2.5M $CaCl_2$ and made up to 250 µL with mQ H_2O. 250 µL 2x BES buffer was added, the solution was mixed, incubated at 25°C for 20 min, then added dropwise to

cells and incubated at 37°C in 3% CO_2. Cells with transfection mixture were cultured for 20-22 h before harvesting.

24 hrs prior to transfection, 10 cm tissue culture plates were seeded with $1.2x10^6$ P19 cells or $1x10^6$ Cos-7 cells and incubated overnight. P19 and Cos-7 cells were transfected with Fugene 6 or HD using the following protocol:
4.5 µL Fugene (Promega, cat. # E2691 (6) or E2311 (HD)) and 2 µg expression vector (9:4 (v/w) Fugene to DNA ratio) was added to 100 µL of appropriate serum-free media. Solution was mixed and incubated at 25°C for 10 min, then added dropwise to cells and incubated at 37°C in 5% CO_2. Cells with transfection mixture were cultured for 20-22 h before harvesting.

In each cell transfection experiment, a sample of cells were transiently transfected with a GFP in the pcDNA3.1 vector to provide evidence of successful transfection. Routinely, 40-50% of HEK-293T and Cos-7 cells, and 20-30% of P19 EC cells were found to express GFP in these samples.

Fgf-2 stimulation

24 hrs prior to transfection, 10 cm tissue culture plates were seeded with $1x10^6$ HEK-293T cells and incubated overnight. Cells were washed with 5 mL of 1x KHB, then incubated for 60 min in 5 mL of 1x KHB at 37°C in 5% CO_2. 20 ng/mL of Fgf-2 (Jomar Bioscience, cat. #: CYT-386) and 10 µg/mL of heparin (Sigma Aldrich, cat. #: H3149-10KU) was added to appropriate plates of cells and incubated for 10 min. All plates of cells were washed twice with 1x PBS and lysed in-plate by adding 300 µL of cell lysis buffer, scraping and pipetting cells to disrupt the membrane. TCL was spun at 13,000 rpm for 15 min at 4°C and supernatant collected, labelled as “soluble CL” and stored at -20°C.

2.2.3 Sample analysis techniques

Bradford assay

30 µL of soluble CL was added to 270 µL of mQ H_2O to make a 1:10 dilution. 10 µL of BSA standard solutions (2 mg/mL stock diluted to 0 – 1 mg/mL in 0.1 mg/mL increments) and soluble CL dilutions was added to a 96-well flat bottom clear plate in duplicate. 200 µL of 1:5 dilution of Bradford reagent (Bio-Rad, cat. #: 500-0006) in mQ H_2O was added to each well. The plate was incubated at 25°C for 5 min and then absorbance at 620 nm was measured. A standard curve was created using absorbance of the BSA standard solutions and concentration of soluble CL calculated from this.

Western blot

A 10% resolving SDS-PAGE gel was made by combining 4.1 mL H_2O, 3.3 mL acrylamide/bis (30% 29:1, Sigma Aldrich, cat. # A3574-100), 2.5 mL 1.5 M Tris-HCl pH 8.8, 100 µL 10% (w/v) SDS in H_2O, 10 µL TEMED (Sigma Aldrich, cat. #: T9281-50), 32 µL 10% (w/v) ammonium sulfate and pouring into a mini gel cassette (Invitrogen, cat. #: C2015), until approximately 2 cm from the top. Upon complete polymerisation, the stacking gel was made by combining 6.1 mL H_2O, 1.3 mL acrylamide/bis (30% 29:1, Sigma Aldrich, cat. #: A3574-100), 2.5 mL 1.5 M Tris-HCl pH 6.8, 100 µL 10% (w/v) SDS in H_2O, 10 µL TEMED (Sigma Aldrich, cat. #: T9281-50), 100 µL 10% (w/v) ammonium sulfate and pouring into the top of the cassette until full. A comb was immediately inserted and the stacking gel left to polymerise. 6x PLB is mixed with the 35 µg of soluble CL and boiled at 95^{o}C for 5 min. Samples were loaded into individual wells with 1 lane of 10 µL of Precision Plus Protein Dual Color Standards (Bio-Rad, cat. #: 161-0374). SDS-PAGE was run at a constant voltage of 110 V in NuPAGE MES SDS running buffer (Invitrogen, cat. #: NP0002) until protein/s of interest are sufficiently resolved. Using Western blot transfer buffer, a “wet transfer” sandwich with PVDF membrane (Millipore, cat. #: IPVH00010) was made and the transfer was run in Western blot transfer buffer for 90 min at 250 mA at 4^{o}C. The membrane was incubated in Ponceau stain for 5 min, then washed in RO water to confirm protein transfer. The membrane was washed with 1x PBST for 5 min, then incubated in the appropriate blocking solution (see Table 8) for 90 min. The primary antibody was diluted in the appropriate antibody incubation solution (see Table 8) to a 1:1000 (v/v) dilution and incubated with the membrane overnight at 4^{o}C. The membrane underwent 3x 5 min and 1x 15 min wash with base buffer, then incubated with appropriate secondary antibody, diluted in the appropriate antibody incubation solution (see Table 8) to a 1:5000 (v/v) dilution, for 90 min. The membrane was washed for 3x 5 min then 3x 15 min in base buffer before being exposed to ECL Select Western Blotting Detection Reagent (Sigma, cat #: GERPN2235) for 5 min. Chemilumiscent bands were detected using the ChemiDoc MP (Bio-Rad). The membrane was washed for 5 min in base buffer and then stripped by incubating with Restore PLUS Western Blot Stripping Buffer (Thermo Scientific, cat. #: 46430) for 10 min, then re-blocked in blocking solution. Antibody incubation and membrane development was then undertaken as previously mentioned above.

Table 8. Western blot primary antibodies and solutions used for blocking and antibody incubation: For each western blot, depending on the antibody used to probe the membrane, the membrane was blocked in the appropriate blocking solution, and antibody diluted in the appropriate antibody incubation solution before adding to the membrane for probing.

Antibody	Blocking solution	Antibody incubation solution
4G10® Platinum Anti-phosphotyrosine (pY)	3% skim milk TBS	3% skim milk TBST
HA-Tag (6E2)	5% skim milk TBST	5% skim milk TBST
Anti-FLAG M2	3% skim milk TBS	3% skim milk TBS
ERK1 (K-23)	5% BSA PBS	5% BSA PBST
p-ERK (E-4)	5% BSA PBS	5% BSA PBST

Immunoprecipitation assay

50 µL of soluble CL was set aside as IP input. 23 µL of Dynabeads Protein G (Dynabeads) (Invitrogen, cat. #: 100.03D)/sample had the supernatant removed and washed twice with 500 µL of RIPA buffer, then resuspended in 23 µL of RIPA buffer/sample. 20 µL was added to the remaining soluble CL supernatant and samples were pre-cleared by rotating overnight at 4°C. Supernatant was removed from the Dynabeads and placed in a clean eppendorf. 4 µL of antibody for immunoprecipitation was added to the sample and rotated for 60 min at 4°C. 20 µL of washed Dynabeads was added to the soluble CL and antibody mixture and rotated for 60 min at 4°C. Supernatant was removed and Dynabeads washed twice with 1x TBST. Dynabeads were transferred to a clean eppendorf and washed once more with 1x TBST. 20 µL of 6x PLB was added and samples were boiled at 95°C for 5 min and loaded onto an appropriate SDS-PAGE gel and run as a Western blot alongside the IP inputs.

RNA extraction and DNAse treatment

All pipette tips and reagents used are RNAse free. Cells were scraped from base of plate into 1 mL of 1x PBS and transferred to a clean eppendorf tube. The tubes were centrifuged for 5 min at 4,000 rpm at 25°C and supernatant discarded. RNA was extracted using Trizol Reagent (Invitrogen, cat. #: 15596018) as per manufacturer's instructions. RNA pellet was redissolved in 100 µL of mQ H_2O. 11 µL of 10x DNAse buffer and 1 µL of DNAse I was added and incubated at 37°C for 10 min. 1 µL of 0.5 M EDTA was added and the solution was incubated at 75°C for 10 min. Samples were incubated on ice for 1 min. 100 µL of phenol/chloroform (Sigma, cat. #: P3803) was added, mixture vortexed to combine and sample spun for 5 min at 13,000 rpm at 25°C. Resulting aqueous layer was transferred to a new eppendorf tube and precipitated by addition of 10 µL of 3 M NaAc and 250 µL of EtOH and incubation at -20°C for 60 min. Mixture was spun for 15 min at 13,000 rpm at RT and supernatant disposed of. Pellet was washed with 100 µL of 70% EtOH by centrifuging for 5 min at 13,000 rpm at 25°C. Supernatant was disposed of, pellet dried for 10 min in 37°C heating block and resuspended in 20 µL mQ H_2O and stored

at -20°C. Samples were visualised using agarose gel electrophoresis to confirm RNA integrity (prominent bands at approximately 5 kb (28S rRNA) and 2 kb (18S rRNA)), as well as completion of gDNA degradation. RNA concentration and purity was assessed by Nanodrop analysis using 2 µL of sample. $A_{260/280}$ values of approximately 2.0 indicated pure RNA.

Complementary DNA (cDNA) synthesis

1 µg of RNA was added to 10 µL of 2x RT buffer and 1 µL of 20x enzyme mix from the High Capacity RNA-to-cDNA Kit (Life Technologies, cat. #: 4387406). Mixture was made up to 20 µL with mQ H_2O and incubated for 60 min at 37°C, 5 min at 95°C, then stored at -20°C.

Quantitative real-time polymerase chain reaction (qRT-PCR)

For each gene, 15 ng of cDNA (3 µL) was added to 27.35 µL of Fast SYBR Green Master Mix (Life Technologies, cat. #: 4385617) and made up to 50 µL with mQ H_2O. 46 µL of this template mixture was added to $2.5x10^{-12}$ mole (4 µL of 1.25 µM primer pair mix) of each primer of the target gene's primer pair. 15 µL of this mixture was added to a well of a MicroAmp® Fast Optical 96-well reaction plate (Life Technologies, cat. #: 4346907) in triplicate. PCR and analysis was undertaken by StepOne Plus Real Time PCR System with StepOne Software v2.1. Levels of cDNA in each sample were normalised using expression levels house-keeping genes GAPDH and eEF2. In each qRT-PCR run, 2 types of negative controls were run; (i) each RNA sample was analysed by qRT-PCR using primers for GAPDH in the absence of reverse transcription, and (ii) a sample containing all reaction components except cDNA was analysed for each primer pair. All samples and reactants were shown to be not contaminated with DNA (no amplification observed in the negative controls).

Immunofluorescence microscopy

Cells were grown on sterile microscope cover-slips in a 6-well tissue culture tray and treated as per experiment details. Cells were washed twice with PBS, fixed for 15 min with 4% (w/v) paraformaldehyde and washed three times with PBS. Cells were permeabilized by washing with PBT-1% for 10 min at 25°C, then blocked by incubating with BS for 30 min at 25°C. Appropriate dilution of primary antibody was made using BS and incubated with cells overnight at 4°C. Cells were washed twice with PBS and once with PBT-0.25%. Secondary antibody was appropriately diluted in BS and incubated with cells for 2 h at 25°C. Cells were washed twice with PBS and once with PBT-0.25%, then the cover-slips were mounted onto microscope slides with Prolong Gold Antifade Reagent with DAPI (Life Technologies, cat. #: P-36931). Cover-slips were sealed on the microscope slide with nail polish and incubated overnight at 25°C in the dark before viewing the slide. Slides were imaged on a Zeiss

deconvolution microscope (located in the Molecular Life Sciences building, University of Adelaide), or with Leica SP5 Spectral Scanning confocal microscope (located at the Adelaide Microscopy facility, University of Adelaide), using the same exposure times, laser and gain settings between slides to ensure accurate representation of fluorescence intensity. Images were false coloured and merged (where appropriate) using Adobe Photoshop.

Dual-Luciferase assays

P19 cells were plated in a 24-well tissue culture plate and transfected 4 h later with 500 ng of the appropriate *Flrt3* pGL3 firefly luciferase vector and 1 ng of renilla luciferase vector using the Fugene 6 protocol outlined above in Cell transfection, appropriately scaled down. Differentiation of the appropriate samples occurs 18 h later, and samples harvested at appropriate time-points and prepared for luminometer analysis following the protocol from the Dual-Luciferase Reporter Assay System (Promega, cat. #: E1910) without variation. Samples were loaded into individual wells of a 96-well plate in triplicate and luminescence measured using the LUMIstar Omega (BMG Labtech) luminometer.

Statistical analysis

All statistical analysis of data obtained was performed using the Student's t-test within the GraphPad Prism software package. At least 3 biological replicates were obtained for all data undergoing statistical analysis. Data was said to be significantly different from the null hypothesis if $p<0.05$.

3. Analysis of Flrt3 localisation and activity using an over-expression system

3.1 Introduction

Flrt proteins have been shown to interact with Fgf receptor 1 (FgfR1), with Flrt1 being implicated in altering ERK phosphorylation, a downstream signalling output of FgfR1 [5, 41]. Over-expression of Flrt1 in HEK-293T cells and stimulation with Fgf-2 results in a rapid and robust increase of phosphorylated ERK (pERK), which is used as a measure of ERK activation and Fgf receptor signalling. Upon induction with Fgf2, increased levels of pERK are measured within 1 min, peaking at an approximate 2-fold induction after 10 min and remain increased after 30 min. Mechanistic studies on the Flrt1 protein have shown that three tyrosine residues (predicted to be Y^{600}, Y^{633} and Y^{671}) in a conserved region of the intracellular domain of Flrt1 are phosphorylated by FgfR1 upon interaction. Mutation of the phosphorylated tyrosine residues results in elimination of Flrt1 tyrosine phosphorylation and constitutive ERK phosphorylation, which is dependent on FgfR activity, thus suggesting that the inability of FgfR1 to phosphorylate the mutated tyrosines results in constitutive FgfR activation [41]. To further understand Flrt-dependent regulation of Fgf signalling, an analysis of the effect of Flrt3 expression on FgfR signalling output was performed. Experiments were based on those carried out by Wheldon *et al.* (2010), in the aim to further elucidate if characteristics identified for Flrt1 over-expression are representative of the Flrt family.

3.2 Results

3.2.1 Localisation of over-expressed Flrt3 and FgfR1

Using tagged proteins, an interaction between Flrt3 and FgfR1 has been shown, with the interaction facilitated in part by the transmembrane and fibronectin domains on Flrt3 [5, 8]. These interactions have been shown using immunoprecipitation and BRET assays, both of which do not visually show the location of interacting proteins in cells. To determine the co-location of the FgfR1 and Flrt3 proteins, immunofluorescence experiments of cultured cells over-expressing Flrt3 and FgfR1 were performed (Figure 3.1).

A

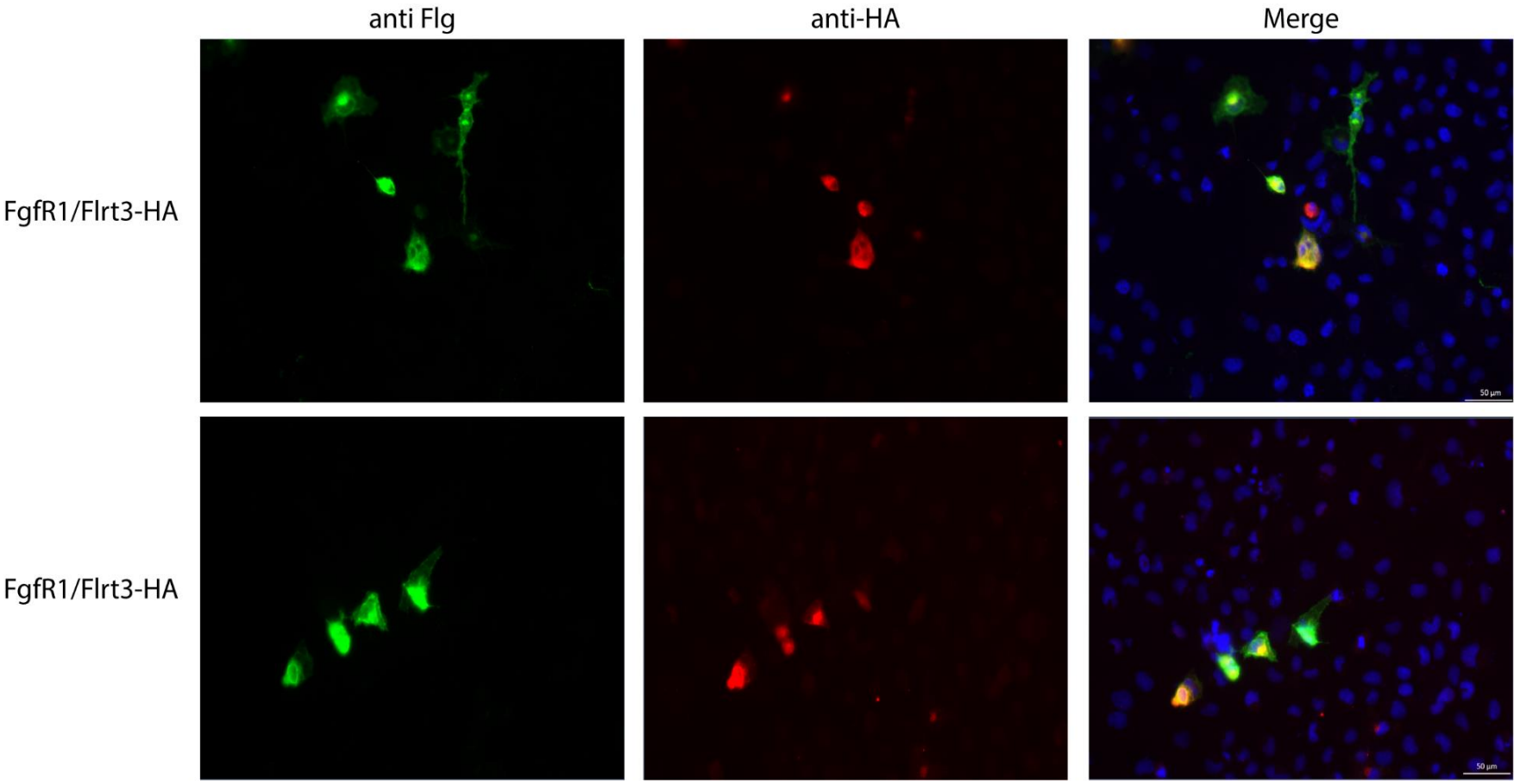
anti Flg
anti-HA
Merge
FgfR1/Flrt3-HA
FgfR1/Flrt3-HA
50 µm
50 µm

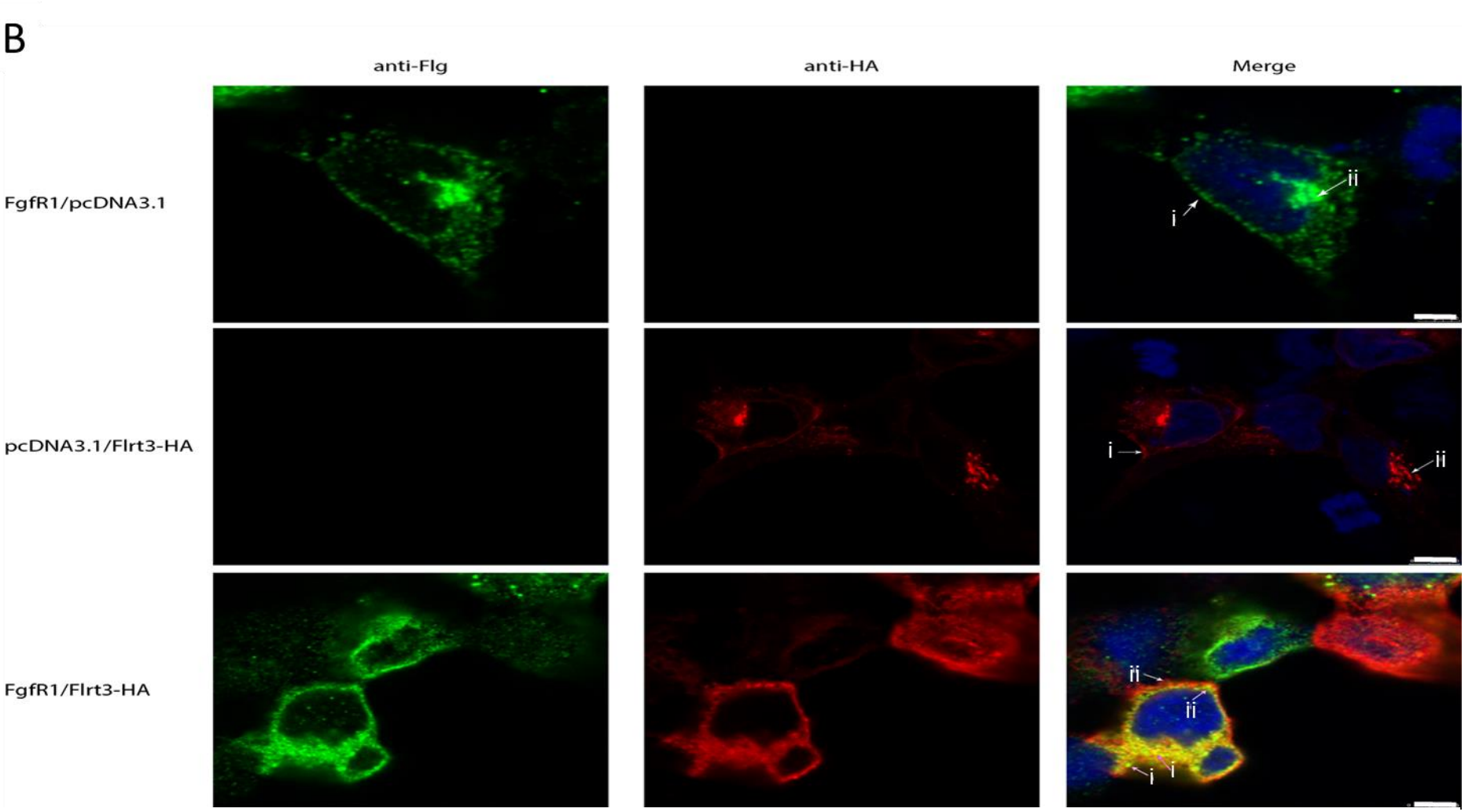

Figure 3.1. Flrt3-HA co-localises with FgfR1: Immunofluorescence images of Cos-7 cells transiently co-transfected with 3'HA-Flrt3 and FgfR1. Cells stained with anti-FgfR1 (green) and anti-HA (Flrt1, red). Merged images show co-localisation in yellow. Nuclei shown in blue (DAPI stain). A) Images taken with Zeiss deconvolution microscope. 20x magnification. Scale bars are 50 µm B) Images (in section) taken with Leica SP5 Spectral Scanning confocal microscope. 100x magnification. FgfR1/pcDNA3.1 (scale bar is 2.5 µm) and pcDNA3.1/Flrt3-HA (scale bar is 10 µm) samples used to show specificity of HA and Flg antibodies respectively. FgfR1/Flrt3-HA (scale bar is 5 µm). pcDNA3.1 is the empty vector control for FgfR1 and Flrt3-HA. Arrows labelled (i) indicate regions of non-overlapping expression of FgfR1 or Flrt3-HA, while (ii) indicates regions of overlapping expression.

Cos-7 cells were transfected with expression vectors encoding cDNAs from Flrt3 and Fgfr1. Transfections using the empty expression vector (pCDNA3.1) were used as controls for this experiment. When FgfR1 and pcDNA3.1 are co-transfected into cells (FgfR1/pcDNA3.1), they act as a negative control for the HA-antibody, which detects HA-tags. Analysis reveals that using the HA-antibody on these cells results in no detectible signal. This is expected as these cells are not expressing a protein containing a HA-tag. In the same way, when Flrt3 and pcDNA3.1 are co-transfected into cells (pcDNA3.1/Flrt3-HA), they act as a negative control for the Flg-antibody, which detects FgfR1. No signal is detected using the Flg-antibody on the cells as these cells are not expressing FgfR1 at high enough levels to be detected in the exposure time used. Use of the appropriate antibody to detect the over-expressed protein results in detectible signal for both transfection set-ups, acting as positive controls for the experiment. The results of these controls show the signals in the expected cells, validating the experiment.

When over-expressed alone (FgfR1/pcDNA3.1), FgfR1 localises within the cell membrane (Figure 3.1 FgfR1/pcDNA3.1 'i'), but is predominantly localised to structures in the cytoplasm reminiscent of intracellular vesicles (Figure 3.1 FgfR1/pcDNA3.1 'ii') consistent with previously described localisation of FgfR1 to these structures. High levels of expression are seen adjacent to the nucleus suggesting that over-expressed FgfR1 protein accumulates in the Golgi and endoplasmic reticulum due to high-level protein over-expression.

Expression of Flrt3 alone (pcDNA3.1/Flrt3-HA) reveals localisation at the cell surface membrane (Figure 3.1 pcDNA3.1/Flrt3-HA arrow 'i') and at intracellular membranes within the cytoplasm (Figure 3.1 pcDNA3.1/Flrt3-HA 'ii'). Cell surface expression was more extensive than that seen for FgfR1, observed as more staining at the "apparent" cell membrane (no membrane marker used, therefore an assumption is made as to the location of the cell membrane based on the staining pattern). Expression in the cell surface membrane appears concentrated in specific regions including, but not limited to, areas of the cell facilitating cell-cell contacts. Overall, cells expressing Flrt3 may occur in small clusters, although lone single cells expressing Flrt3 were also observed.

Co-expression of Flrt3 and FgfR1 (FgfR1/Flrt3-HA) showed overlapping domains (Figure 3.1 FgfR1/Flrt3-HA 'i') of co-expression as well as distinct domains of individual protein expression (Figure 3.1 FgfR1/Flrt3-HA 'ii') (Figure 3.1). Co-localisation of FgfR1 and Flrt3 exists mostly in the vesicles and membranes within the cytoplasm, adjacent to the nucleus. Some co-localisation between Flrt3 and Fgfr1 that occurs at the cell surface may be a result of re-localisation of FgfR1 to the cell surface by

interaction with Flrt3. Co-localisation does not occur only in the cytoplasm or only in the intracellular vesicle membranes, but is present in both of these membranes concurrently. Flrt3 expression is not co-localised with FgfR1 appears at the extremities of the cell at the cell surface.

Flrt3 and FgfR1 have been previously shown to interact by immunoprecipitation and have now been shown they co-localise in the same membranes within the cell, providing an *in vivo* context for the interaction [5]. Co-localisation of Flrt3 and Fgfr1 in intracellular membranes is similar to that observed for Flrt1 and Fgfr1 interaction [41]. Flrt3 and FgfR1 are co-localised in the same membranes of the cell, and with Flrt3 being shown to interact with FgfR1 by immunoprecipitation, an effect on FgfR1 signalling is possible [41]. Interestingly, it is thought that a lot of signalling from FgfR occurs within intracellular membranes and not at the cell surface [26]. Assignment of the specific membrane structures would provide valuable information on the identity of vesicles where interaction occurs and would require co-staining with appropriate markers for various membranes.

3.2.2 Effect of Flrt3 over-expression on FgfR1 signalling

Similar to Flrt1, the majority of Flrt3 interaction with FgfR1 co-localisation occurs within intracellular vesicles, which positions Flrt3 in the correct location to be able to influence the output of FgfR1. Wheldon *et al.* (2010) showed that over-expression of Flrt1 caused a subtle but consistent change in ERK phosphorylation, a measure of FgfR1 signalling via the MAPK pathway output, when analysed using a time course of Fgf-2 stimulation [41]. A change in FgfR1 signalling due to the expression of Flrt3 and the mechanism associated with the interaction can be assessed in a similar manner. By transiently co-transfecting HEK-293T cells with Flrt3-HA and FgfR1 and stimulating the cells with Fgf-2, FgfR1 signalling was evaluated by measuring pERK levels by Western blot (Figure 3.2).

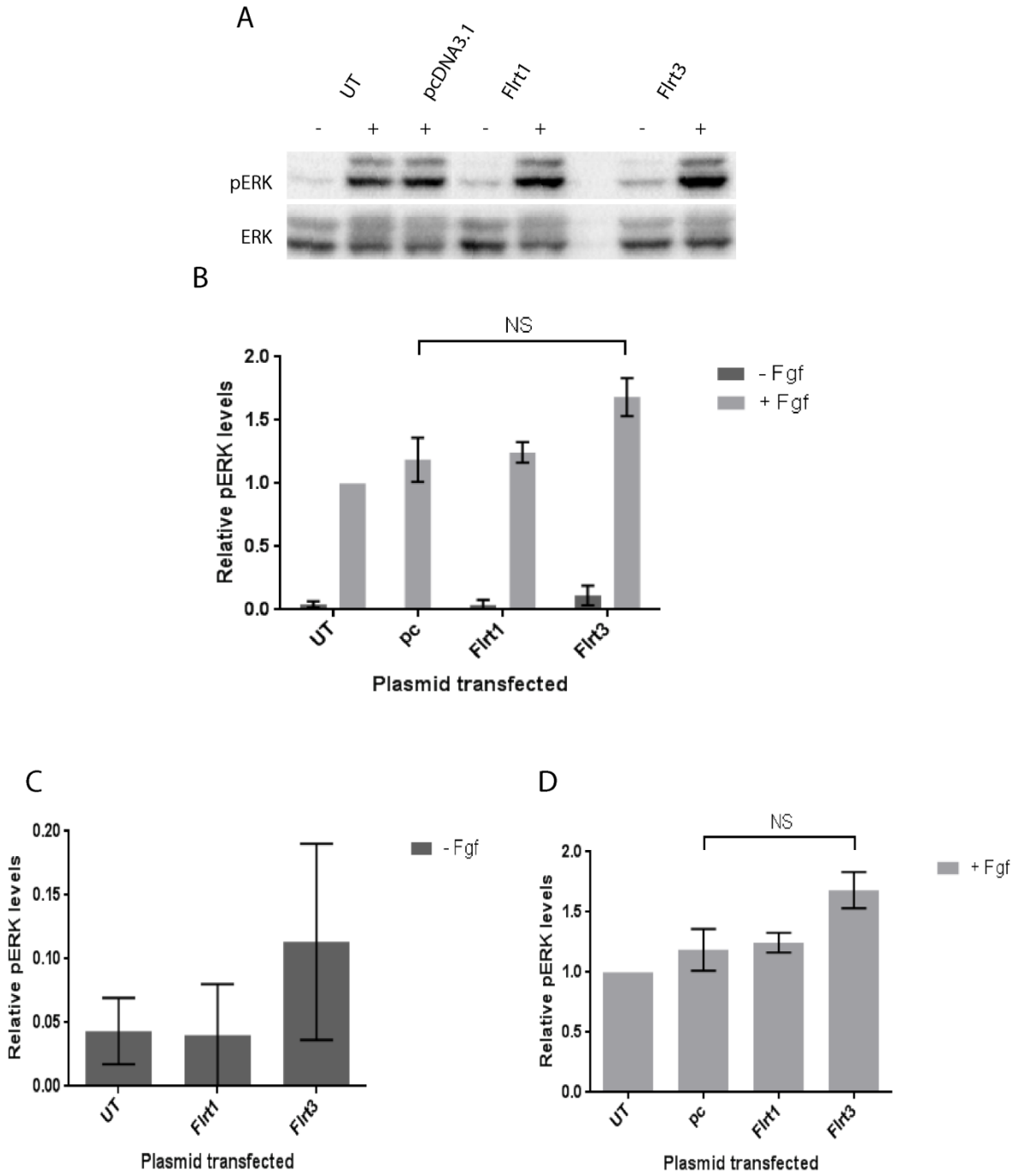

Figure 3.2. Over-expression of Flrt3 produces a trend towards increased pERK levels: Western blot of HEK-293T cells transiently transfected with indicated plasmids (UT = untransfected cells, pc and pcDNA3.1 = pcDNA3.1 transfected cells (vector only control)) for 20 h, then stimulated with Fgf-2 and heparin for 10 min. A) Western blot probed with anti-pERK and anti-ERK (for pERK normalisation). + = with Fgf-2 and heparin stimulation, - = without Fgf-2 and heparin stimulation. Representative of 3 independent experiments. B) Normalised quantification of pERK levels (normalised to total ERK levels using densitometric analysis) between unstimulated and Fgf-2 stimulated cells relative to untransfected Fgf-2 stimulated cells. C) Quantification of pERK levels in unstimulated cells. D) Quantification of pERK in Fgf-2 stimulated cells. Data for (C) and (D) is drawn from (B). Error bars are S.E.M, n=3, Student's t-test performed to determine significant difference of results, NS = no significant difference ($p>0.05$).

Basal levels of ERK phosphorylation (pERK) are observed in untransfected, unstimulated cells (Figure 3.3A, UT -) which are significantly increased (23.25-fold) upon stimulation with Fgf-2 (Figure

3.2A, UT +), showing that Fgf-2 stimulation is inducing FgfR activation and subsequent ERK phosphorylation (based on Student's t-test, $p<0.05$). In this experiment, untransfected (UT) and pcDNA3.1-transfected cells (pc) are used as controls for basal pERK levels when unstimulated and for Fgf-2 stimulation as pERK levels rise upon stimulation. The stimulated pcDNA3.1-transfected cells show no difference in pERK levels upon showing transfection and expression vector alone does not drastically alter ERK phosphorylation.

Cells transfected with Flrt1 show no significant difference in ERK phosphorylation when compared to untransfected cells or cells transfected with empty expression vector pcDNA3.1 (pc) ($p>0.05$), whether unstimulated or stimulated with Fgf-2 (Figure 3.2). This is consistent with previous data for over-expression of Flrt1 at this time point [41]. Unstimulated cells over-expressing Flrt3 (Flrt3 -) showed a 2.63-fold increase in the average level of ERK phosphorylation levels compared to empty vector (Figure 3.2). However, this is not significant due to the large degree of variability in the data. Flrt3 over-expressing cells stimulated with Fgf-2 for 10 min also showed a 1.41-fold increase in the amount of phosphorylated ERK (Figure 3.2, Flrt3) when compared to cells transfected with empty vector. However, again this data was not-significant using a Student's t-test ($p>0.05$).

The results show pERK levels increase upon over-expression of Flrt3 and Fgf-2 stimulation of cells. However, this increase is not significant ($p>0.05$). It also showed that Flrt3 over-expression in non-Fgf-2 stimulated cells resulted in a slightly elevated level of pERK activity, albeit statistically insignificant at a 95% confidence interval due to variability in the assay. Despite the lack of significance, in both the stimulated and unstimulated case Flrt3 exhibited a trend towards increased ERK phosphorylation.

While Flrt3 does not show a significant increase in FgfR1 activity via the MAPK pathway, independent of Fgf-2 stimulation, a trend exists for an increase in pERK levels due to the over-expression of Flrt3, possibly caused by the interaction with FgfR1. To determine that the increase in ERK phosphorylation identified in cells over-expressing Flrt3 is dependent on activation of the Fgf receptor, the Fgf receptor inhibitor SU5402 was utilised. Flrt3 or empty vector (pcDNA3.1) transiently transfected HEK-293T cells were serum-starved for 60 min with SU5402 (50 μM) where indicated. Cells were then stimulated with Fgf-2 for 10 min and cell lysates analysed for levels of pERK by Western blot (Figure 3.3).

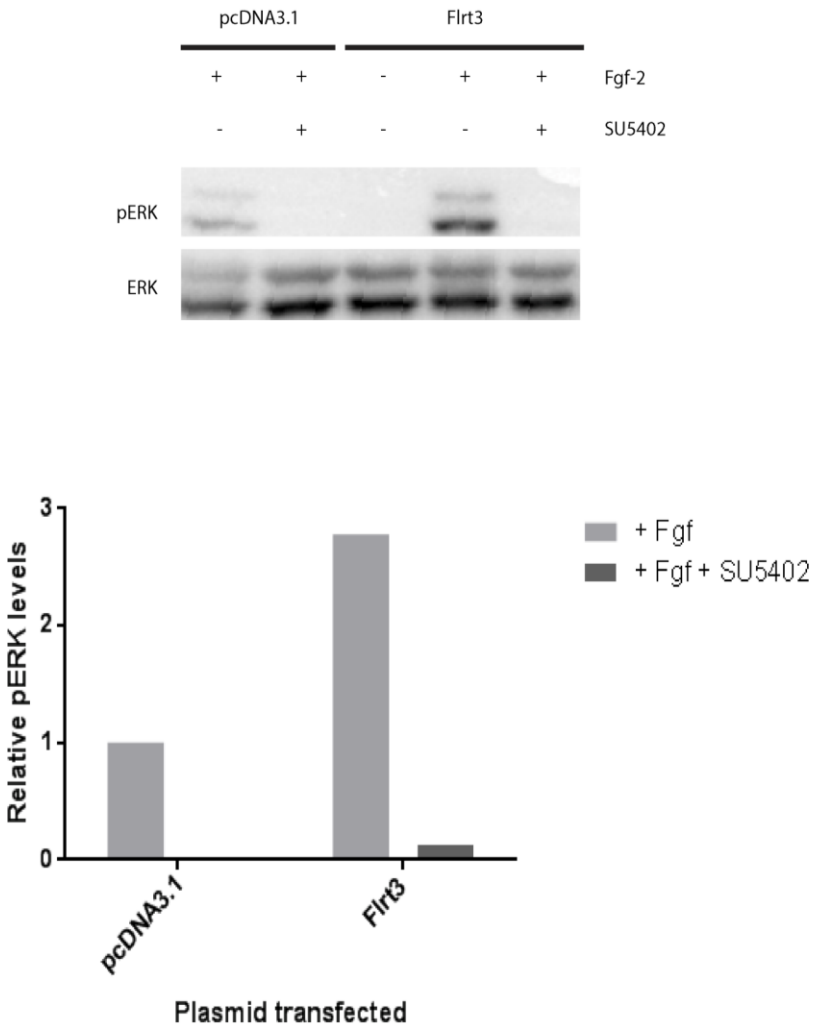

Figure 3.3. Increased pERK levels caused by Flrt3 over-expression require FgfR activity: Western blot of HEK-293T cells transiently co-transfected with FgfR1 and pcDNA3.1 (vector only control) or Flrt3 for 20 h, then stimulated with Fgf-2 and heparin for 10 min. Appropriate samples were incubated with 50 μM SU5402 during Fgf-2 stimulation. Blot probed with anti-pERK and anti-ERK (for pERK normalisation). Bar graph represents the normalised quantification of pERK levels between Fgf-2 stimulated cells with and without SU5402 treatment relative to untransfected Fgf-2 stimulated cells without SU5402 treatment (normalised to total ERK levels using densitometric analysis). n=1.

Fgf-2 stimulation of pcDNA3.1-transfected cells (pcDNA3.1 + -) results in activation of Fgf receptor and subsequent ERK phosphorylation (Figure 3.3). The inclusion of SU5402 in Fgf-2 stimulated pcDNA3.1-transfected cells (pcDNA3.1 + +) results in complete absence of pERK, showing the effectiveness of the inhibitor in blocking activation of the FgfR1 signalling, and consequently the MAPK pathway. As previously shown, stimulation of Flrt3 (Flrt3 + -) over-expressing cells with Fgf-2 results in a higher level of pERK than stimulation of pcDNA3.1-transfected cells. In this case, the level of pERK is slightly higher (2.78-fold increase) than previously shown (1.41-fold increase) for Flrt3 over-expressing cells in comparison to pcDNA3.1-transfected cells. When Flrt3 over-expressing Fgf-2 stimulated cells are incubated with 50 μM SU5402 (Flrt3 + +), the levels of pERK are essentially eliminated.

This data shows that the trend identified in our previous experiments of an increase in pERK levels in cells over-expressing Flrt3 is due to increased activity of the Fgf receptor, and not through an Fgf receptor independent mechanism. Therefore, if this trend is real, increased activity of the FgfR1 is responsible for the increase in pERK levels in Flrt3 over-expressing cells, with the interaction between Flrt3 and FgfR1 the likely mechanism.

3.2.3 Investigation of Flrt3 tyrosine phosphorylation

Increased levels of pERK seen upon over-expression of Flrt1 and Flrt3 are dependent on the activation of the Fgf receptor tyrosine kinase domain ([41] and Figure 3.3). Using NetPhos 2.0 to predict tyrosine phosphorylation sites, Wheldon, *et al.* (2010) proposed that three tyrosine residues on the intracellular tail of Flrt1 were highly likely to be phosphorylated upon activation of FgfR1 activity. Analysis of tyrosine phosphorylation using a phosphotyrosine specific antibody identified tyrosine phosphorylation of Flrt1 and subsequent mutation of the three tyrosines to phenylalanine caused a loss of this phosphorylation [41] (Chapter 1, Figure 26). In this study, it was predicted that the intracellular domain of Flrt3 may also undergo tyrosine phosphorylation. Tyrosine residues within the intracellular domain that have a strong consensus sequence for tyrosine phosphorylation were identified using the NetPhos 2.0 prediction algorithm (http://www.cbs.dtu.dk/services/NetPhos/) (Figure 3.4).

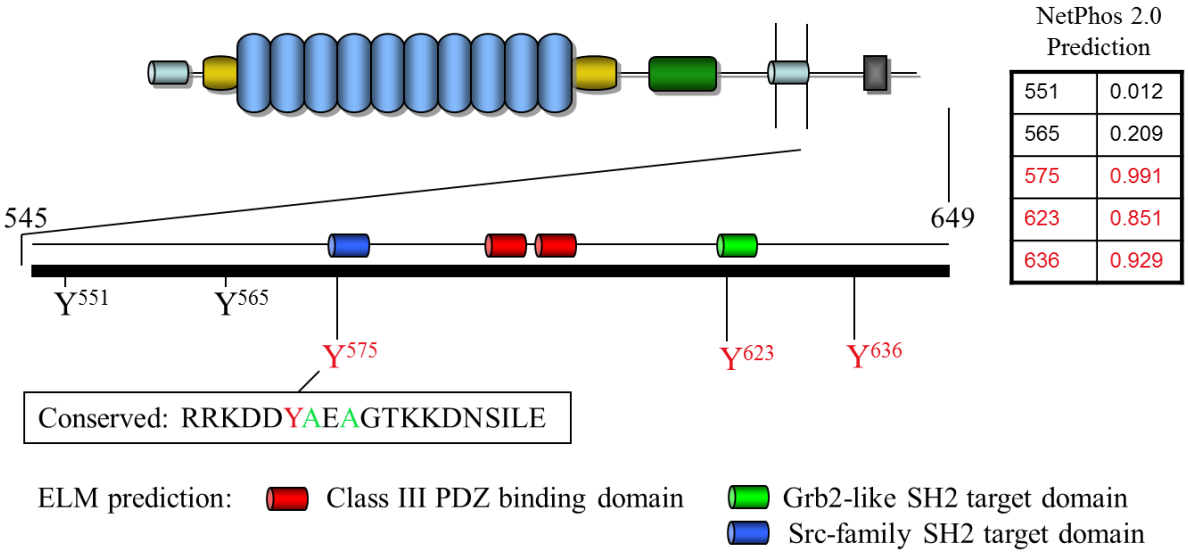

Figure 3.4. Predicted sites of tyrosine phosphorylation in the intracellular domain of Flrt3: Using the NetPhos2.0 server, tyrosine residues 575, 623 and 636 (red text) of Flrt3 were identified as being the most likely to be phosphorylated [43].

Out of the 5 Flrt3 intracellular tyrosine residues, 3 were identified as being highly likely to be phosphorylated (Figure 3.4). A sequence conserved between all Flrt members contains a single tyrosine

residue, Y^{575}, which is the most likely of the three residues in the intracellular domain of Flrt3 to be phosphorylated (99.1% likelihood). The remaining two tyrosines are found further towards the C-terminal of Flrt3, Y^{623} and Y^{636} (85.1% and 92.9% likelihood of phosphorylation respectively). Using co-transfection of HA-tagged Flrt proteins and FgfR1 with immunoprecipitation of HA-tagged proteins, tyrosine phosphorylation of Flrt3 in response to Fgf-2 stimulation was investigated (Figure 3.5).

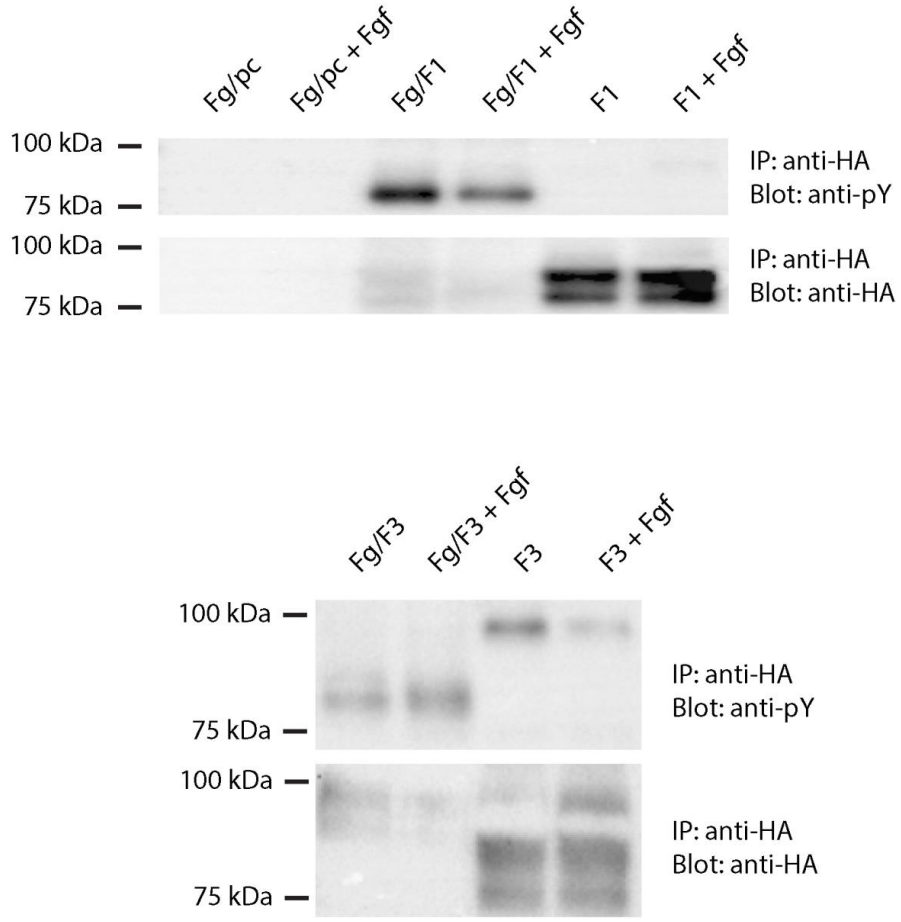

Figure 3.5. Flrt proteins contain phosphorylated tyrosines: Western blot of HEK-293T cells transiently co-transfected with indicated plasmids (Fg = FgfR1, pc = pcDNA3.1 (vector control), F1 = Flrt1-HA, F3 = Flrt3-HA) for 20 h, then appropriately stimulated with Fgf-2 and heparin (+ Fgf) for 10 min. Resulting WCL underwent immunoprecipitation for HA-tagged proteins. Blot probed with anti-pY and anti-HA (control for success of immunoprecipitation). n=2.

Immunoprecipitation of samples transfected with FgfR1 and pcDNA3.1 (Fg/pc and Fg/pc + Fgf) showed no bands when probed for phosphorylated tyrosine or for the HA tag, as expected (Figure 3.5) as no HA tagged proteins are present in these samples, showing the HA antibody showed no non-specific precipitation. Wheldon *et al.* (2010) have previously shown by immunoprecipitation that Flrt1 is phosphorylated when co-expressed with FgfR1 which we used as a positive control [41]. Cells transfected with FgfR1 and Flrt1 (Fg/F1 and Fg/F1 + Fgf) and immunoprecipitated with HA-antibody, independent of Fgf-2 stimulation, show phosphorylation of tyrosine residues, with a single band in each lane at approximately 75 kDa. When probed for HA, two bands are seen; one at approximately 75 kDa,

and the other at approximately 92 kDa, showing that the immunoprecipitation of HA-tagged proteins occurred. Over-expression of Flrt1 alone (F1 and F1 + Fgf) results in no Flrt1 tyrosine phosphorylation. Flrt1 expression results in two bands at approximately 75 kDa and 92 kDa when probed for HA. This blot shows lower levels of HA-tagged protein in Fgf-2 stimulated samples, indicating that either transcription or translation of Flrt1 was lower, or the immunoprecipitation did not occur as effectively as the unstimulated sample. These results show that Flrt1 is phosphorylated when over-expressed with Fgfr1 in this experiment.

Co-expression of Flrt3 and FgfR1 (Fg/F3) results in phosphorylated tyrosine on an 80 kDa and 85 kDa species of Flrt3. Fgf-2 stimulation (Fg/F3 + Fgf) results in a single band at approximately 80 kDa. Interestingly, the associated HA-probed blot shows expression of 1 species of Flrt3 of approximately 100 kDa in size, suggesting that the form of Flrt3 that is phosphorylated is a minor component of the Flrt3 present in the lysate. When over-expressed alone (F3 and F3 + Fgf), a 100 kDa tyrosine phosphorylated species of Flrt3 exists, with stronger tyrosine phosphorylation present in unstimulated samples. Multiple forms of Flrt3 are being expressed in the cell, demonstrated by the bands present at approximately 75 kDa, 87 kDa and 100 kDa in the HA-blot. Levels of different species are expressed the same between F3 and F3 + Fgf with the exception of the 100 kDa species, which shows higher expression with Fgf-2 stimulation. Similar to experiments with Flrt1, the overall levels of Flrt3 present in immunoprecipitations where Flrt3 and Fffr1 are over-expressed, compared to Flrt3 alone are reduced.

Similar to Flrt1, Flrt3 contains tyrosines that become phosphorylated. This phosphorylation occurs independently of Fgf-2 stimulation. Interestingly, different forms of Flrt3 appear to have tyrosine phosphorylation depending on the co-expression of FgfR1. With FgfR1 co-expression, a 75 kDa species of Flrt3 is tyrosine phosphorylated, yet does not appear when probed for HA so is likely to be present at low levels. Co-expression of FgfR1 also results in expression of differing amounts and species of Flrt3 protein.

3.2.4 Role of Flrt3 domains in increased FgfR1 activity

In this study, over-expression of Flrt3 appears to result in a 1.41-fold increase in ERK phosphorylation due to increased FgfR1 activity (Figure 3.2) that is likely mediated by the interaction of Flrt3 and FgfR. The interaction between Flrts and FgfR has been postulated to be mediated by the fibronectin domain, but a Flrt1 molecule can interact with a FgfR without an extracellular domain (L.

Wheldon, pers. comm.), but the kinetics of these interactions have not been elucidated [8]. The investigation of Flrt3 mutants is a good method to identify a specific motif that is common amongst the Flrt family that may mediate FgfR interaction and cause an increase in FgfR signalling.

To examine the domains of Flrt3 involved in ERK activation a number of mutations of Flrt3 were constructed. Mutations were generally a loss of a domain, but also included individual amino acid mutations. Mutated Flrt3 constructs include Flrt3 without the intracellular domain (F3-IC), Flrt3 without the LRR domains (F3-LR), Flrt3 without the fibronectin domain (F3-FN), Flrt3 without the LRR and fibronectin domains (F3-LRFN), Flrt3 without an intracellular microtubule binding domain (F3-KKD), and Flrt3 with the intracellular tyrosine residues predicted to be phosphorylated (F3-3YF) (as described in Figure 3.4). The effect of these Flrt3 mutations on pERK levels was assessed. HEK-293T cells were transiently transfected with FgfR1 and appropriate Flrt3 mutant expression plasmid, followed by Fgf-2 stimulation and analysis of cell lysates by Western blot for pERK (Figure 3.6).

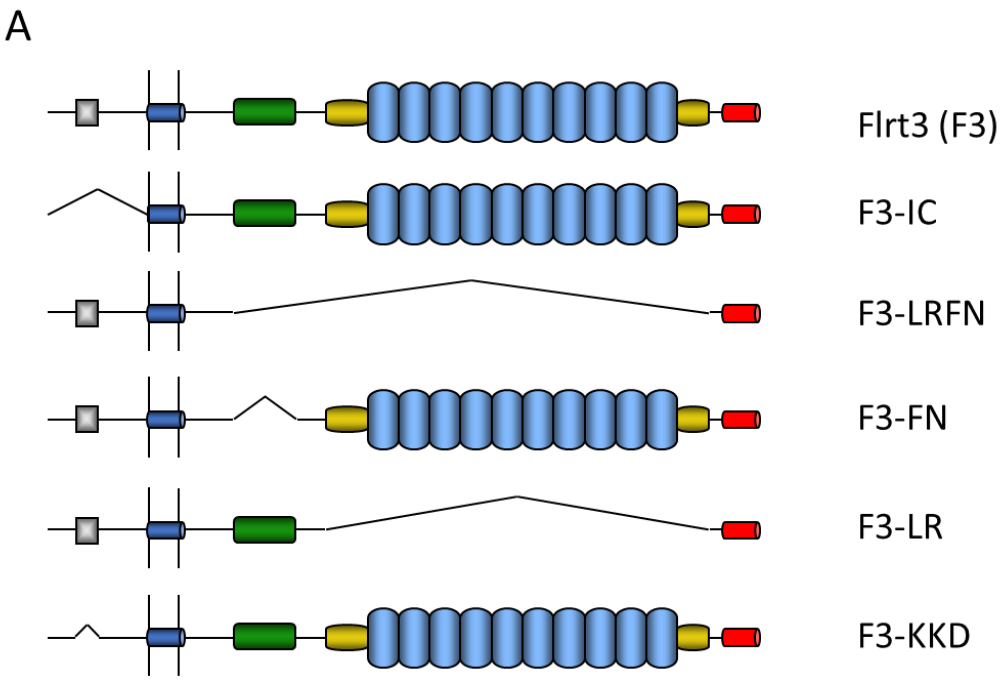

B

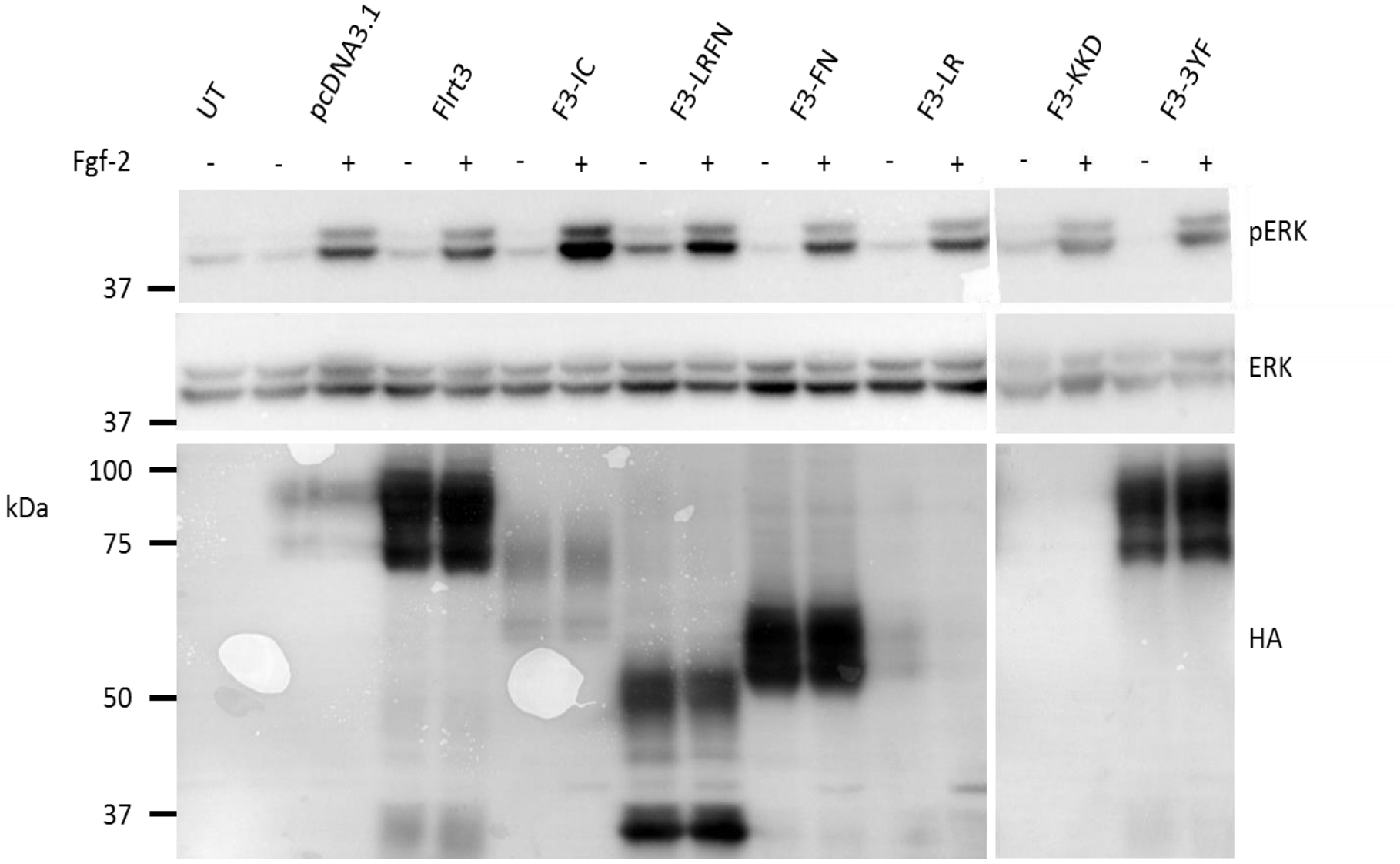
UT
pcDNA3.1
Flrt3
F3-IC
F3-LRFN
F3-FN
F3-LR
F3-KKD
F3-3YF
Fgf-2
- - + - + - + - + - + - + - + - +
pERK
ERK
HA
kDa
100
75
50
37
37
37

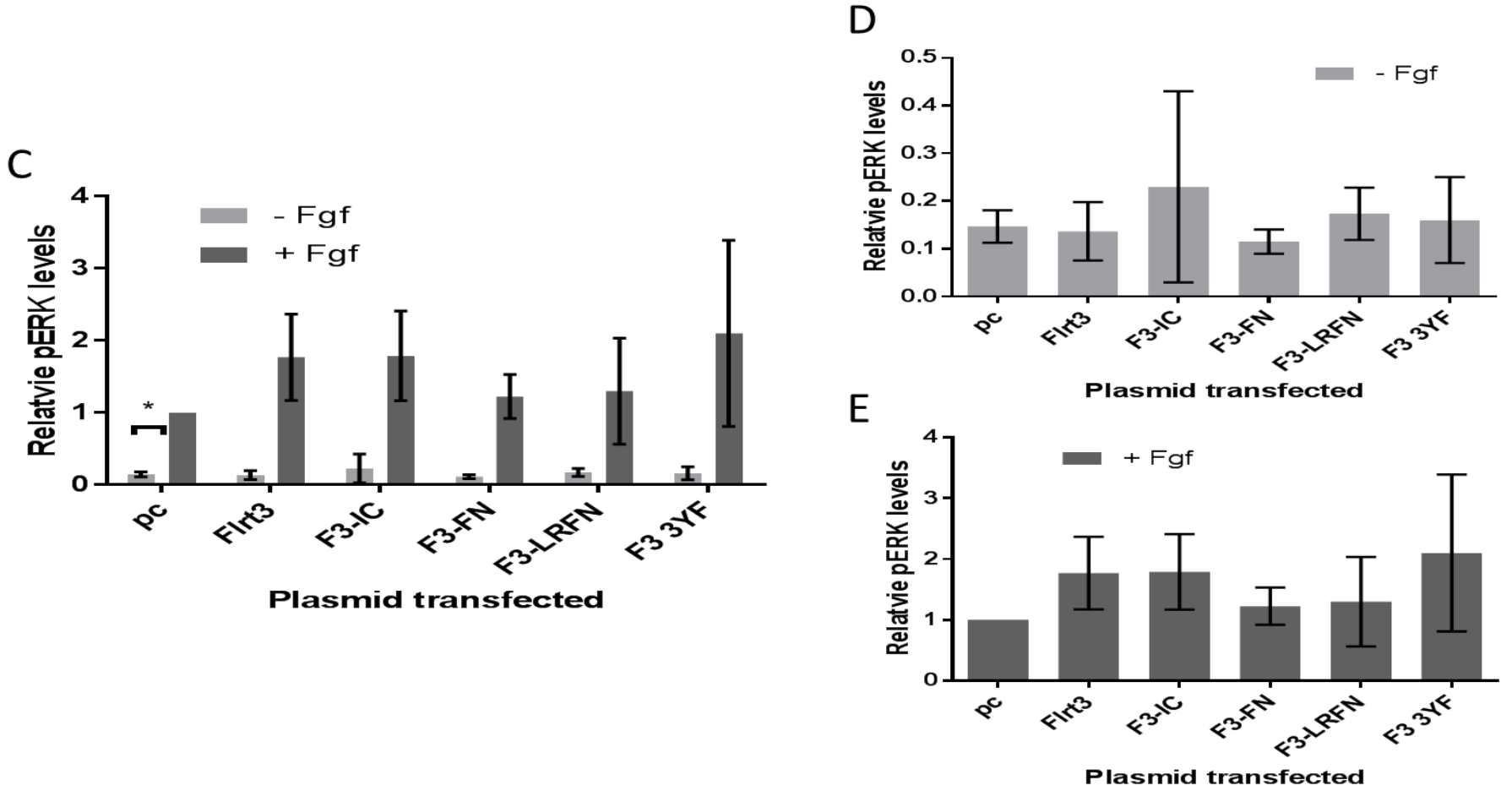

Figure 3.6. Over-expression of selected Flrt3 mutations causes no change in pERK levels: Western blot of HEK-293T cells transiently co-transfected with FgfR1 and indicated plasmids (pc = pcDNA3.1 (vector only control), F3-IC = Flrt3 intracellular domain only, F3-LR = Flrt3 LRR domain only, F3-FN = Flrt3 fibronectin domain only, F3-LRFN = Flrt3 LRR domain and fibronectin domain as encoded by ORF, F3-KKD = Flrt3 without intracellular microtubule binding domain, F3-3YF = Flrt3 with the 3 tyrosines identified as potentially phosphorylated mutated to phenylalanine) for 20 h, then stimulated with Fgf-2 and heparin (+) for 10 min or were left unstimulated. A) Schematic representation of Flrt3 mutants assessed B) Western blot probed with anti-pERK, anti-ERK (for pERK densitometric normalisation), and anti-HA (to show HA-tagged protein expression). C) Normalised quantification of pERK levels between unstimulated and Fgf-2 stimulated cells relative to pcDNA3.1+ transfected Fgf-2 stimulated cells. D) Quantification of pERK levels in unstimulated cells. E) Quantification of pERK in Fgf-2 stimulated cells. Error bars are S.E.M, n=3. Statistics analysed using Student's t-test, *=p<0.05.

Lysates from cells transfected with HA tagged mutant Flrt3 constructs were assessed for protein expression by Western blot that showed all the constructs transfected are being expressed (Figure 3.6 B) except F3-LR and F3-KKD. Therefore results with these constructs must be excluded the analysis. All Flrt3 mutant proteins were expressed at different levels compared to each other (Figure 3.6 B). Flrt3, F3-FN and F3-3YF are expressed at similar levels, with the remaining Flrt3 mutant proteins expressed at lower levels. Multiple bands appear in all Flrt3 mutant and Flrt3 samples, indicating different sized species. Bands present in the pcDNA3.1 sample are at the same size as the bands in the adjoining Flrt3 lane. The band in the pcDNA3.1 sample was due to over-loading of the Flrt3-Fgf over-expressing sample. No bands appear in the untransfected cell lysates (Figure 3.6 B). pcDNA3.1 transfected cells show the background levels of pERK caused by the transfection of the empty vector and pERK levels rise with stimulation of these cells with Fgf-2 as expected allowing any change in pERK levels to be attributed to the expression of mutant Flrt3 proteins ($p<0.05$).

Unstimulated cells over-expressing all Flrt3 mutants show no statistically significant difference in pERK levels (Figure 3.6 B, C and D) compared to Flrt3 transfected cells ($p>0.05$). Levels of pERK in Flrt3 over-expressing cells showed a non-significant trend towards higher levels of pERK when compared to cells transfected with expression vector alone, as previously observed. The levels of pERK show a non-significant change in cells transfected with all mutant Flrt3 constructs when stimulated with Fgf-2 (Figure 3.6 B and C) ($p>0.05$).

The trend towards an increase in pERK with over-expression with Flrt3 was repeated in this assay but is again not significant. Alteration of the domains within the Flrt3 coding sequence gave no significant, repeatable changes in ERK phosphorylation when over-expressed in cells. Therefore, we were unable to identify any Flrt3 mutants that affect FgfR1 activity or ERK phosphorylation in any way.

3.3 Discussion

Previous studies have shown that Flrt1 can interact with FgfR1, co-localise with FgfR1 in intracellular vesicles, and influence the phosphorylation of ERK, the output of FgfR1 [5, 41]. In this chapter, the characteristics of Flrt3 and its influence on FgfR1 signalling were assessed. These experiments were carried out to determine if the effects of Flrt3 over-expression on FgfR1 signalling were similar to those of Flrt1. Immunolocalisation of over-expressed Flrt3 and FgfR1 determined that overlap existed, providing the first evidence of cellular co-localisation of these proteins (Figure 3.1).

These results draw similarities with Flrt1 and FgfR1 which showed overlapping expression patterns [41]. Flrt3 shows a similar expression pattern to Flrt1, with localisation of the protein shared between intracellular membranes and the cell surface membrane. Localisation of the proteins when not over-lapping is also consistent between studies [41]. Transfection of Flrt3 and FgfR1 proteins resulted in localisation to intracellular membrane structures such as the rough ER and/or Golgi body and intracellular vesicles. Accumulation in the rough ER and/or Golgi is likely to be due to the large levels of over-expression. The co-localisation assay results suggest that Flrt3 and FgfR1 are co-localised to a number of different undefined cellular membranes (Figure 3.1). It is important to note that Flrt3 co-localisation in these over-expression assays is similar to that of Flrt1, which was subsequently shown to co-localise with endogenously expressed FgfR1 and Fgf signalling components, and influence FgfR1 output [41].

Over-expression of Flrt1 in HEK-293T cells results in a subtle increase in pERK levels as a result of FgfR1 activation, with a more rapid increase of pERK after just 1 min that is sustained at a higher level for at least 30 min [41]. To analyse the effect of Flrt3 over-expression on pERK levels we attempted to repeat this analysis with Flrt3. We had multiple difficulties with these assays, including large levels of variability between experiments, which meant we had difficulty in verifying previous experiments to then extrapolate this to our new data for Flrt3. However, we obtained some repeatable results with our initial experiments which were performed with Flrt over-expressing cells stimulated for 10 min. Surprisingly, this experiment resulted in no increase in FgfR1 activation in Fgf-2 stimulated, Flrt1 over-expressing cells, which is in contrast to previous data despite all efforts made to replicate experimental conditions [41]. It was also noted that the constitutive activation of pERK seen in cells transfected with a mutant version of Flrt1 that was unable to be phosphorylate on tyrosines was also absent in our assays [41]. There could be multiple reasons why Flrt1 may not activate pERK in our assays, including differences in cell lines, culture conditions or different batches of reagents used which may have altered the response to Flrt1 over-expression. The 23.26-fold increase in pERK levels in untransfected cells upon Fgf-2 stimulation indicates that activation of Fgf receptors is occurring as expected in our cells, and it is clear to see that the stimulation is also successful in the Flrt1 and Flrt3 over-expressing samples due to the large increase in pERK levels (Figure 3.2 A + B).

Flrt3 over-expressing cells showed an average 1.41-fold increase in pERK levels after 10 minutes stimulation (Figure 3.2 A + B + D) that was consistent over 3 experiments, but statistical analysis showed was not significant using a Student's t- test. The consistency of this increase suggested that with further repeats of this experiment we may have obtained a significant increase. This

increase in pERK may also be larger at a different time-point, making the increase in FgfR1 activation statistically significant. Furthermore, in unstimulated cells we saw a trend towards increased pERK in cells over-expressing Flrt3 but this was not significant due to the low levels of pERK present and the associated large errors involved. It is interesting to note in stimulated and unstimulated cells that pERK levels in Flrt3 over-expressing samples show an increasing trend in pERK levels compared to Flrt1 over-expressing cells (Figure 3.2) suggesting Flrt3 may be more influential in FgfR activation than Flrt1. No difference in pERK levels between pcDNA3.1 and Flrt1 over-expressing cells exists, which is not consistent with published data [41]. This further suggests that the loss of Flrt1-related significance may be a difference in our cells or the experimental system.

Despite the lack of significance in the above experiments we were confident that Flrt3 was causing an increase in the output of FgfR through increased phosphorylation of ERK in our HEK-293T cells. Although pERK is a signalling molecule for many different receptors, the increase in pERK levels observed in Flrt3 over-expressing samples was attributed predominantly to activation of the Fgf receptors (Figure 3.3). The Fgf receptor inhibitor was effective in blocking Fgf receptor activation, with levels of pERK in Fgf-2 stimulated, SU5402 treated cells being only slightly higher than the level of unstimulated cells. When Flrt3 over-expressing cells are stimulated with Fgf-2 in the presence of the inhibitor, pERK levels are almost abolished, suggesting the increase in pERK levels is due to the influence that Flrt3 has on the activation of the Fgf receptor and not a result of activation of some other signalling receptor or cascade. Combined, this data suggests that Flrt3 over-expression results in increased stimulated FgfR activation compared to non-Flrt3 over-expressing and Flrt1 over-expressing cells.

Based on studies of Flrt1, we predicted that Flrt3 may be phosphorylated on tyrosine residues within its intracellular tail and that Y^{575}, Y^{623} and Y^{636} are the most likely candidates for phosphorylation upon Fgf receptor activation (Figure 3.4). As previously mentioned, Y^{575} is within a region of conserved sequence across the Flrt family, with the corresponding tyrosine in Flrt 1, Y^{600}, being shown to be phosphorylated, hinting to a potentially important role in Flrt function as a FgfR1 regulator [41]. Using immunoprecipitation and Western blotting with anti phospho-tyrosine antibody Flrt3 was shown to contain phosphorylated tyrosine residues, with the absence of a signal from FgfR1 and pcDNA3.1 transfected cells indicating that any signal produced in the phospho-tyrosine (pY) blot for the Flrt over-expressing samples is due to phosphorylation of tyrosines on the HA-tagged Flrt proteins, and not from FgfR1 phosphorylated tyrosines. Tyrosine phosphorylation of Flrt1 when co-expressed with FgfR1 is evident, similar to the result obtained by Wheldon *et al.* (2010) [41]. Flrt3 shows robust tyrosine

phosphorylation when over-expressed with FgfR1 with a species of approximately 80-85kDa observed. Interestingly, when the experiment is performed without over-expression of FgfR1, an approximately 100 kDa species of Flrt3 showed tyrosine phosphorylation when over-expressed (Figure 3.5). This is the largest of the 3 species of Flrt3 to be immunoprecipitated, indicating different post-translationally modifications forms of Flrt3 are tyrosine phosphorylated in these two situations. The most obvious explanation of this is that the interaction between over-expressed FgfR1 and Flrt3 protein retains and phosphorylates more Flrt3 within the endoplasmic reticulum/Golgi where it contains less post-translational modifications. We observe the retention of Flrt3 adjacent to the nucleus when we over-express it with FgfR1 in Cos-7 cells compared to expression of Flrt3 alone, which shows more localisation to the cell surface. The expression of multiple forms of Flrt3 when over-expressed alone (seen by the HA blot), yet the presence of only the largest form having phosphorylated tyrosines suggests that the smaller forms may be restricted to the Golgi or endoplasmic reticulum (ER) due to large over-expression. Without over-expression of FgfR1, tyrosine phosphorylation cannot occur in the Golgi or ER, and therefore only the largest species is observed in the pY blot, presumably phosphorylated by endogenous proteins outside of the Golgi /ER. In the HA-blot of Flrt3 and FgfR1 over-expressing cells two species of Flrt3 protein are observed; an approximately 100 kDa and an approximately 92 kDa Flrt3 species, and not the smaller species visualised in the pY blot suggesting the phosphorylated Flrt3 is a minority component of all cellular Flrt3. These results show that Flrt3 is tyrosine phosphorylated and that this phosphorylation can be altered by its co-over-expression with FgfR1, similar to that of Flrt1.

In our assay, we demonstrated that Flrt3 showed a consistent trend of increased FgfR1 activation (Figure 3.2). This, combined with our demonstrated phosphorylation of Flrt3 and the role that the phosphorylated tyrosines of Flrt1 had on FgfR1 activation (Wheldon *et al.* (2010)) lead us to believe we could use this assay to analyse the importance of the different domains within the Flrt3 protein within its role in FgfR1 signalling regulation [41]. No significant changes in FgfR1 activity were detected. As previously seen, cells over-expressing Flrt3 that are stimulated with Fgf-2 result in higher levels of FgfR1 activity than those not over-expressing Flrt3. This has been observed consistently over 3 different assays, meaning there is support that there is a small, but real difference in pERK levels due to Flrt3 over-expression. It was surprising that with the combination of mutated sequence tested no significant change in FgfR1 activity was seen in any of these assays. This could be due to all the constructs possessing a transmembrane domain, which is the vital feature for FgfR1 interaction (L. Wheldon, pers. comm.) therefore interaction could still occur [8]. Another explanation could be that over-expression of

the constructs affects intracellular signalling pathways that interfere with correct signalling pathway function such that it may not be the best method to investigate this phenomena.

3.4 Conclusion

From our experiments, we have confirmed that Flrt3 can act in a similar way to Flrt1 by interacting and localising with FgfR1 and being phosphorylated by FgfR1 on tyrosine residues within its intracellular domain. Over-expression experiments using the HEK-293T cell line with transient transfection of appropriate expression vectors has been previously used to analyse Flrt1 dependent alteration of Fgf signalling. This system over-expressing Flrt3 protein within HEK-293T cells to analyse the output of Fgf receptor signalling using pERK was problematic in our hands. This system showed a consistent trend with Flrt3 over-expression of increasing pERK levels, with or without Fgf-2 stimulation, that was however not significant. This was attributed to the activity of FgfR1. This increase was observed despite our positive controls with Flrt1 not showing increased FgfR signalling as in previous studies, suggesting our assay system was not acting as previously reported. While the data gathered here infers a role for Flrt3 in regulating FgfR signalling our investigations suggest that this high-level over-expression system may not be the best system available for analysis of Flrt regulation of Fgf signalling. This could be overcome with the discovery of a cell system to study endogenous Flrt3 expression and function. The discovery of a cell system would also allow investigation of the role of endogenous Flrt3 in the regulation of pERK levels due to interaction with FgfR1 and provide more developmentally relevant data, which will be the focus of Chapter 4.

4. P19 EC cell line: A cell model for studying endogenous *Flrt3* function in neural differentiation.

4.1 Introduction

Chapter 3 has provided some functional insight into the role of Flrt3 in an over-expression context. However, the relevance of this functional data to an *in vivo* setting is uncertain due to the high levels of protein expression when compared to the levels of endogenous Flrt3 expression. This can result in localisation and activity that is not a true representation of the protein in an endogenous *in vivo* context. A common method of studying *in vivo* protein function is using knockout mouse models. Phenotypic and genetic analysis can identify differences between wild-type and knockout animals, providing insight into the roles of Flrt3. As presented in Chapter 1, a *Flrt3*$^{-/-}$ mouse model has been studied in an attempt to elucidate a role for Flrt3 during embryonic development, but due to the early lethality of the Flrt3 null mouse, it was difficult to assess the effect of Flrt3 on Fgf signalling. The knockout does not survive past mid-gestation, dying at approximately the same time-point as the initiation of *Flrt3* expression at the midbrain-hindbrain boundary (MHB). Therefore, the embryo does not survive to stages where the well-studied models of Fgf signalling, such as the MHB and the developing limb, have formed. This makes the knockout model unsuitable to study of the effect of endogenous *Flrt3* function on Fgf signalling in neural development [5].

The identification of an *in vitro* cell culture model to study the role of endogenous Flrt would be advantageous due to its simplicity, ease of use and greater scope for manipulation. A pluripotent or multipotent cell line would be a useful tool to study the function of Flrt genes during cellular differentiation. The ability to differentiate these cells down a number of cellular pathways that are directly relatable to those *in vivo,* may lead to direct comparisons to embryonic development. Expression of the *Flrt* family is present during early development of the mouse in the three embryonic germ layers, in neural development in the early neurectoderm and at later stages at the MHB boundary [5], so may show interesting expression in early pluripotent stem cell differentiation.

In this chapter, different pluripotent cell differentiation regimes are examined in an attempt to identify a cell model system to analyse Flrt function. Specifically, the P19 embryonic carcinoma (P19 EC) cell line and the D3 ES cell line were examined. The P19 EC is a euploid pluripotent cell line isolated from murine teratocarcinomas that can be differentiated to different cell fates with the aid of different chemicals and cell culture conditions. For example, differentiation with retinoic acid (RA)

promotes neural differentiation, whilst differentiation with dimethyl sulfoxide (DMSO) promotes cardiomyocyte differentiation [44, 45]. D3 ES cells are the mouse equivalent of the inner cell mass and can also be differentiated down various cellular differentiation pathways, reminiscent of those in the early mouse embryo, using various cell culture conditions.

4.2 Results

4.2.1 Analysis of *Flrt* expression in neural-differentiated P19 EC cells

To determine the expression of Flrt genes *in vitro* in models of early embryogenesis, I utilised the differentiation of two stem cell based systems. Firstly, a time-course of differentiation of P19 EC cells in the presence of retinoic acid, which directs differentiation towards a neural lineage, was analysed using quantitative real-time PCR (qRT-PCR) to detect the expression of *Flrt1*, *Flrt2*, and *Flrt3* (Figure 4.1).

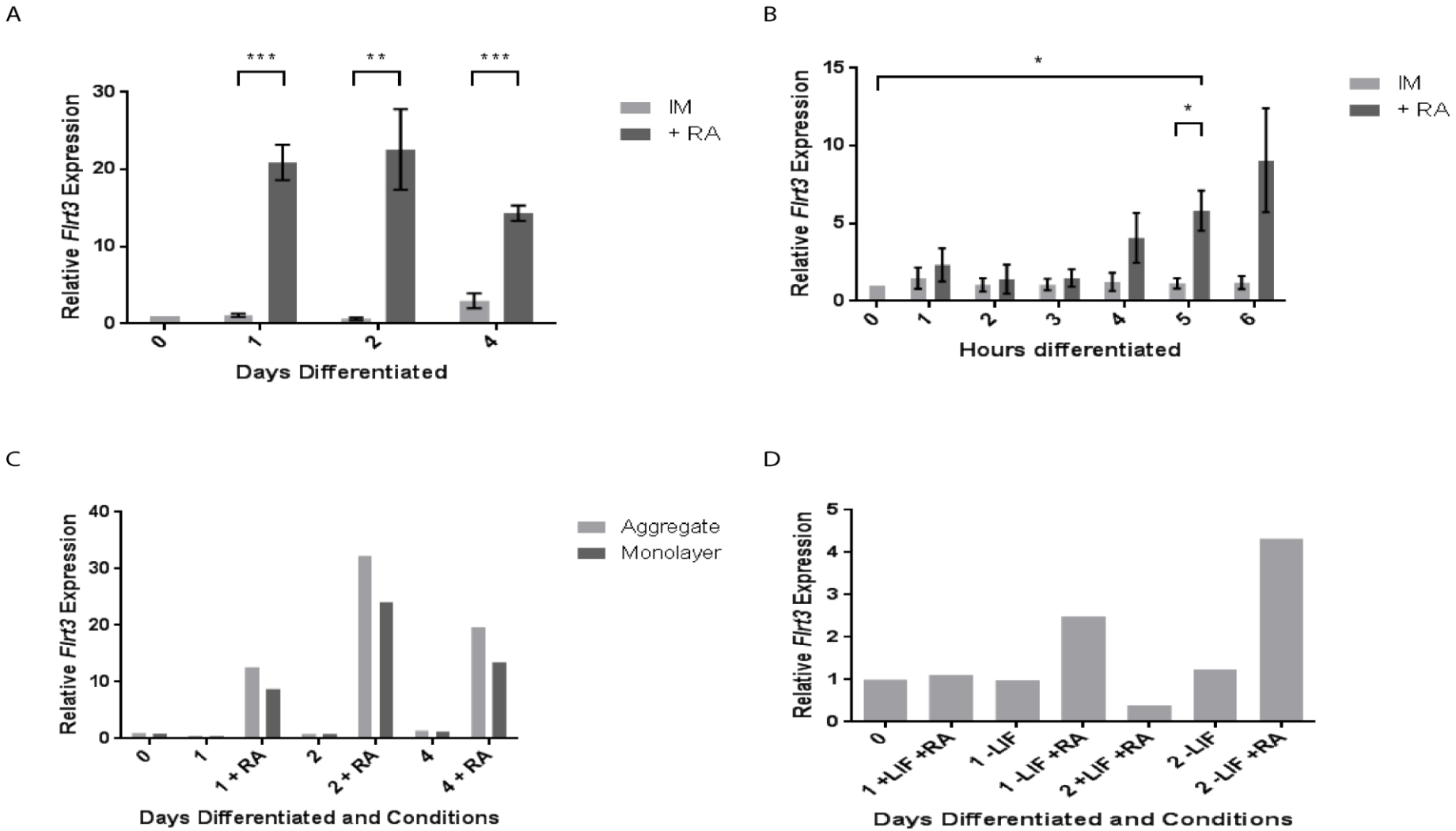

Figure 4.1. *Flrt3* is induced during the retinoic acid driven differentiation of P19 EC cells: qRT-PCR analysis of RNA from P19 EC cell aggregates (A and B) or, monolayer (C) and mouse D3 ES (D) cell lines after induction with 5 mM retinoic acid (RA). A) *Flrt3* expression in cells differentiated over a 4 day period with or without RA. n=3. B) *Flrt3* expression in cells differentiated over a 6 h period with or without RA. n=3. C) *Flrt3* expression in P19 EC cells grown in aggregates and in a monolayer over 4 days with or without RA. n=1. D) *Flrt3* expression in cells differentiated over a 2 day period with or without LIF and RA. Error bars are S.E.M. Statistics analysed using Student's t-test, *=p<0.05, **=p<0.01, ***=p<0.005.

To identify if the RA-differentiated P19 EC cell model can be used to study *Flrt* function, gene expression over 4-days of differentiation was assessed. Analysis of *Flrt3* mRNA shows a rapid and robust induction of expression upon early retinoic acid dependent neurectoderm differentiation (Figure 4.1 A). This is in contrast to expression of *Flrt1* and *Flrt2* that show negligible expression over the four days of differentiation (data not shown). Upon differentiation with RA, *Flrt3* expression increases rapidly, with a 20.9-fold increase after 1 day (1 + RA) compared to undifferentiated cells (0) (Figure 4.1 A). Expression remained steady after 2 days (2 + RA), with a 22.6-fold increase compared to undifferentiated cells, before appearing to slightly decrease to a 14.3-fold increase compared to undifferentiated cells after 4 days (4 + RA), with all changes noted being statistically significant (Figure 4.1 A). When compared to differentiation in the absence of RA (- RA), RA-directed neural differentiation of P19 EC cells significantly increased endogenous *Flrt3* expression in each of the 4 days measured, with statistically significant increases of 18.9-fold ($p=9.9x10^{-4}$), 35.8-fold ($p=0.014$) and 4.82-fold ($p=1.2x10^{-3}$) respectively (Figure 4.1 A). When differentiated in the absence of RA, expression of *Flrt3* does not significantly change from undifferentiated cells (Figure 4.1 A). Therefore, this model allows analysis of Flrt3 function without expression of the closely related *Flrt1* and *Flrt2* genes, allowing for easier data analysis and interpretation.

As *Flrt3* is induced within the initial 24 hours of induction, a short time-course differentiation experiment was carried out to determine when an increase in *Flrt3* transcription first appears. In comparison to non-RA differentiated cells, the presence of RA P19 EC cells show a statistically significant 3.7-fold increase in *Flrt3* expression after 4 h of differentiation when compared to cells differentiated for 4 h without RA. A statistically significant increase is maintained throughout the remaining time-points when comparing RA- and non-RA differentiated cells ($p<0.05$) (Figure 4.1 B). A significant 6.5-fold increase in *Flrt3* expression is observed after 5 h by RA-driven differentiation when compared undifferentiated (0 h) P19 EC cells, with expression continuing to increase beyond this time as observed in A (Figure 4.1). In the absence of RA, *Flrt3* levels do not change over the first 6 h of differentiation, remaining at the same level as undifferentiated cells (0 h) ($p>0.05$).

Our previous experiments analysing the expression of the Flrt genes during the RA directed differentiation relied upon aggregation of P19 cells during differentiation. To determine if cell-cell communication that occurs during cellular aggregation plays a role the ability of RA to induce *Flrt3* expression, or if this induction is directed by RA alone, P19 cells grown in a monolayer and treated with RA, rather than as aggregates, were analysed. Expression of *Flrt3* over the 4-day differentiation period

replicates that of cells grown in aggregates (Figure 4.1 C). *Flrt3* expression increases in cells grown in a monolayer with RA-differentiation after 1 day, remains steady after 2 days, and marginally decreases after 4 days (Figure 4.1 C). The induction of *Flrt3* expression by RA in cells grown in monolayer will provide many advantages for the downstream analysis of Flrt3 expression and function, such as a clearer cell morphology for the localisation of Flrt3 protein within these cells.

Investigation into *Flrt3* expression during RA-guided early neurectoderm differentiation in mouse D3 ES cells was undertaken to determine if induction of *Flrt3* is specific to P19 cells and if this system could provide a more embryonically relevant model to study Flrt3 function. ES cells can be differentiated into different cell types using different methods. The presence of leukaemia inhibitory factor (LIF) in the media inhibits ES cell differentiation maintaining ES cells in an undifferentiated state (0). The addition of RA to LIF-containing media (+ LIF + RA) resulted in no change to *Flrt3* expression after 1 day, and an apparent decrease in expression after 2 days (Figure 4.1 D). Removing LIF from lower serum media promotes differentiation to occur, replicating similar conditions to that of P19 EC cells differentiating without RA. Levels of *Flrt3* in these samples (-LIF) remain similar to that of undifferentiated cells, and are similar in pattern to that of P19 EC cells differentiated without RA (Figure 4.1 D). When early neurectoderm differentiation was promoted by lowering serum levels, removing LIF and adding RA, *Flrt3* expression appears to increase when compared to undifferentiated D3 ES cells and to differentiating cells without addition of RA over the first 2 days of differentiation (Figure 4.1 D). Expression of *Flrt3* in cells differentiated for 1 day (1 –LIF +RA) showed a 2.5-fold increase compared to undifferentiated cells, while differentiation for 2 days (2 –LIF +RA) showed a 4.3-fold increase (Figure 4.1 D). This expression pattern is similar to that observed in P19 EC cells, albeit with a much reduced level of induction (Figure 4.1 A), identifying the RA-differentiation of P19 EC cells the better of the 2 models investigated to study endogenous Flrt3 function.

To ensure the validity of the results, a number of controls were used in this experiment. The primers used are designed against the *Flrt3* open reading frame, which is a single exon. This means that primers crossing exon boundaries cannot be utilised, resulting in the implementation of a number of controls, including DNAse treatment to eliminate contaminating gDNA, analysis of samples that were not reverse transcribed to obtain cDNA, and the use of reference genes as a part of the analysis. These controls are further outlined in Chapter 2.

Early neurectoderm differentiation of the P19 EC cell line with RA is a good model to study the function of *Flrt3*. Expression of *Flrt3* is rapidly and robustly increased upon differentiation with RA, with

this increase consistent between cell lines (P19 EC and D3 ES), and cell monolayer and aggregate growth. An increase in *Flrt3* is observed within 5 hours of induction of differentiation and continues to increase towards a maximum around 48 hours after neurectodermal differentiation begins, with expression beginning to fall again after this period of time. *Flrt3* was the only family member to show a sustained increase in expression using RA-differentiation of P19 EC cells, while negligible change in expression of *Flrt1* and *Flrt2* was observed. Importantly, these results may allow the use of this model to analyse the function of Flrt3 without any influence from Flrt1 and Flrt2 which may act as a compensation mechanism. Protein expression levels will need to be analysed to ensure that there is no compensation for the increase in *Flrt3* expression at the protein level. This would confirm the ability to use this model. Expression of *Flrt3* in non-RA differentiated cells remains low over the initial 4 days of differentiation. With the induction of *Flrt3* occurring rapidly, a direct response of the gene to exposure of RA may exist.

4.2.2 *Flrt3* promoter response to RA

The rapid nature of the induction of *Flrt3* expression by RA-induced differentiation suggested that this induction may be a direct transcriptional activation by RA. Therefore, we used two methods to identify elements within the *Flrt3* promoter region that may control retinoic acid dependent induction of *Flrt3* expression.

Visual analysis of the *Flrt3* promoter up to 10 kb upstream of the *Flrt3* start site has failed to reveal any obvious sequence that matches the $^{5'}$PuGGTCAxxxxxPuGGTCA$^{3'}$ consensus sequence (where Pu is any purine, and x is any nucleotide) of an RA response element [46]. As the expression pattern of *Flrt3* is highly conserved between mouse and chicken, we performed an analysis of the *Flrt3* upstream sequence using the Evolutionary Conservation of Genomes (ECR) browser (http://ecrbrowser.dcode.org/), which compares genomic DNA sequences between species to identify conserved regions, and then searched these sequences for conserved transcription factor binding sites. We identified a conserved DNA sequence approximately 5 kb upstream of the transcriptional start site that contained a conserved retinoic acid orphan receptor (ROR) binding site that is a good candidate for a direct response to retinoic acid exposure (https://rvista.dcode.org/cgi-bin/rVA.cgi). It lies within a region of approximately 600 bp that shares high sequence homology between higher order vertebrates (ECR browser, http://ecrbrowser.dcode.org) (Figure 4.2).

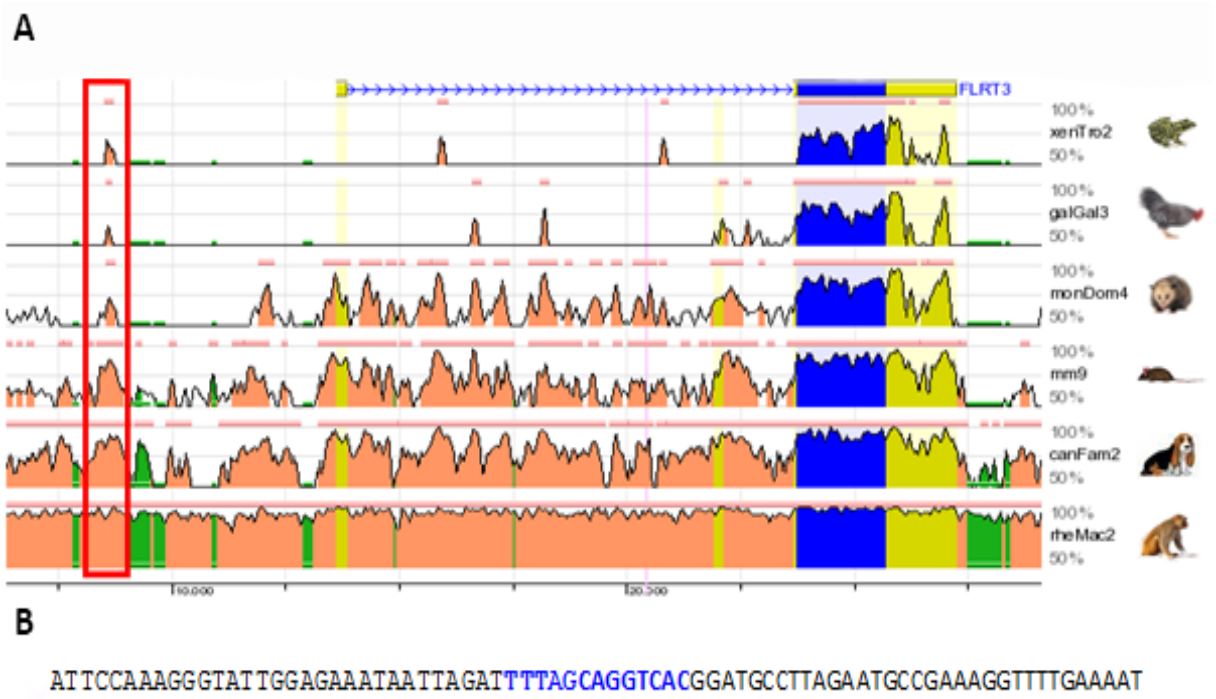

Figure 4.2. Alignment of DNA sequences reveals a conserved element upstream of the *Flrt3* promoter containing a ROR element: A) Flrt3 gene alignment showing percentage sequence identity between various species relative to human (yellow and blue boxes with blue arrows at top of figure), including higher order mammals. Yellow shading indicates exons, orange shading indicates introns, blue shading indicates ORF, red box highlights conserved portion of DNA sequence further investigated (http://ecrbrowser.dcode.org/xB.php?db=hg18&location=chr20:14252643 -14266270). B) Sequence analysis revealed the location of a potential retinoic acid response element (RORA1, blue text) within the conserved element in both the human and mouse sequences (human sequence shown) (https://rvista.dcode.org/cgi-bin/rVA.cgi).

The nuclear orphan receptor family consists of a number of subfamilies, including the ROR subfamily. The subfamily consists of 3 different members; alpha, beta and gamma, of which beta and gamma are responsive to retinoic acid [47]. These comprise of a highly-conserved DNA-binding domain across the family, and a moderately conserved ligand binding domain. They are defined as orphan receptors due to the conflicting reports over the identification of binding ligands. Isoforms differing only in their amino terminus, are formed due to alternative promoter usage and splicing. RORs bind to specific ROR response elements, which consist of a core motif AGGTCA preceded by a 5 bp A/T-rich sequence, as a monomer, with binding to co-repressors and co-activators discovered. RORβ is expressed in mouse pineal gland and suprachiasmatic nuclei, localising it within the correct tissue-type to influence *Flrt3* expression during neurogenesis [48]. Using PCR, the conserved element (CE) was isolated and using traditional cloning methods, luciferase constructs containing the CE were cloned with the minimal SV40 promoter.

In the second approach, regions of DNA 5' of the *Flrt3* transcriptional start site of varying sizes (2 kb, 4 kb and 6 kb of *Flrt3*) were isolated and used to analyse whether the sequence that mediates RA-mediated *Flrt3* induction is present close to the *Flrt3* transcriptional start site. Variations of the

sequence upstream of *Flrt3* in the presence or absence of the native *Flrt3* transcriptional start site (labelled +pr and –pr respectively) were cloned into the luciferase containing vector pGL3 B, under the control of the endogenous *Flrt3* promoter, or pGL3 P, under the control of the minimal SV40 promoter, to also assess the importance of the native promoter (Figure 4.3).

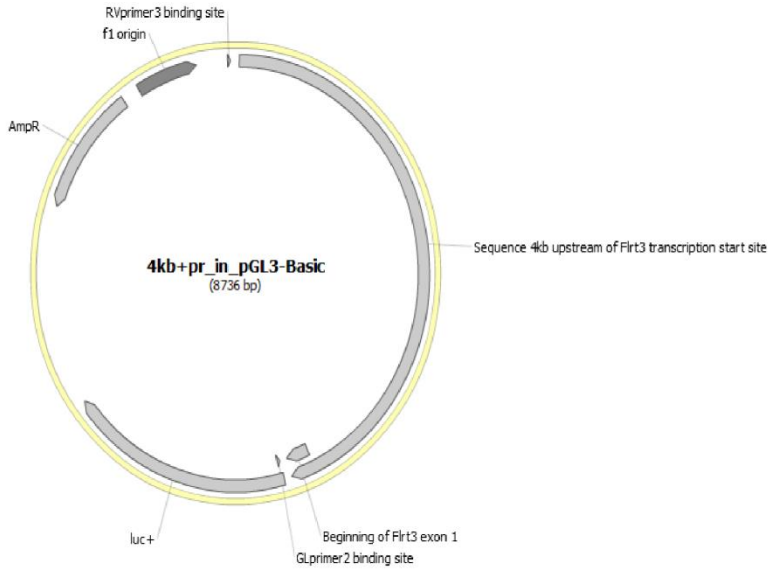
RVprimer3 binding site
f1 origin
AmpR
4kb+pr_in_pGL3-Basic
(8736 bp)
Sequence 4kb upstream of Flrt3 transcription start site
luc+
Beginning of Flrt3 exon 1
GLprimer2 binding site

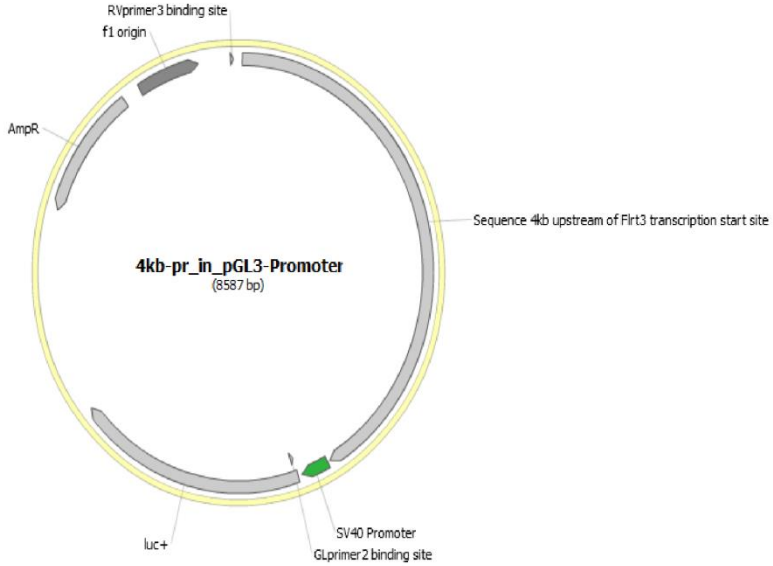
RVprimer3 binding site
f1 origin
AmpR
4kb-pr_in_pGL3-Promoter
(8587 bp)
Sequence 4kb upstream of Flrt3 transcription start site
luc+
SV40 Promoter
GLprimer2 binding site

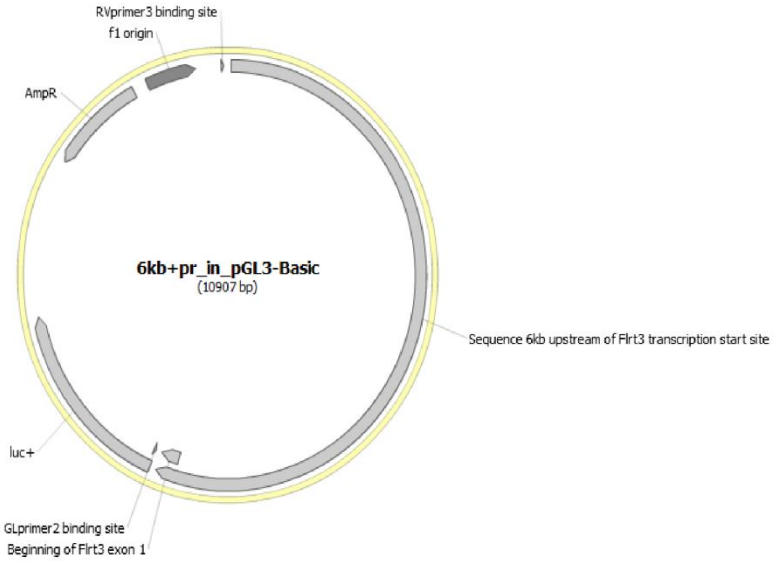
RVprimer3 binding site
f1 origin
AmpR
6kb+pr_in_pGL3-Basic
(10907 bp)
Sequence 6kb upstream of Flrt3 transcription start site
luc+
GLprimer2 binding site
Beginning of Flrt3 exon 1

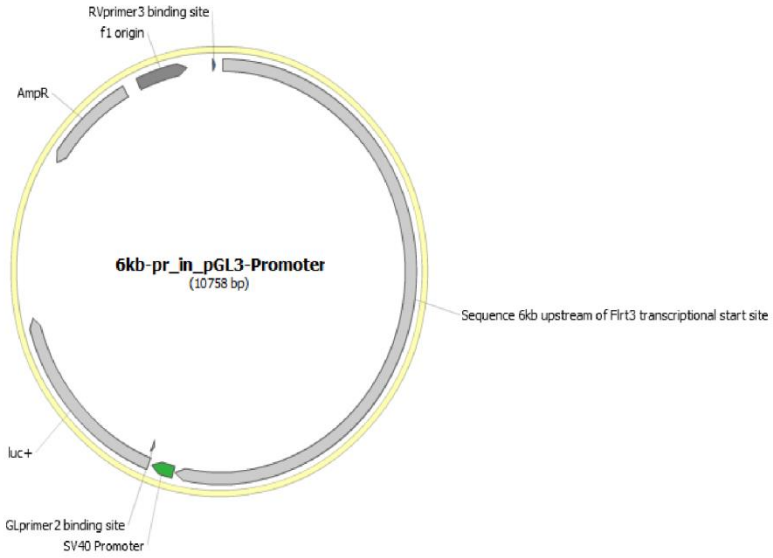
RVprimer3 binding site
f1 origin
AmpR
6kb-pr_in_pGL3-Promoter
(10758 bp)
Sequence 6kb upstream of Flrt3 transcriptional start site
luc+
GLprimer2 binding site
SV40 Promoter

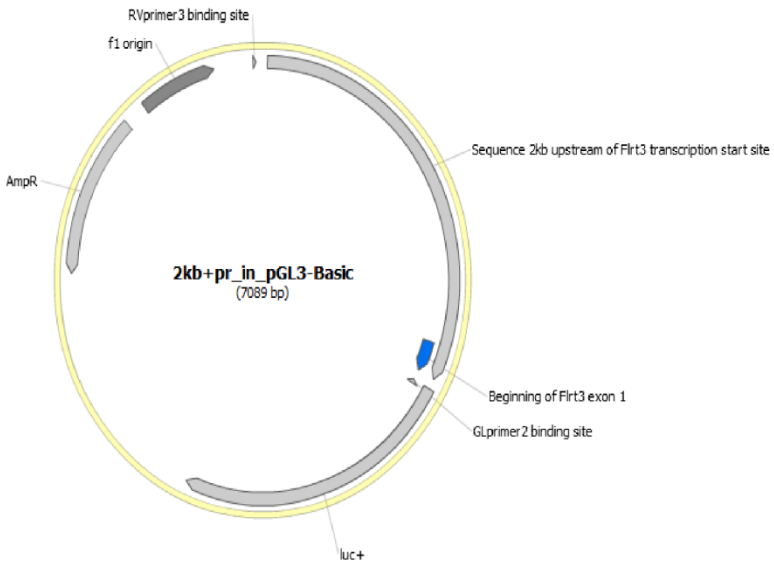
RVprimer3 binding site
f1 origin
Sequence 2kb upstream of Flrt3 transcription start site
AmpR
2kb+pr_in_pGL3-Basic
(7089 bp)
Beginning of Flrt3 exon 1
GLprimer2 binding site
luc+

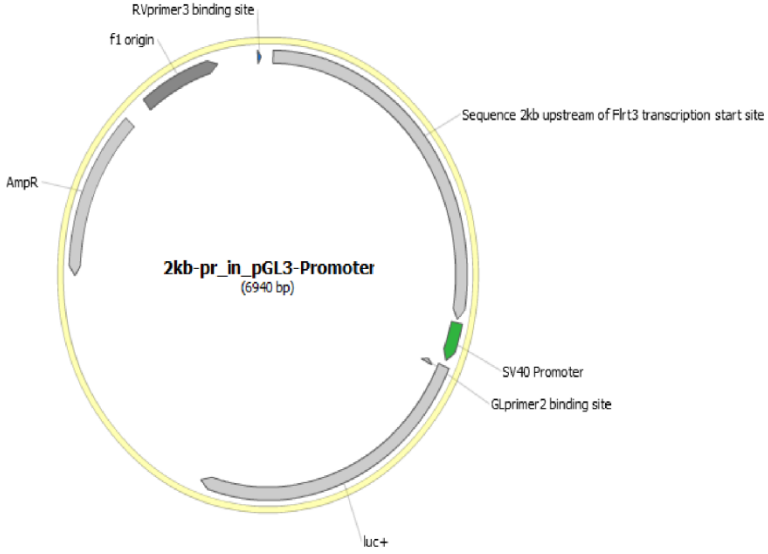
RVprimer3 binding site
f1 origin
Sequence 2kb upstream of Flrt3 transcription start site
AmpR
2kb-pr_in_pGL3-Promoter
(6940 bp)
SV40 Promoter
GLprimer2 binding site
luc+

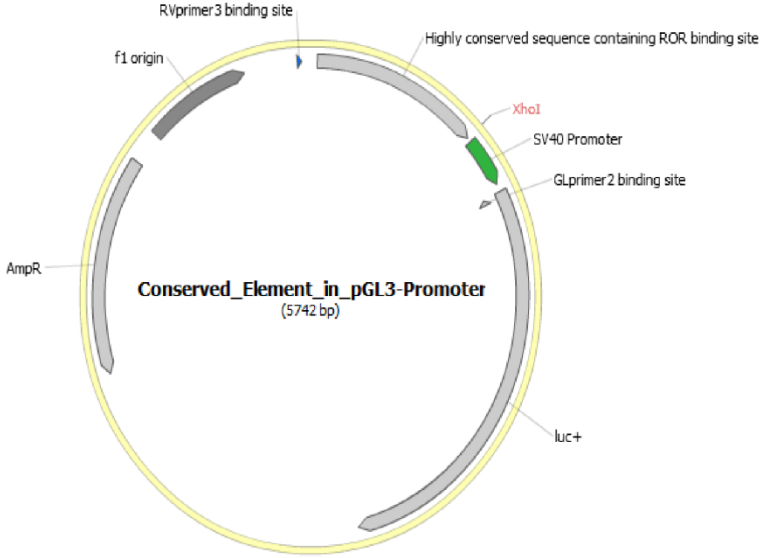
RVprimer3 binding site
Highly conserved sequence containing ROR binding site
f1 origin
XhoI
SV40 Promoter
GLprimer2 binding site
AmpR
Conserved_Element_in_pGL3-Promoter
(5742 bp)
luc+

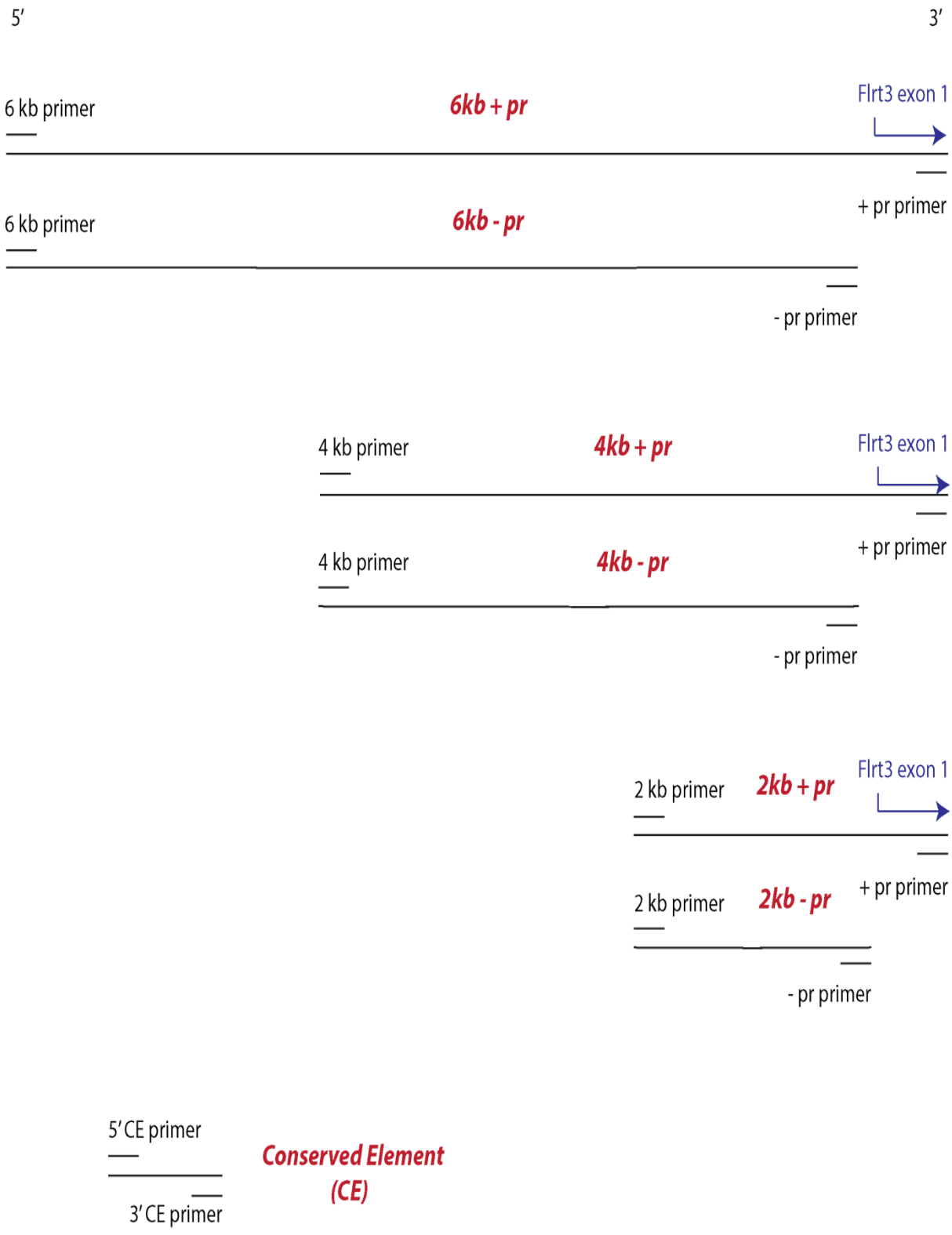

Figure 4.3. Luciferase constructs cloned to analyse *Flrt3* promoter regions response to RA differentiation of P19 EC cells: Vector maps showing the structure of the cloned luciferase vectors (previous 2 pages), and a schematic of the regions of the *Flrt3* promoter investigated (current page). +pr = including *Flrt3* transcriptional start site, -pr = excluding *Flrt3* transcriptional start site

To analyse the output from the cloned Flrt3 regulatory elements we transfected the luciferase constructs into P19 EC cells and differentiated them with or without RA (Figure 4.4).

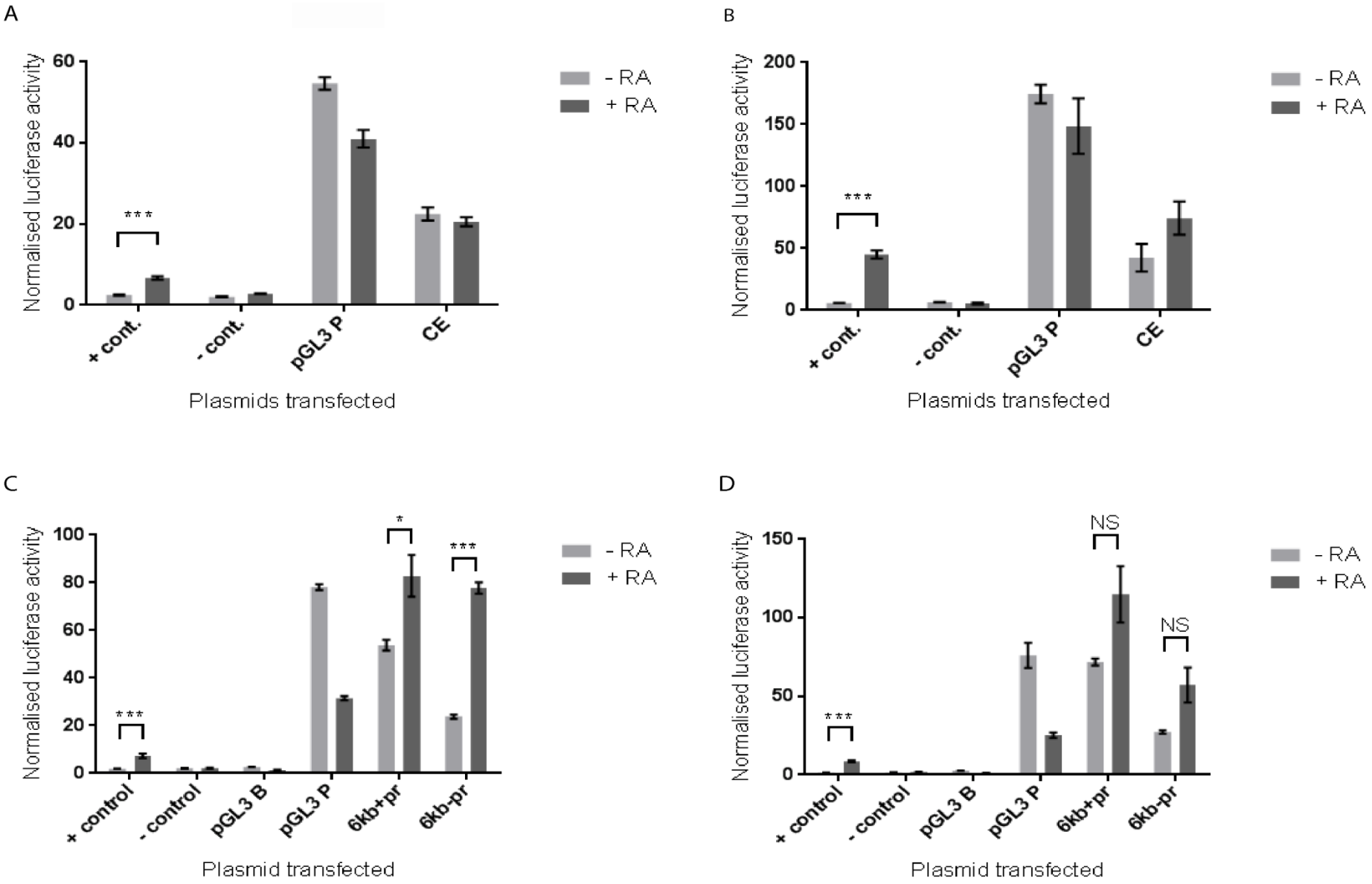
A
Normalised luciferase activity
60
40
20
0
***
+ cont.
- cont.
pGL3 P
CE
Plasmids transfected
- RA
+ RA
B
Normalised luciferase activity
200
150
100
50
0
***
+ cont.
- cont.
pGL3 P
CE
Plasmids transfected
- RA
+ RA
C
Normalised luciferase activity
100
80
60
40
20
0
***
*
***
+ control
- control
pGL3 B
pGL3 P
6kb+pr
6kb-pr
Plasmid transfected
- RA
+ RA
D
Normalised luciferase activity
150
100
50
0
***
NS
NS
+ control
- control
pGL3 B
pGL3 P
6kb+pr
6kb-pr
Plasmid transfected
- RA
+ RA

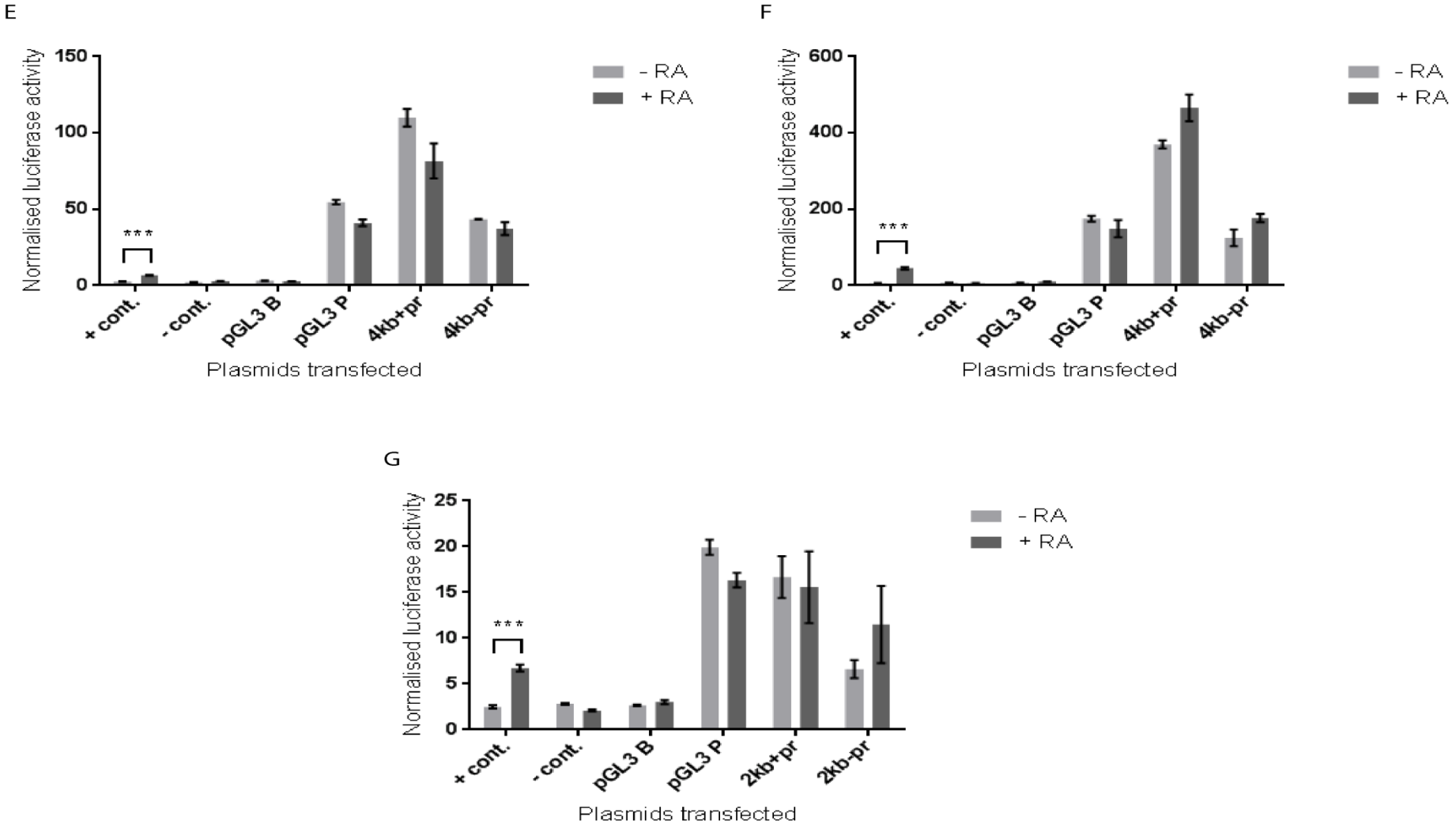

Figure 4.4. An RA response is initiated from within a 1.7 kb region between 4 kb and 6 kb upstream of the *Flrt3* transcription start site: Normalised luciferase activity from luciferase assays of P19 EC cells transfected with indicated plasmids (+ cont. is a known RA-responsive element in pTK-LUC, - cont. is empty pTK-LUC, pGL3 B is pGL3 Basic (no promoter) without an insert, pGL3 P is pGL3 Promoter (minimal SV40 promoter) without an insert, CE is the conserved element of the *Flrt3* promoter) and differentiated ± RA for 1 (A, C, and E) or 2 (B, D, F, and G) days. Error bars are S.E.M, n=3. Statistics analysed utilising the Student's t-test, *=p<0.05, **=p<0.01, ***=p<0.005.

Using RA-differentiation of luciferase vector-transfected P19s, we analysed all the constructs for the ability to be induced by RA and found no significant increase in luciferase activity with all except the 6 kb constructs (Figure 4.4). Here we observed a 1.54-fold increase in luciferase activity in cells transfected with 6 kb + pr ($p<0.05$), while cells transfected with 6 kb – pr resulted in a 3.26-fold increase in luciferase activity ($p<0.05$) when differentiated with RA for 1 day (Figure 4.4 C) compared to those differentiated without RA.

The results of this experiment were shown to be valid using several controls. The transfection of P19 EC cells was shown to be successful by using a GFP-expression vector control. A transfection efficiency of approximately 30-40% was routinely observed. To validate the luciferase assay with retinoic acid induced P19 cells, a positive (+ cont.) and negative (- cont.) control were utilised. The + cont. was a luciferase vector containing a known retinoic acid response element, which was confirmed to exhibit retinoic acid dependent induction of luciferase. In each case, the + cont. showed a significant increase in luciferase activity when transfected cells are differentiated in RA ($p<0.05$) compared to those differentiated without RA (Figure 4.4). The - cont. consisted of the same vector sequence as the + cont., except without the known response element, consistently resulting in no change in luciferase activity when differentiated in RA or differentiated without RA ($p>0.05$) (Figure 4.4). The influence of the pGL3 luciferase vectors in the absence of the DNA to be analysed was assessed using the pGL3 promoter vector alone (pGL3 P) and the pGL3 basic vector alone (pGL3 B). The pGL3 B and pGL3 P-transfected P19 EC cells showed no positive response to RA-differentiation (Figure 4.4). Interestingly, when P19 EC cells containing pGL3 P are differentiated in RA, levels of luciferase expression are consistently decreased compared to those cells differentiated without RA (Figure 4.4). All results observed for the controls were as expected, validating the data obtained.

Upon differentiation of P19 EC cells with RA, expression of endogenous *Flrt3* is seen to significantly increase nearly 36-fold (Figure 4.1). An increase in luciferase activity was observed in cells containing 6kb of DNA sequence upstream of *Flrt3* coding region differentiated in RA compared to these cells differentiated without RA for 1 day, although this does not account for the substantial increase in endogenous *Flrt3* expression (Figure 4.4). This difference in luciferase activity is not observed in the cells transfected with the 4kb *Flrt3* promoter sequence or within the conserved element. This implies that while there is a region of DNA between 4 kb and 6 kb 5' of the gene that is responsive to RA treatment, the extent of induction with the 6 kB constructs was far less than the induction of endogenous *Flrt3* levels. Therefore, the majority of RA responsive elements must exist elsewhere to justify the increase in endogenous *Flrt3* expression observed.

4.2.3 Flrt3 protein expression during RA-mediated differentiation of P19 EC cells

In Section 4.2.1, a large increase in *Flrt3* mRNA expression in P19 EC cells differentiated with retinoic acid was observed. To determine if this increased mRNA expression translates into increased levels of Flrt3 protein, we utilised a commercial antibody produced to the extracellular domain of the Flrt3 protein (MAB2795, R&D systems). Unfortunately, this antibody was problematic in Western blot analysis for endogenous Flrt3 protein. Therefore, we used immunofluorescence assays of RA-differentiated P19 EC cells to analyse endogenous Flrt3 protein expression. To validate the use of the Flrt3 antibody in these assays, two experiments were run to test the ability to specifically detect endogenous Flrt3. Firstly, HA-tagged Flrt3 was transfected into Cos-7 cells and expression was assessed using an anti-HA antibody and the anti-Flrt3 antibody (Figure 4.5).

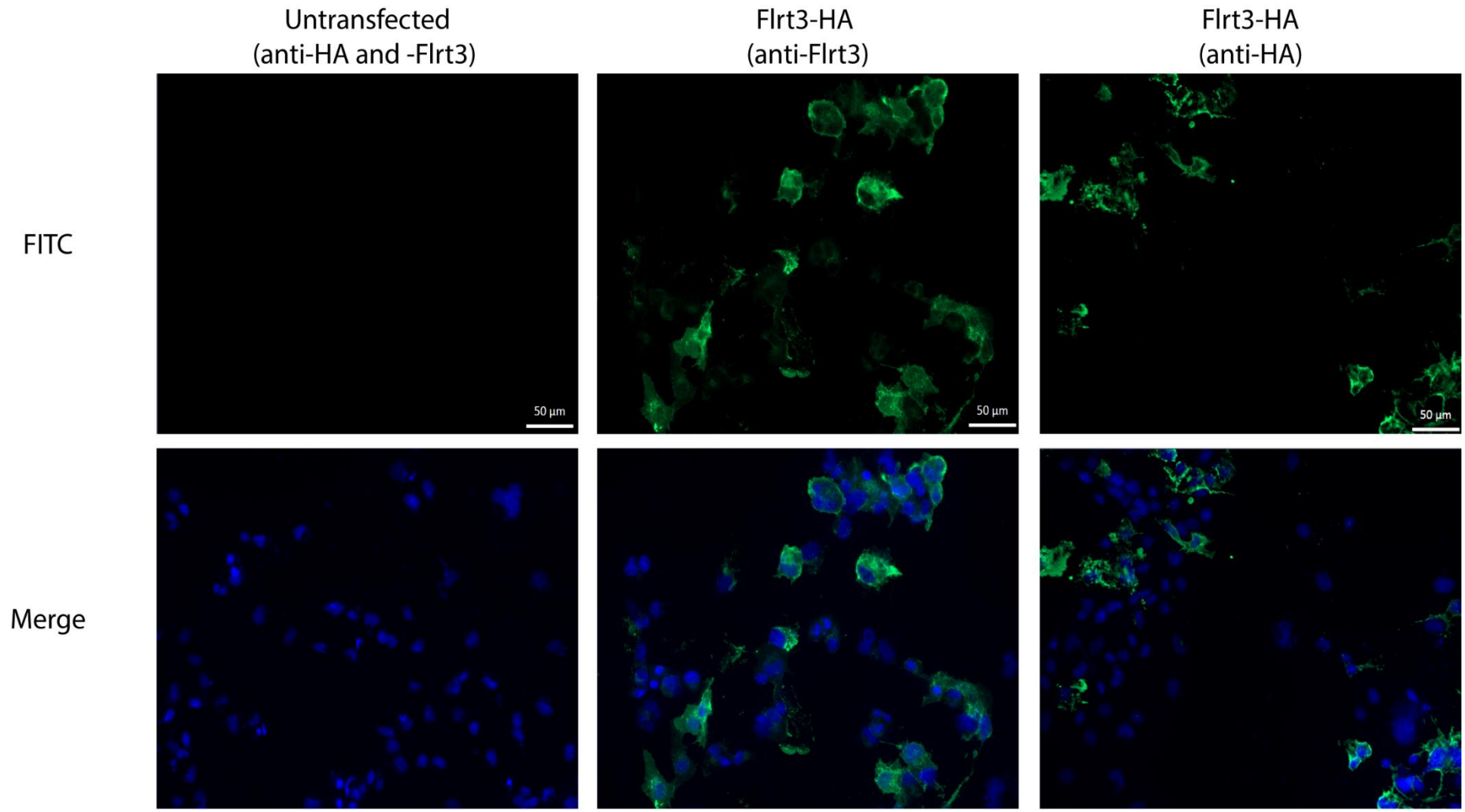

Figure 4.5. Flrt3 antibody recognises Flrt3 over-expressed in Cos-7 cells: Immunofluorescence assay of Cos-7 cells over-expressing Flrt3-HA (Flrt3-HA), and untransfected cells. Cells stained with anti-Flrt3 and anti-HA (green, FITC) and DAPI (blue). Images taken on a Zeiss deconvolution microscope. 20x magnification.

Cos-7 cells over-expressing Flrt3-HA probed with Flrt3 antibody resulted in immunofluorescence consistent with the membrane localisation of Flrt3. Cells exhibited protein localisation to perinuclear structures within the cell cytoplasm consistent with intracellular membranes or uniform cytoplasmic staining consistent with localisation to the cell surface membrane. Cells adjacent to other Flrt3 over-expressing cells showed localisation to the site of cell-cell contacts (Figure 4.5 Flrt3-HA (anti-Flrt3)). This is consistent with the previous cellular localisation of over-expressed Flrt3 [5]. This staining pattern is also observed when over-expressing cells are probed for HA (Figure 4.5 Flrt3-HA (anti-HA)), while both antibodies reveal no non-specific binding to untransfected cells (Figure 4.5, Untransfected (anti-HA and -Flrt3)). This assay confirms that the Flrt3 antibody selectively binds to Flrt3 protein in an over-expression system.

Endogenous *Flrt3* mRNA levels increase in RA-differentiated P19 EC cells but are low undifferentiated cells. To confirm that the antibody is suitable to determine an increase in endogenous Flrt3 protein expression in this system, the specificity of the Flrt3 antibody in P19 EC cells was assessed (Figure 4.6).

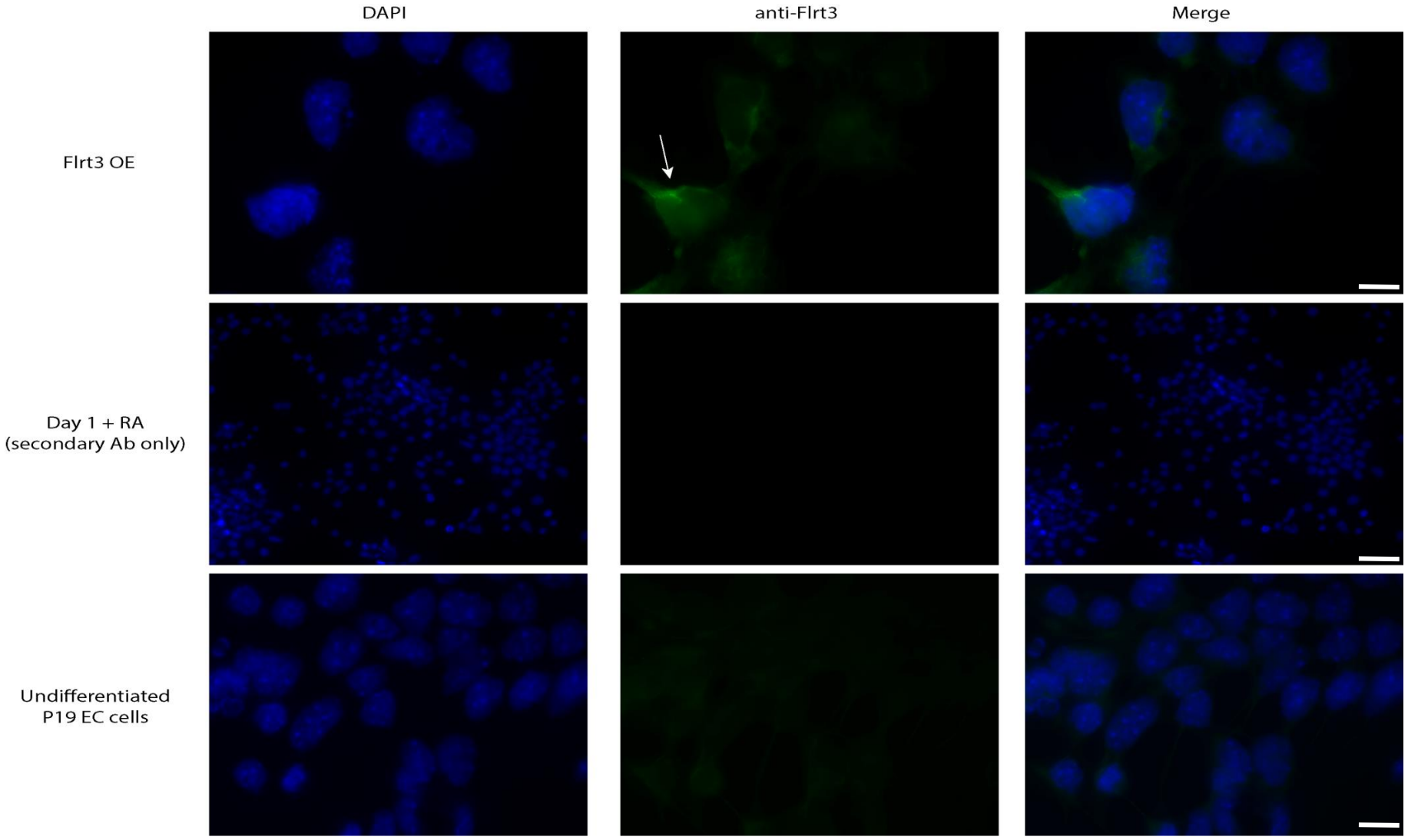

Figure 4.6. The Flrt3 antibody is specific for Flrt3 in P19 EC cells: Immunofluorescence staining of P19 EC cells over-expressing Flrt3 (Flrt3 OE), differentiated with RA for 1 day (Day 1 + RA), and undifferentiated (Undifferentiated P19 EC cells). Cells stained with anti-Flrt3 (green) and DAPI (blue). Arrow indicates intracellular localisation of Flrt3. Top and bottom panels are 100x magnification (scale bar is 5 µm), middle panels are 20x magnification (scale bar is 25 µm).

To demonstrate that the Flrt3 antibody is specific for the Flrt3 protein in this system, P19 EC cells were transiently transfected with an expression vector to over-express Flrt3 (Flrt3 OE). Expression of Flrt3 is detected with the Flrt3 antibody, demonstrated by green immunofluorescence (arrow), with expression concentrated adjacent to the nucleus (Figure 4.6 Flrt3 OE). Undifferentiated P19 EC cells show very low to no expression of Flrt3, consistent with the mRNA expression of Flrt3 and showing no non-specific background staining with the Flrt3 antibody (undifferentiated P19 EC cells, Figure 4.6). This eliminates the possibility of the signal being observed from the secondary antibody binding non-specifically. These controls produced the expected results, and therefore validate the use of the antibody in determining an increase in Flrt3 expression using the RA-differentiation P19 EC cell differentiation system.

To determine if the increase in *Flrt3* mRNA expression reported in Chapter 4.2.1 translates to an increase in endogenous Flrt3 protein, P19 EC cells differentiated for 1 day with or without RA were assessed for changes in Flrt3 antibody staining (Figure 4.7).

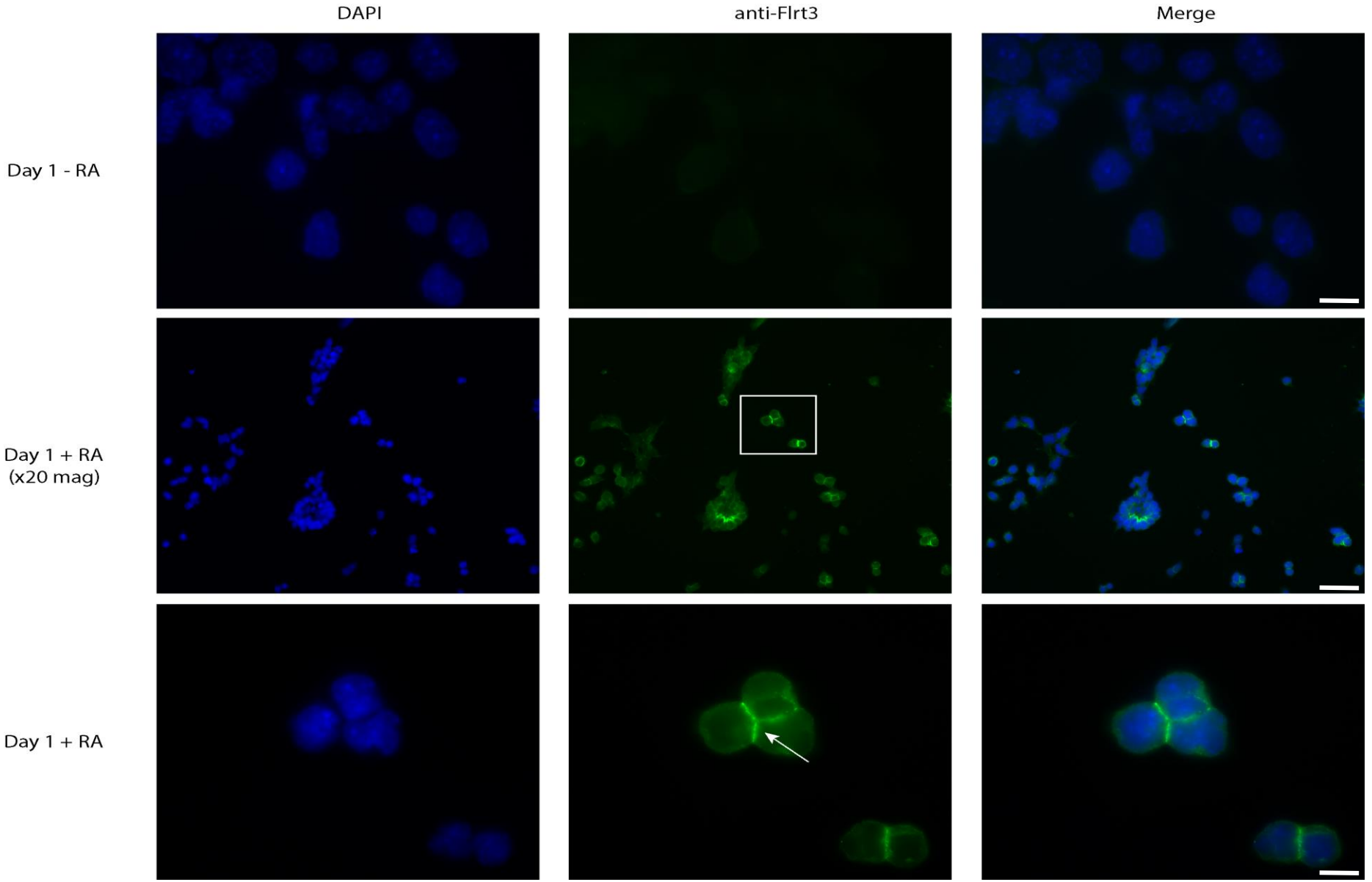
DAPI
anti-Flrt3
Merge
Day 1 - RA
Day 1 + RA
(x20 mag)
Day 1 + RA

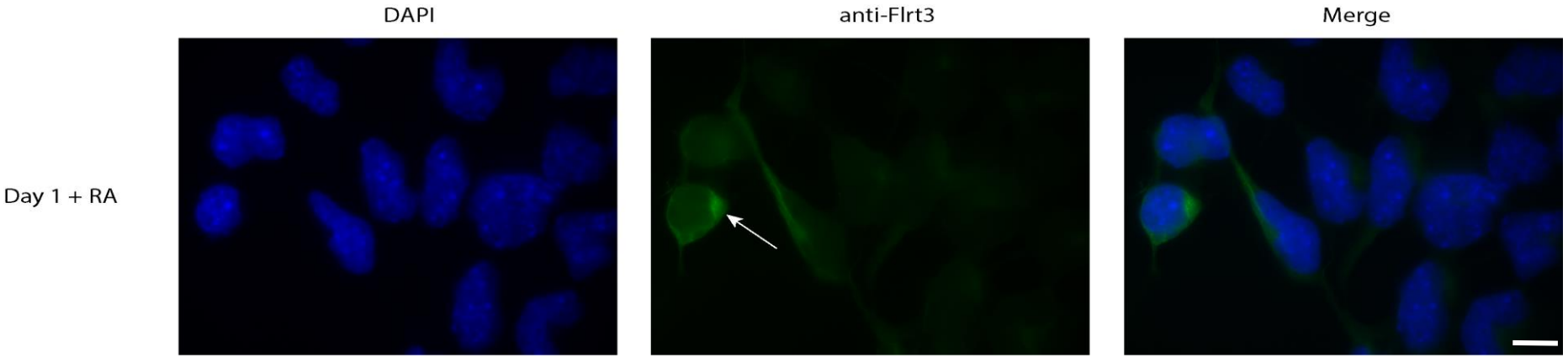

Figure 4.7. Flrt3 expression increases in RA-differentiated P19 EC cells: Immunofluorescence assay of P19 EC cells differentiated with or without RA for 24 h. Cells stained with anti-Flrt3 (green) and DAPI (blue). Third row images (previous page) are the zoom of white square in Day 1 + RA (20x mag, scale bar is 25 µm). Arrows indicate regions of Flrt3 localisation. Images taken on Leica SP5 Spectral Scanning confocal microscope and are representative cells from 5 total fields of cells. 100x magnification unless stated otherwise, scale bars are 5µm.

Differentiation for 1 day in the absence of RA (Day 1 - RA, Figure 4.7) reveals low levels of Flrt3 expression. Upon differentiating for 1 day in the presence of RA (Day 1 + RA, Figure 4.7), an increase in Flrt3 immunostaining was observed in comparison to Day 1 – RA cells, correlating to an increase in Flrt3 protein expression. Cells expressing increased levels of Flrt3 are estimated to make up approximately 20% of cells in the sample, demonstrating the heterogeneous nature of Flrt3 expression in P19 cells at this stage of differentiation. Interestingly, cells that do show an increase in Flrt3 appear to occur in clusters (Day 1 + RA third panel, arrow). Flrt3 immunostaining was present in the cytoplasm in a pattern suggesting localisation to intracellular membranes (Figure 4.7, Day 1 + RA fourth panel, arrow) and was observed to be stronger at cell-cell boundaries when two cells showing high Flrt3 expression are in contact (Figure 4.7, Day 1 + RA second and third panel, arrow), which has been previously observed in cells over-expressing Flrt3 [5, 10].

This experiment shows that expression levels of Flrt3 protein increase in a subset of P19 EC cells during RA-differentiation in comparison to those differentiated in the absence of RA, meaning that the increase in *Flrt3* transcription identified in Figure 4.1 does translate to an increase in endogenous Flrt3 protein expression. Localisation of endogenous Flrt3 protein is similar to that reported for over-expressed Flrt3 protein. Therefore, the increase in endogenous Flrt3 expression due to RA-differentiation of P19 EC cells may provide a mechanism for regulating FgfR1 signalling, as alluded to in Chapter 3, during this differentiation process.

4.2.4 ERK phosphorylation during P19 EC cell differentiation: Evidence for a role for Flrt3.

Given that levels of endogenous *Flrt3* mRNA and protein increase (Figure 4.1, 4.7) in RA-differentiated P19 EC cells, and that there are multiple lines of evidence that show Flrt proteins can alter phosphorylated ERK (pERK) levels via the regulation of Fgf signalling upon over-expression ([41], Chapter 3), I investigated whether there is evidence linking the induction of *Flrt3* to the regulation of ERK phosphorylation in P19 cells.

To assess the regulation of ERK phosphorylation during P19 EC cell differentiation with or without retinoic acid, Western blot analysis of whole cell lysates (WCL) was used to investigate the levels of pERK (Figure 4.8).

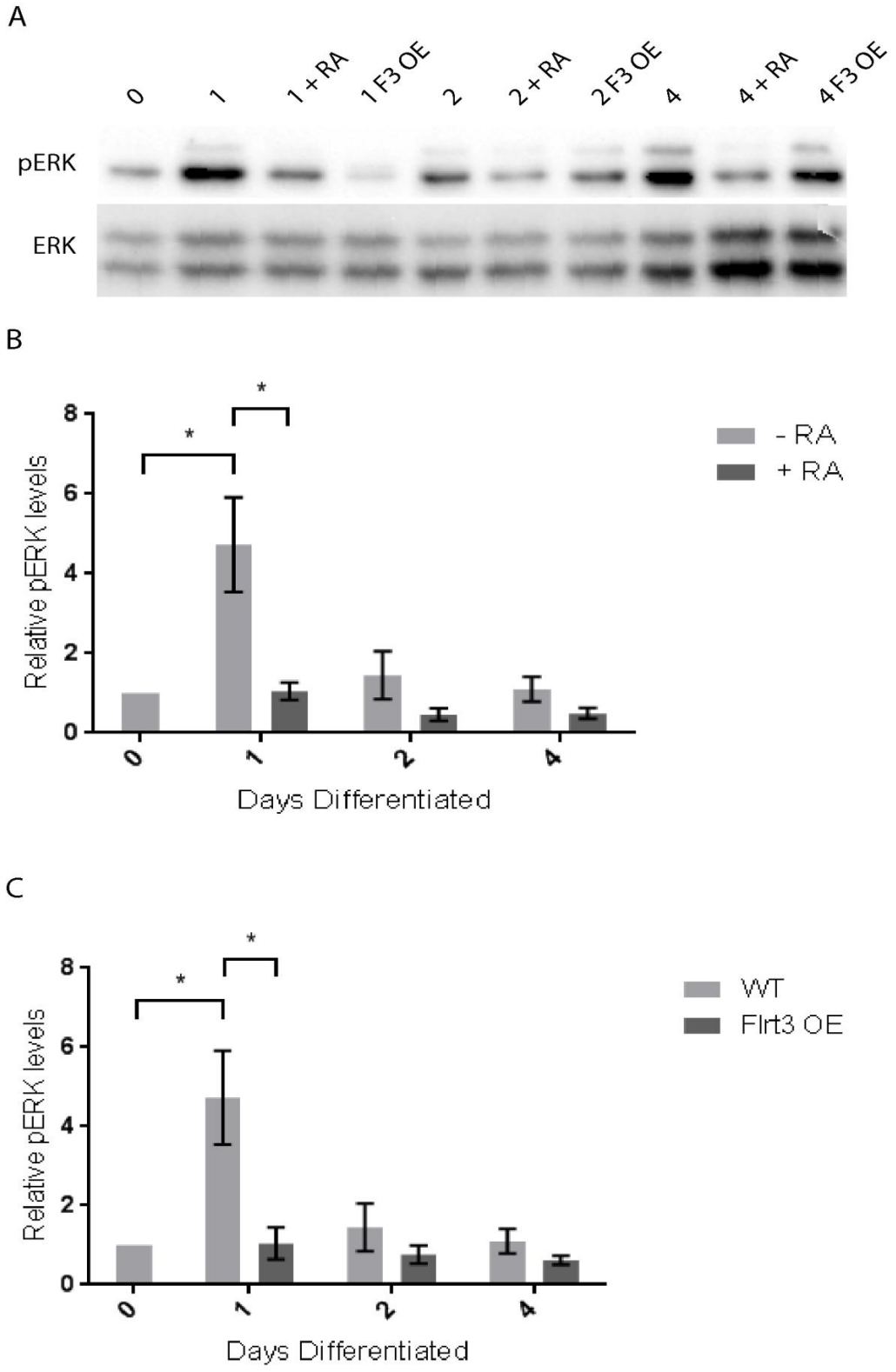

Figure 4.8. Increased expression of Flrt3 by RA differentiation and over-expression decreases ERK phosphorylation in differentiating P19 EC cells: P19 EC cells were differentiated either without RA (day number only), with RA (day number + RA) or while over-expressing Flrt3 (day number F3 OE) for 1 – 4 days, then lysed. WCLs were analysed by Western blot using pERK and ERK (for pERK densitometric normalisation) antibodies. A) Western blot representative of 3 independent experiments. pERK levels compared between cells differentiated without RA (day number only (A), - RA (B)) and those differentiated in RA (day number + RA) (B), and untransfected cells (day number only (A), WT (C)) compared to over-expressing Flrt3 cells (Flrt3 OE) (C) relative to undifferentiated cells (0). Error bars are S.E.M, n=3. Statistics analysed utilising Student's t-test, *=p<0.05.

By comparing the pERK:total ERK ratio between samples, it was found that differentiation of P19 EC cells without RA causes a transient increase in the amount of pERK by a significant 4.7-fold compared to undifferentiated cells after 1 day (Figure 4.8). Levels of pERK in cells differentiated without RA (- RA) returned to levels of undifferentiated cells after 2 days of differentiation and remain unchanged after 4 days. Differentiation for 1 day with RA (+ RA) shows no significant change in pERK levels from undifferentiated cells. When compared to cells differentiated without RA, cells differentiated with RA display a significant 4.5-fold increase in pERK levels (Figure 4.8 A and B). pERK levels in cells differentiated with RA for 2 and 4 days remain unchanged compared to undifferentiated cells, and are no different to cells differentiated without RA beyond the first day differentiation. Although not statistically significant, there is a trend for cell populations that express *Flrt3* at higher levels due to RA-differentiation to have slightly lower pERK levels than non-RA differentiated cells after 2 and 4 days (Figure 4.8 B and C) ($p>0.05$). Differentiation of cell lines was confirmed by qRT-PCR, with results showing a decrease in *Oct4* expression upon introduction of differentiation-promoting conditions, i.e. the lowering of HI-FCS levels from 10% to 5% (data previously shown).

As an increase in Flrt3 expression induced by RA correlated with an alteration in the level of pERK during P19 cell differentiation, the effect of over-expression of Flrt3 on pERK levels during P19 cell differentiation in the absence of RA was analysed. P19 EC cells were transiently transfected with an expression vector containing Flrt3 (Flrt3 OE) or untransfected (WT) and differentiated in the absence of RA for 4 days, with whole cell lysates (WCLs) analysed for levels of ERK phosphorylation (Figure 4.8 A and C).

Interestingly, Flrt3 OE cells show an identical expression profile of ERK phosphorylation as + RA differentiated cells over the four days of differentiation (Figure 4.8). Throughout the 4-day differentiation, Flrt3 OE cells have a statistically similar amount of pERK as day 0 WT cells. In keeping with the pattern observed for + RA differentiated cells, Flrt3OE cells show a 4.4-fold reduction in pERK level compared to WT cells. As previously described (Figure 4.8 B), WT cells reveal an increase in pERK after the first day of differentiation without RA, which then recedes to levels similar to that of undifferentiated cells for the remaining 3 days. Similar again to the observations made with the differentiation of P19 EC cells with and without RA, a statistically insignificant trend exists for cell populations that express *Flrt3* at higher levels, due to over-expression in this situation (Flrt3 OE), to have slightly lower pERK levels than WT differentiated cells after 2 and 4 days (Figure 4.8 B and C)

(p>0.05). A comparison of pERK levels in untransfected cells and cell transfected with empty pcDNA3.1 vector revealed no differences in ERK phosphorylation (data not shown).

When P19 EC cells undergo random differentiation, levels of pERK rise on the first day before returning to levels observed in undifferentiated cells. When these cells are differentiated towards a neural fate by the addition of RA, we see a rapid induction of *Flrt3* mRNA and protein, while an increase in pERK does not occur. Analysing ectopically over-expressed Flrt3, we see a similar abolishment of the increase in pERK levels. This is provocative evidence suggesting that the increased expression of Flrt3 in P19 cells may be responsible for the reduction in pERK levels, with its ability to regulate Fgf receptor providing a possible mechanism for this regulation. This reduction of ERK phosphorylation is in contrast to the increase in ERK phosphorylation seen for the over-expression studies in HEK-293T cells carried out in Chapter 3. However it is the first evidence to link endogenous Flrt3 expression and the regulation of a key signalling protein downstream of FgfR signalling.

4.2.5 *Flrt3* is expressed before *Sox1*, but is not solely responsible for *Sox1* expression in P19 EC cell neurectodermal differentiation.

The differentiation of P19 EC cells in the presence of RA results in a neurectodermal cell fate, an early step along the pathway to neural cell lineages [49]. A marker of early neurectodermal cell commitment is the expression of *Sox1*. The importance of this transcription factor in neural differentiation has been highlighted by the over-expression of *Sox1* being able to drive neural differentiation of P19 EC cells in the absence of RA, with robust expression within 24 h in P19 aggregates [50]. To compare the timing of *Flrt3* and *Sox1* expression, qRT-PCR analysis of *Sox1* expression was undertaken on P19 EC cells differentiated for up to 6 h in RA (Figure 4.9A).

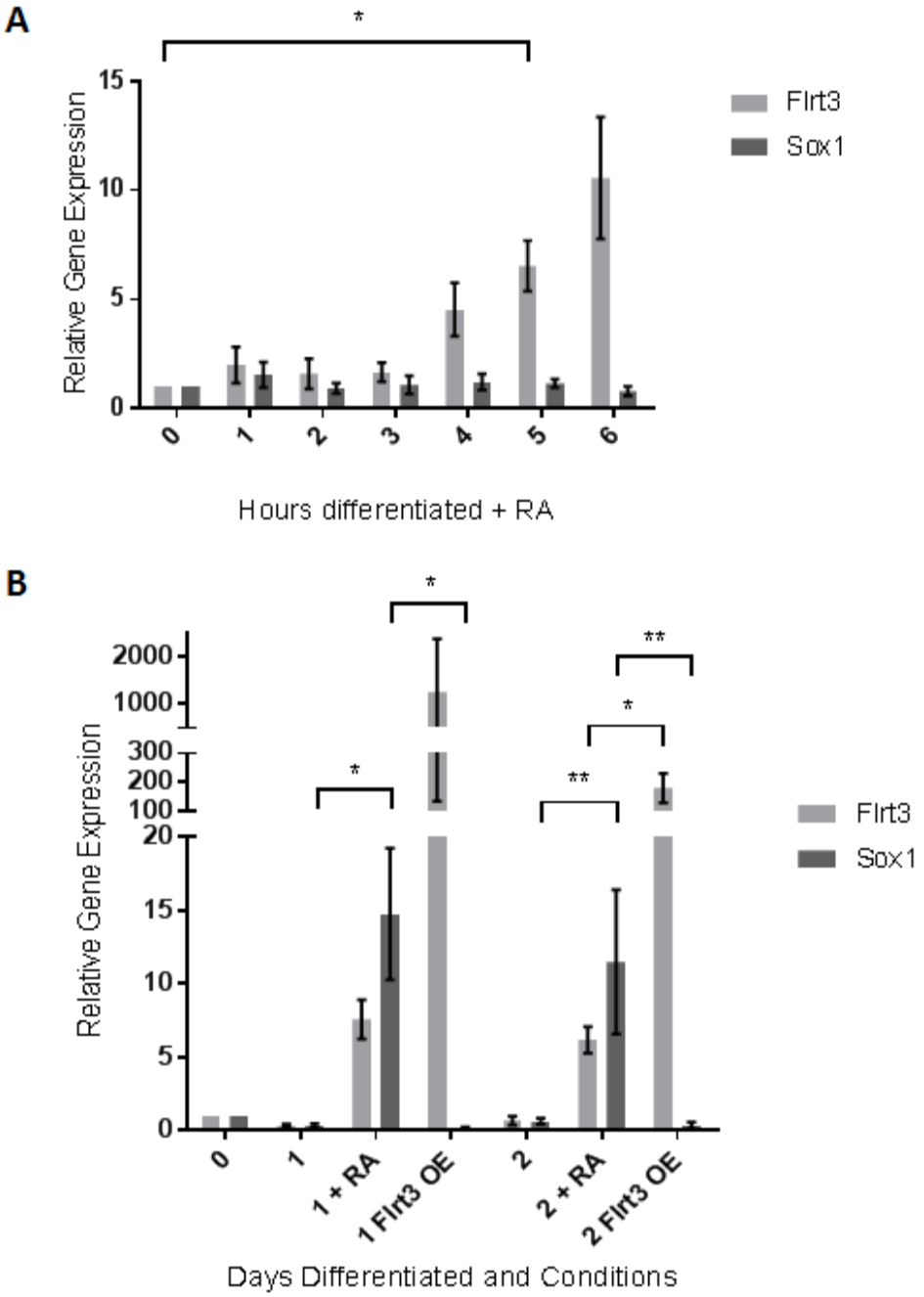

Figure 4.9. Expression of *Sox1* is induced by RA differentiation of P19 EC cells, but not Flrt3 OE: qRT-PCR analysis of RNA isolated from P19 EC cells. A) Cells were differentiated for up to 6 h with retinoic acid and expression of *Flrt3* and *Sox1* analysed B) Cells were differentiated up to 2 days with RA (number + RA) or without RA (number alone), or over-expressing Flrt3 (number + Flrt3 OE), and expression of *Flrt3* and *Sox1* analysed. Error bars are S.E.M, n=3. Statistics analysed utilising the Student's t-test, *=p<0.05, **=p<0.01.

During the first 6 h of differentiation, expression of *Sox1* does not vary between undifferentiated P19 EC cells (0) and cells differentiated with RA (1, 2, 3, 4, 5, and 6) (Figure 4.9 A). This is in contrast to *Flrt3*, with expression showing a significant increase in RA-treated cells compared to those without RA after 5 hours, with an 8.3-fold difference observed after 6 hours. After 1 day of differentiation, *Sox1* expression is shown to increase (Figure 4.9 B). Compared to cells differentiated without RA, *Sox1*

expression shows a significant 39.4-fold increase ($p<0.05$) after 1 day (1 vs 1 + RA), while after 2 days, a significant 22.4-fold increase ($p<0.01$) is observed (2 vs 2 + RA) in cells differentiated with RA (Figure 4.9 B). RA-induced differentiation results in a 14.7-fold increase in *Sox1* expression after 1 day compared to undifferentiated cells ($p<0.05$), with expression levels remaining consistently greater, and a 11.5-fold increase after 2 days in comparison to undifferentiated cells ($p<0.05$). No significant difference between day 1 or 2 differentiated cells is observed (Figure 4.9 B) ($p>0.05$). Cells differentiated for 1 and 2 days in media without RA (1 and 2) results in *Sox1* expression levels equivalent to those of undifferentiated cells. This therefore demonstrates that up-regulation of *Flrt3* expression precedes that of *Sox1* during neural differentiation of P19 EC cells.

As *Flrt3* expression is up-regulated prior to increased *Sox1* expression, it is possible that the increase in *Flrt3* expression may lead to up-regulation of *Sox1*. To determine if expression of *Flrt3* in the absence of RA was sufficient to induce *Sox1* expression, a Flrt3-containing expression vector was transiently transfected into P19 EC cells, with the cells differentiated without RA, and *Sox1* transcript levels measured by qRT-PCR (Figure 4.9B).

Flrt3 over-expression does not show any effect on *Sox1* levels after 1 or 2 days of differentiation, with *Sox1* expression levels remaining similar to cells differentiated without Flrt3 over-expression (Figure 4.9 B). Expression of *Flrt3* was at least 5-fold higher in Flrt3 OE samples than RA-differentiated samples (Figure 4.9 B), indicating successful plasmid transfection.

During RA-mediated differentiation, *Sox1* expression has been shown to increase after *Flrt3* expression is up-regulated. Increased expression of Flrt3 using an over-expression system does not result in an increase in *Sox1* expression over two days of differentiation, inferring that the increased expression of Flrt3 alone is not sufficient to drive *Sox1* expression in this cell system and there must be other factors involved in the ability to induce *Sox1* in RA-guided neural differentiation.

During early neural differentiation with RA, it has been shown that expression of *Flrt3* increases after just 5 h (Figure 4.1 C), with *Sox1* being expressed after this, but still within the first 24 hours (Figure 4.9 B). These experiments were performed using qRT-PCR on an entire population of cells, so it is unclear whether the individual cells that increase expression of *Flrt3* during RA-mediated differentiation also increase *Sox1* expression, or if *Sox1* is increased in cells that do not increase *Flrt3* expression. Using immunofluorescence assays, expression of Flrt3 and Sox1 in RA-differentiating P19 EC cells was investigated (Figure 4.10).

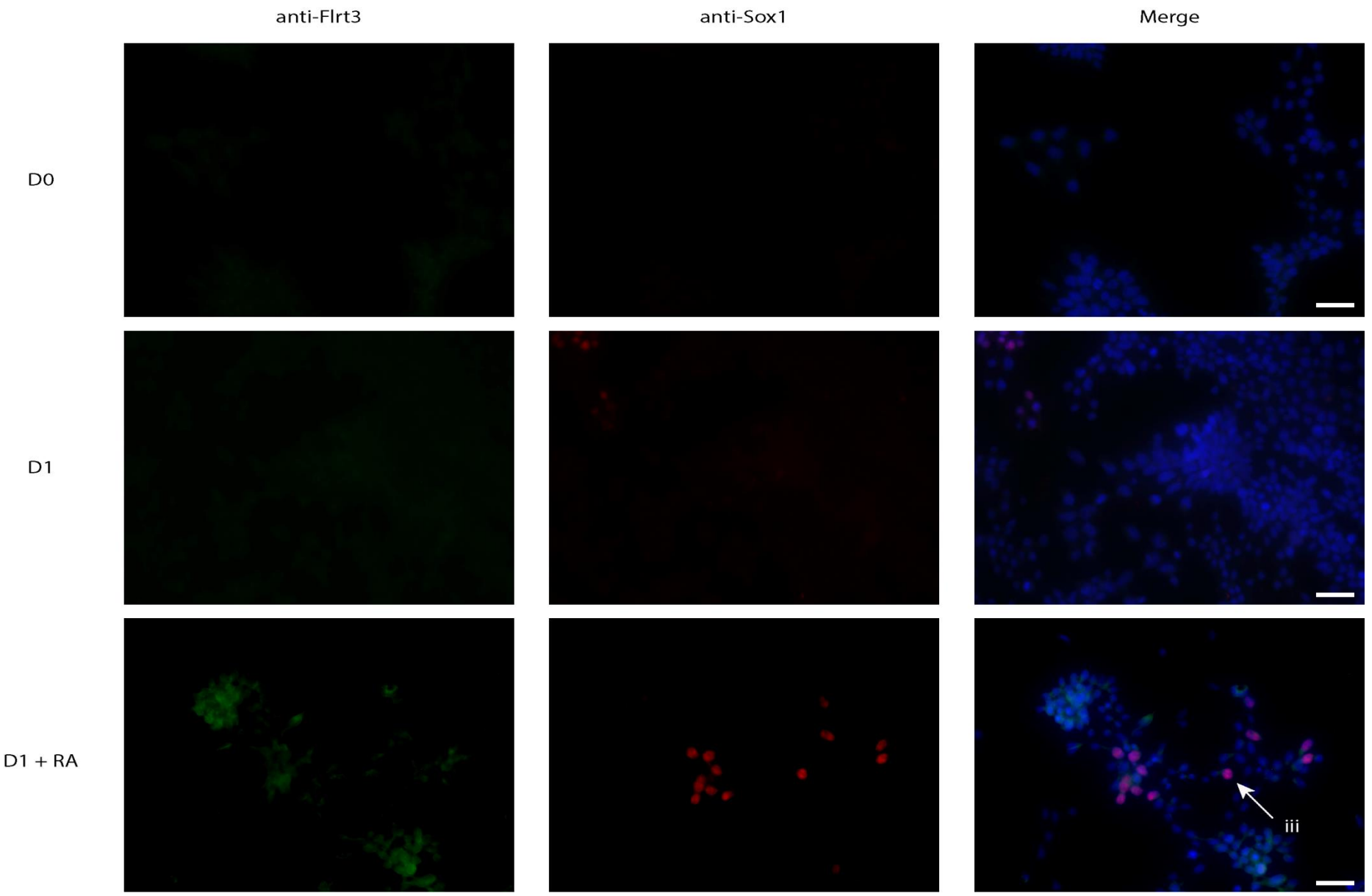
anti-Flrt3
anti-Sox1
Merge
D0
D1
D1 + RA
iii

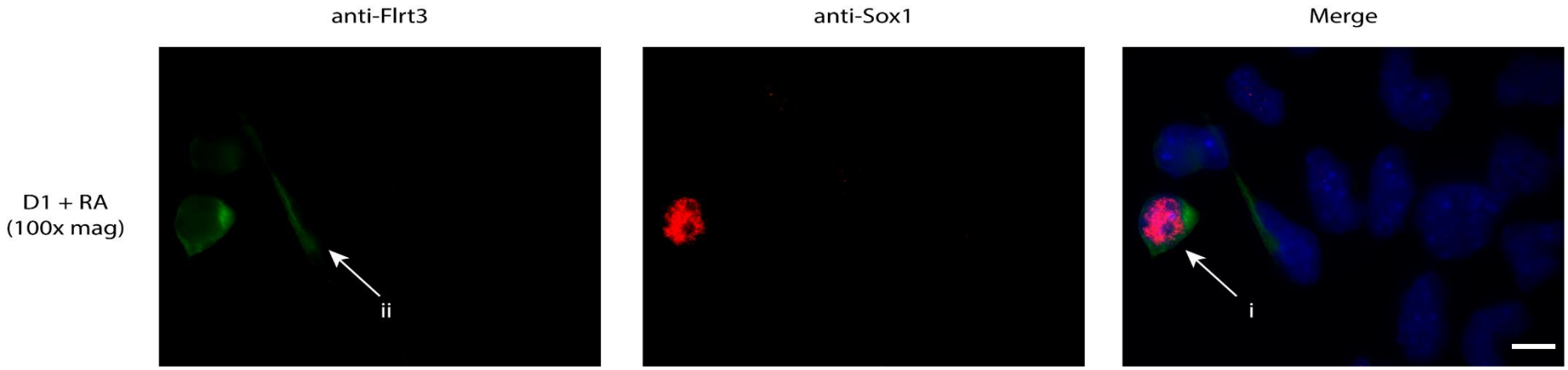

Figure 4.10. Sox1 expression is increased in P19 EC cells that have increased Flrt3 expression due to RA-mediated differentiation: Immunofluorescence assays of P19 EC cells differentiated for 1 day with (D1 + RA) or without RA (D1). Cells stained with anti-Flrt3 (green) and anti-Sox1 (red). Images taken on a Leica SP5 Spectral Scanning confocal microscope and are representative of cells from 5 total fields of cells. 20x (scale bar is 25 μm) or 100x (where noted, scale bar is 5 μm) magnification. Representations of i) Flrt3+ and Sox1+ cells, ii) Flrt3+ Sox1- cells, iii) Sox1+ Flrt3- cells. n=1.

Localisation of Flrt3 using antibody staining was similar to that observed in Figure 4.7, while Sox1 localisation was observed in the nucleus, consistent with its role as a transcription factor (Figure 4.10). Very little non-specific staining was observed for either of the antibodies. Cells observed during analysis of the immunofluorescence assay revealed a combination of expression profiles; cells that expressed Flrt3 and Sox1 (Figure 4.10 i), cells that expressed Flrt3 but not Sox1 (Figure 4.10 ii), cells expressing Sox1 but not Flrt3 (Figure 4.10 iii), and those cells that showed expression of neither protein, which made up the majority of cells counted. Analysis of images determined that undifferentiated P19 EC cells (D0) show little to no expression of Flrt3 or Sox1, as expected from Figure 4.9 and previous published data (five fields of view randomly selected from 3 different transfections, total of 1850 cells counted) [50]. After 1 day of differentiation without RA (D1), 2.95% of cells show Flrt3 expression, and 2.06% of cells show Sox1 expression. Only 0.85% of cells were observed to express both Flrt3 and Sox1 simultaneously (five fields of view randomly selected from 3 different transfections, total of 3059 cells counted). After 1 day of differentiation towards a neurectodermal fate (D1 + RA), approximately 10% of cells express Flrt3, and almost 20% of cells express Sox1, which is consistent with the mRNA expression for both genes. Interestingly, approximately half of the Flrt3 expressing cells (approximately 5% of the total cells) were shown to also express Sox1 (five fields of view randomly selected from 3 different transfections, total of 1950 cells counted).

Detection of Flrt3 protein has given further insight into the role of Flrt3 in neurectodermal differentiation. Flrt3 protein expression increases with differentiation using RA, a change that is consistent with the increase in mRNA levels observed in Figure 4.1 (when compared to cells differentiated without RA), with immunofluorescence staining revealing that detectible Flrt3 expression is observed in approximately 10% of cells (Figure 4.10). Higher levels of Sox1 expression are observed in cells differentiated for 1 day in RA compared to cells undergoing unguided differentiation (Figure 4.10), consistent with that of Sox1 mRNA levels (Figure 4.9). Without more time-points either side of 24 h, it is not possible to determine if all cells that express Flrt3 will show expression for Sox1. This experiment has provided an understanding that Sox1 is increased in nearly half of the cells that up-regulate Flrt3 expression during RA differentiation (Figure 4.10).

4.3 Discussion

The differentiation of P19 EC cells in the presence and absence of RA provides an excellent system for the investigation of the function of endogenous *Flrt3 in vitro*. The P19 EC cell system shows

a rapid (within 5 hours of the initiation of differentiation) and robust (continues after 4 days of differentiation) increase in *Flrt3* expression, with a maximum difference in *Flrt3* expression between RA- and non-RA differentiated cells of approximately 36-fold (Figure 4.1). Low expression of *Flrt3* in cells differentiated without RA suggests that spontaneous neural differentiation is slower or occurs rarely. The variation in *Flrt3* expression levels between experiments, exemplified in Figure 4.1, is caused by subtle variations in the proportion of cells responding to RA and a resulting heterogeneous cell population, confirmed by immunofluorescence analysis (Figure 4.7). Potential functional redundancy and compensation between Flrt family members is avoided using this system, as *Flrt1* and *Flrt2* expression is negligible and unaltered by RA-differentiation, making this a uniquely specific system for studying Flrt3 function. The use of the P19 EC cell line differentiated with RA as a model for the investigation of Flrt3 function is further strengthened by the induction of *Flrt3* expression in monolayer as well as aggregate differentiation models. Expression of *Flrt3* in P19 EC cell monolayers during RA-differentiation is comparable to that of those grown in aggregation as embryoid bodies. This therefore provides a simpler differentiation system without the complex cell-cell interactions that occur during embryoid body, and will aid the investigation into Flrt3 function and localisation, using experiments such as immunofluorescence assays. The induction of *Flrt3* in D3 ES cell aggregates treated with RA will allow any results found in P19 EC cells to be confirmed in ES cells. ES cells may allow comparisons between *in vitro* experiments and what occurs *in vivo*, with this RA-differentiation system somewhat replicating cellular organisation in the developing embryo. It is interesting to note the lack of change in *Flrt3* expression when D3 ES cells are cultured in the presence of LIF and RA. LIF is used to maintain ES cells in their pluripotent state, so a possible explanation for the lack of change in *Flrt3* expression in these cells is that the LIF is inhibiting RA signalling, and/or the expression of *RORα* is inhibited in the presence of LIF due to inactivity of controlling transcription factors, or the silencing of the promoters of *Flrt3* and *RORα*. While *Flrt3* expression shows a greater increase in P19 EC cells compared to D3 ES cells, *Flrt3* expression during differentiation of the D3 ES cells follows the same pattern of increase. These experiments have identified that the differentiation of the P19 EC cell line with and without retinoic acid is the best model known to date for investigating Flrt3 function.

The rapid nature of transcriptional induction of *Flrt3* suggests direct regulation of expression by RA. Use of luciferase vectors containing regions of the *Flrt3* promoter transfected into RA-mediated differentiating P19 EC cells potentially allowed identification of sites of regulation using the *in vitro* system. The limitation of this experiment includes the absence of potential long-range regulatory elements, and the size limitations of upstream regulatory sequences/elements that could be incorporated into a single vector. A stretch of sequence between 4 kb and 6 kb upstream of the *Flrt3*

start site was identified as responsible for a small portion of the RA induced increase in *Flrt3* expression (Figure 4.4), although the levels of luciferase activity are much less than the level of endogenous *Flrt3* expression. Therefore, elements outside of the 6kb upstream of the *Flrt3* promoter region must be responsible for the majority of the increase in *Flrt3* expression observed during RA-mediated differentiation of P19 EC cells. While a difference in luciferase activity is observed between 6 kb luciferase transfected cells differentiated with or without RA, this is slightly reduced by the second day of differentiation, although this is not significant. The observed lack of difference in luciferase activity after 2 days suggests that this element is potentially involved in the initial rapid increase in *Flrt3* expression, with other elements allowing the maintenance of *Flrt3* expression. The observation of no difference in luciferase activity between vectors with or without the *Flrt3* transcriptional start site implies that sequence spanning approximately 200 bp immediately 5´ and 3´ of the start site is not important in regulating the increased expression of *Flrt3* in this system. It is interesting to note that the stretch of DNA identified using this system partially responsible for the increase in *Flrt3* expression does not reside within the region of DNA found to be highly conserved between organisms. This may therefore be a feature of higher order mammals exclusively, and lie in regions of conservation between higher-order mammals not specifically investigated in this project.

While an increase in gene transcription may logically cause an increase in protein expression, this does not occur in all situations. Immunofluorescent staining shows that an increase in *Flrt3* transcription results in the increased translation of Flrt3 after just one day of differentiation with the levels of protein expression mirroring that of gene expression using this differentiation system (Figure 4.1). Induced Flrt3 protein expression localised to perinuclear membranes, and membrane boundaries between adjacent cells with increased Flrt3 expression (Figure 4.7). Flrt3 protein detection showed a cell population with varying levels of increased Flrt3 expression after treatment with RA, highlighting the homogenous nature of P19 cell differentiation eluded to earlier in this discussion.

Localisation of Flrt3 during RA-mediated differentiation of P19 EC cells to intracellular membranes provides an appropriate cellular localisation for Flrt3 to interact with and regulate membrane receptors that utilise MAPK signalling, such as FgfR1, as has been observed using *in vitro* assays described in Chapter 3, and predicted *in vivo* from Flrt3 expression patterns. ERK phosphorylation was relatively unchanged from basal levels during both RA-mediated neural differentiation of P19 EC cells and differentiation of P19 EC cells over-expressing Flrt3, whereas, a 4.5-fold increase in ERK phosphorylation is observed in P19 EC cells undergoing unguided differentiation (Figure 4.8). This data, combined with previous evidence of Flrt3 function, implicates endogenous Flrt3 in the regulation of

pERK levels. This is a previously unidentified role for endogenous Flrt3, and may be related to a potential interaction with FgfR1, observed using over-expression assays in Chapter 3.

The rapid induction of *Flrt3* upon neurectodermal differentiation identified in the RA-mediated P19 EC cell differentiation system prompted a comparative analysis with *Sox1* expression; the earliest known marker of neural lineage commitment. Interestingly, *Flrt3* induction occurs at least 1 h prior to that of *Sox1* in cells differentiating with RA (Figure 4.9), identifying Flrt3 as a potential very early marker of P19 cell differentiation. In saying this, cells that over-express *Flrt3* and differentiate without RA do not cause induction of *Sox1* expression within the initial two days of differentiation. This may mean that these cells are not undergoing neural differentiation, or that *Flrt3* expression is not sufficient to drive neural differentiation within the 2 days analysed. Due to the presence of a heterogeneous cell population in relation to those cells transiently transfected with Flrt3-expressing vector or those with *Flrt3* induction due to RA-exposure, conclusions cannot be drawn based on assessment of overall cell populations, such as qRT-PCR used here. Analysis of individual cells or populations of cells stable over-expressing *Flrt3* must be undertaken to determine if those that are showing increased expression of *Flrt3* do go on to express *Sox1* and therefore undergo neurectodermal differentiation.

Using immunofluorescence assays of P19 EC cell monolayers, shown to similarly induce *Flrt3* expression, and probing for Flrt3 and Sox1 allowed the confirmation of a heterogeneous population of cells and the extent of the complexity of the system (Figure 4.10). This experiment was undertaken only once to obtain a basic trend of what is occurring within the cell populations, hence the lack of statistics. Approximately 10% of cells differentiating with RA express Flrt3 protein, with 17% of Flrt3-positive cells also expressing Sox1. From this experiment, we can conclude that Flrt3 and Sox1 expression do not correlate well, thus supporting the hypothesis that an increase in Flrt3 expression alone is insufficient to drive neurectodermal differentiation, indicating the importance of other proteins.

The experiments in this chapter have shown that *Flrt3* is induced in P19 EC cells by RA differentiation at both the mRNA and protein level. They have also shown that pERK levels are altered by Flrt3 over-expression and RA treatment during differentiation. Despite these findings, details of how these interactions impact cellular differentiation are unknown due to the limitations of the experiments performed, e.g. the heterogeneous nature of the culture during RA differentiation and transient transfection. Heterogeneity in Flrt3 over-expression results in the ‘diluting’ of observed Flrt3-phenomena by cells that do not over-express Flrt3 for experimental techniques that utilise cell populations rather than individual cell analysis. These include some techniques performed in this chapter, including qRT-

PCR (Figure 4.1 and 4.9), luciferase assays (Figure 4.4), and Western blot (Figure 4.8). This heterogeneity could be overcome in a number of ways, which are described in Chapter 6.3. Using these systems, cultures would be very close to, if not homogeneous in nature, and cells with unaltered Flrt3 expression excluded from analysis. It would then be possible to further elucidate the function and mechanism of endogenous Flrt3 activity.

4.4 Conclusion

The results of experiments presented in this chapter have identified the P19 EC cell RA differentiation system as a suitable model for studying endogenous Flrt3 function. Expression of *Flrt3* occurs in a rapid and robust manner, with induction occurring within 5 h of differentiation, and increased expression maintained beyond 4 days of differentiation. The increase in *Flrt3* expression is primarily due to elements outside of the regions investigated, but a stretch of DNA between 4 kb and 6 kb upstream of the *Flrt3* start site appears to be partially responsible. The induction of *Flrt3* translates into an increased expression of Flrt3 protein, with increased Flrt3 expression appearing to be integral in maintenance of low pERK levels upon differentiation of P19 EC cells. *Flrt3* is expressed before neural lineage marker *Sox1* suggesting it is a very early marker of neurectoderm differentiation, but an increase in Flrt3 expression alone is not sufficient to induce *Sox1* expression during differentiation. Other factors appear to play a role in the induction of neurectodermal differentiation besides Flrt3, with cells expressing Flrt3 under RA-differentiation more likely to show expression of Sox1 compared to Flrt3-transfected cells. Identification of this system will allow further analysis of Flrt3 function during neurectodermal differentiation and a probable role in the regulation of ERK phosphorylation, possibly though modulation of FgfR signalling.

5. Single-pass LRR transmembrane proteins as regulators of FgfR1 activity.

5.1 Introduction

In Chapter 3, I have presented data that infers Flrt3 plays a role in FgfR1 signalling when over-expressed. In conjunction with data showing Flrt1 also increases FgfR1 signalling [41], it is believed that the Flrt family as a whole could regulate FgfR1 signalling by increasing its signalling activity. As previously shown, there are many single-pass LRR protein families in the mammalian genome. The Lrrtm family is closely related to the Flrt family, with both families encoding structurally similar proteins, and some members also showing expression patterns overlapping with FgfR during embryogenesis and in regions where Fgf signalling is known to be functionally important.

The Lrrtm family consists of 4 genes that encode type I transmembrane proteins with 10 extracellular LRR domains, a transmembrane domain, a family-conserved 71 or 72 amino acid intracellular sequence containing a terminal PDZ domain protein docking site consensus sequence, and several potential N-linked glycosylation sites [51]. Sequence identity between the family ranges from 43% to 63% for the human proteins, and sequence identity between human and mouse orthologues shows a high degree of conservation, ranging from 95% - 98%. Post-natal expression profiles of *Lrrtm* members are diverse, with *Lrrtm3* being the most limited. All *Lrrtm* family members are expressed in the neurons of the adult brain at varying levels with various sub-cellular distributions, where they have been shown to act as synaptic organisers [51, 52] (Figure 5.1).

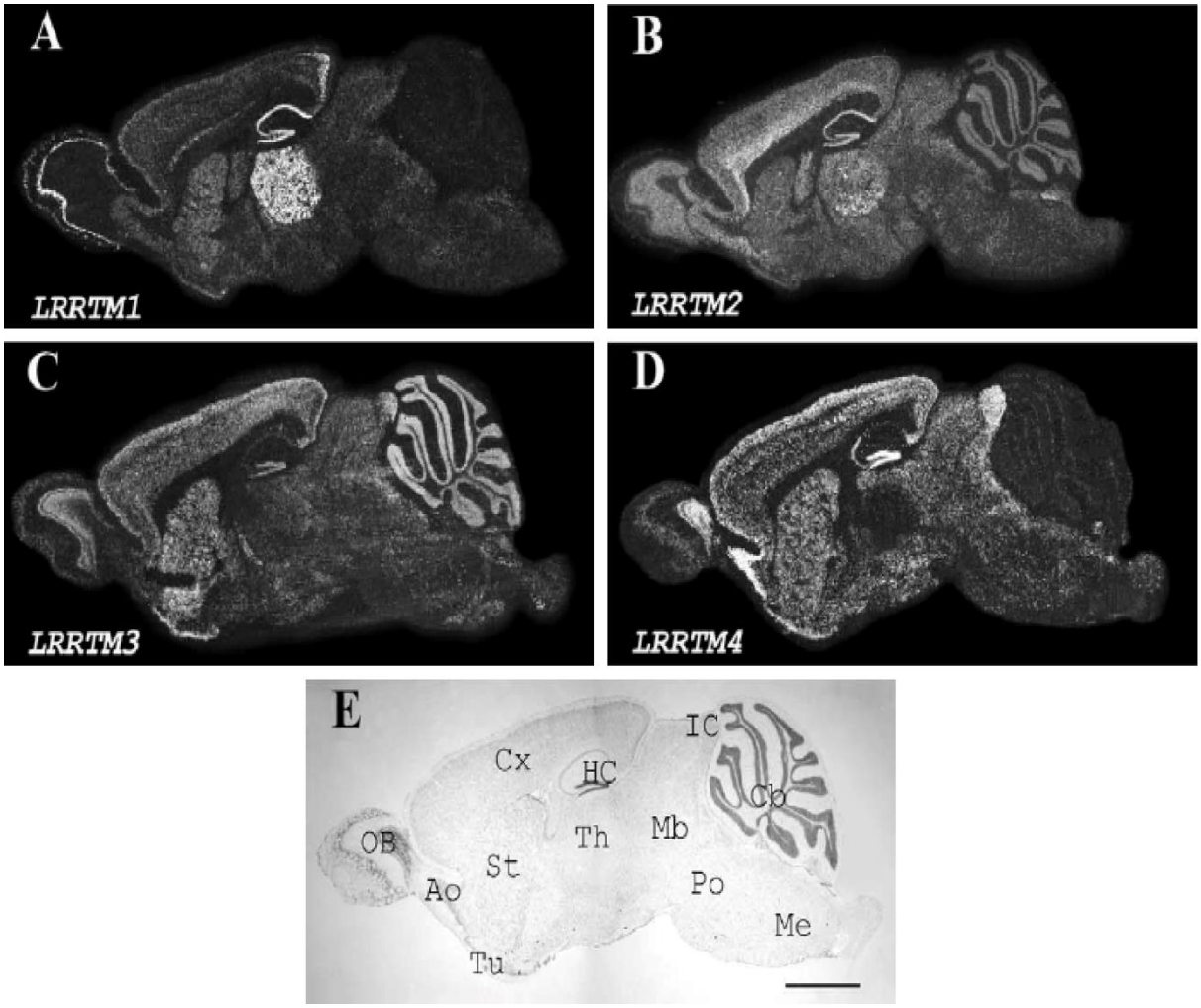

Figure 5.1. *In situ* hybridisation analysis of *LRRTM* family mRNA expression in the adult mouse brain. Shown are dark-field emulsions autoradiographs: A) *LRRTM1*, B) *LRRTM2*, C) *LRRTM3*, D) *LRRTM4*. E) The bright-field image of (D). OB, olfactory bulb; Ao, anterior olfactory nucleus; Tu, olfactory tubercle; St, striatum; Cx, cerebral cortex; Th, thalamus; HC, hippocampus; IC, inferior colliculi; Mb, midbrain; Po, pons; Me, medulla; Cb, cerebellum. Scale bar, 1 mm. Adapted from [51].

Embryonic expression of *Lrrtm1* is first observed at 9 *dpc* in the overlying ectoderm of the developing limb bud that forms the presumptive AER, while neural expression is present in the forebrain, midbrain and hindbrain [53]. Limb expression becomes more restricted by 10 and 11 *dpc*, where it is localised exclusively to the AER. *Lrrtm2* shows restricted expression, observed only within a collection of lateral cells in the motor horn at 10 *dpc* [53]. Expression of *Lrrtm3* in mouse is observed from early- to mid-gestation, with expression present from 8.5 *dpc* (Figure 5.2).

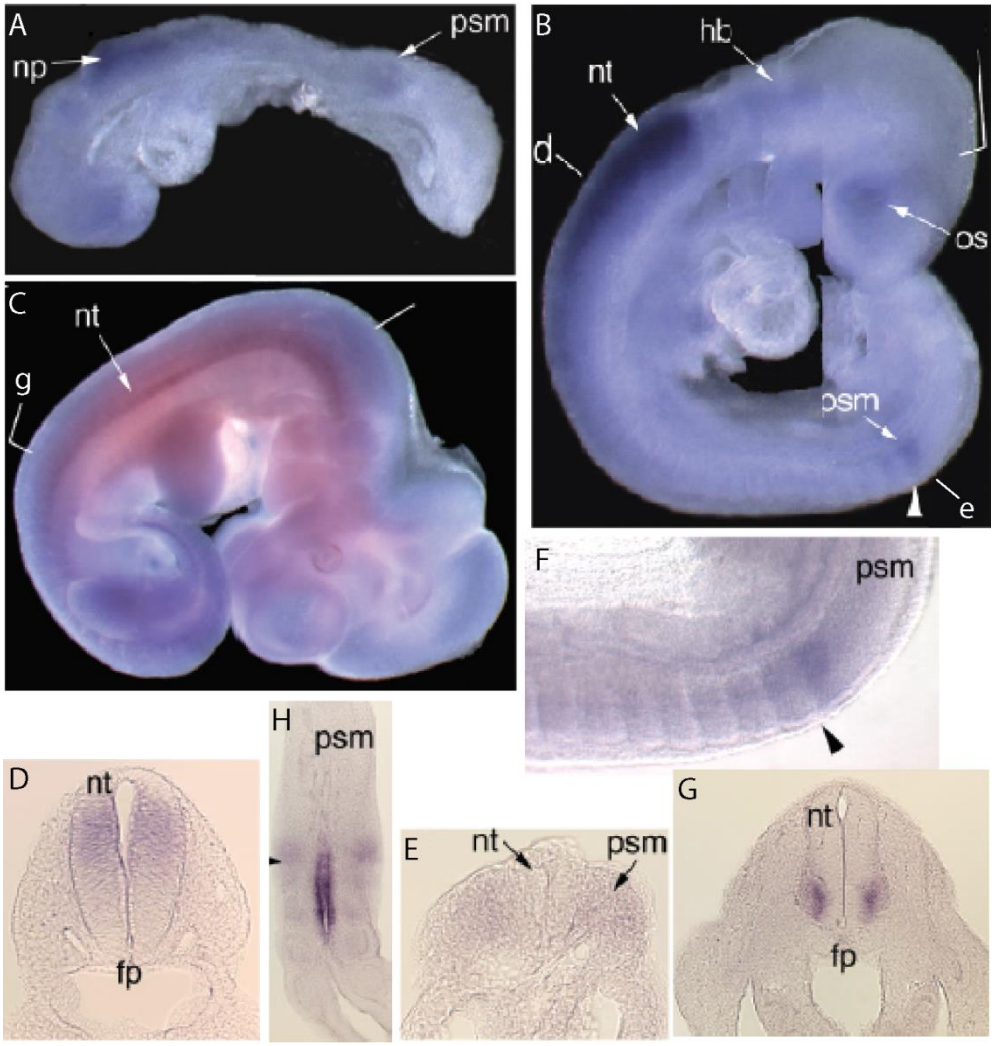

Figure 5.2. Expression of *Lrrtm3* during mid-gestation embryogenesis: *Lrrtm3* expression is detected by whole mount *in situ* hybridisation on 8 *dpc* mouse embryos. A) Expression is evident in the presomitic mesoderm (psm), the rostral neural plate (np), and the head. B) Expression in the rostral neural tube (nt) is present in dorsal neural progenitors at 9 *dpc*. C) Further expression became evident in the neural tube (nt) with expression in the rostral neural tube reducing in dorsal neural progenitors and initiating in centrally located lateral cells at 11 *dpc*. D) Expression is detected in the head, and expression in the presomitic mesoderm (psm) (E) is present in a stripe at the boundary with the most recently formed somites. The approximate plane of section D and E is shown in lower case (B). An interference contrast image of the tail of the embryo in B (F) shows expression at the presomitic mesoderm/somite boundary (arrowhead). Caudal expression localises to a group of cells within the motor horn at 11 *dpc* (G). The approximate plane of section G is shown in lower case (C). H) Expression is present in the hind-gut diverticulum. Adapted from [53].

Neural expression of *Lrrtm3* is strong in anterior neural plate neural progenitor cells (which go on to form the rostral neural tube), forebrain and hindbrain at 8.5 *dpc*, and continues to increase through to and beyond adulthood. Expression is also observed at the presomitic mesoderm/somite boundary and within early somites, which continues beyond 11 *dpc*. As the somite continues to develop, expression gradually decreases and is restricted to the somite boundaries. Expression of *Lrrtm3* is restricted to the brain exclusively post-natally [51, 53]. *Lrrtm4* expression is present at 8.5 *dpc* in embryos in the caudal lateral mesoderm, which persists through to 11 *dpc*, when expression is seen in stripes in the anterior mesoderm in the developing sclerotome. *Lrrtm4* is also present in the limb

mesenchyme in the distal limb bud at 9.5 *dpc*. Neural expression of *Lrrtm4* is seen in the neural tube and the developing brain at 9.5 *dpc*, where expression is maintained throughout development [51].

Functional data for Lrrtm proteins is limited, although Linhoff *et al*. (2009) identified an important role for the Lrrtm family as organisers of excitatory presynaptic differentiation, allowing postsynaptic differentiation. All Lrrtms localise to the cell membrane where over-expression of Lrrtm1, 2, and 4 show a >14-fold increase in synapsin clustering when compared to controls, thought to be due to the LRR domain. In contrast to this, Lrrtm3 only displayed limited activity, suggesting a different role [52, 54]. An *Lrrtm1* knockout has revealed a claustrophobia-like behaviour, whilst single nucleotide polymorphisms of *Lrrtm3* have been identified in increased susceptibility to developing autism spectrum disorders [55, 56]. During development, expression of *Lrrtm1* is observed in the AER and the endolymphatic appendage, and *Lrrtm3* is expressed at the somite/presomitic mesoderm boundary; tissues that rely on FgfR signalling for their correct development. Post-natally, expression of all *Lrrtms* are observed in the dentate gyrus; a region which relies on FgfR signalling for neurogenesis during adulthood [51, 53, 57]. With a similar structure to the Flrt family and expression patterns that overlap with regions of FgfR signalling importance, investigation of an interaction between Lrrtm3 and FgfR1 was performed. Using experiments based on those carried out by Wheldon *et al.* (2010), I attempted to identify novel roles of Lrrtm proteins and to further elucidate if characteristics identified for Flrt1 and Flrt3 over-expression are representative of other LRR proteins.

5.2 Results

5.2.1 Investigation of an interaction between Lrrtm3 and FgfR1

With expression in common tissues, an interaction observed between the Flrt proteins and FgfR1, and the high degree of structural similarity between the Flrt and Lrrtm proteins, there is potential for an interaction to exist between Lrrtm3 and FgfR1. Utilising HEK-293T cells co-transfected with FLAG-tagged FgfR1 and HA-tagged Lrrtm3 and subsequent co-immunoprecipitation, this potential interaction was investigated (Figure 5.3).

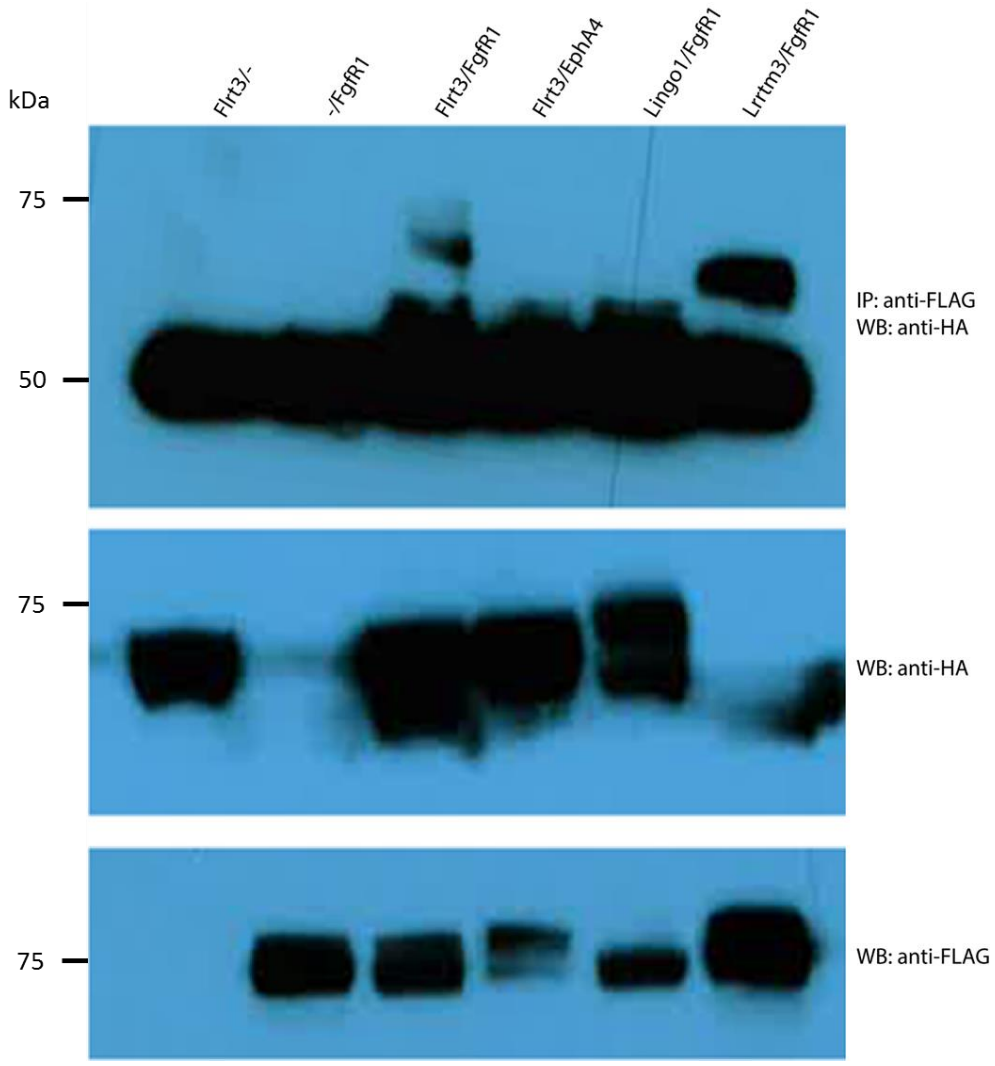

Figure 5.3. LRR protein Lrrtm3 interacts with FgfR1: Expression vectors for HA-tagged LRR proteins Flrt3, Lingo1 and Lrrtm3 were co-transfected into HEK-293T cells with expression vector encoding Flag-tagged FgfR1 and EphA4. Cells were harvested and WCLs underwent co-immunoprecipitation for FLAG-tagged proteins (upper panel). Precipitated proteins were analysed by Western blot, probing for HA to identify LRR proteins interacting with FgfR1/EphA4. Immunoprecipitation inputs were analysed by Western blot using anti-HA (middle panel) and anti-FLAG (lower panel) antibodies to confirm expression of LRR construct and specific pull-down with the FLAG antibody respectively. Input 1° Ab: mouse α-HA (6E2), 2° Ab: donkey α-mouse HRP. Co-immunoprecipitation 1° Ab: mouse α-HA (6E2), 2° Ab: donkey α-mouse HRP. - = pcDNA3.1 transfected (vector control). Representative of 3 independent experiments.

Upon co-expression and immunoprecipitation with anti-FLAG, an interaction between Lrrtm3 and FgfR1 was identified by the presence of a band of the correct molecular weight of Lrrtm3 in the Lrrtm3/FgfR1 transfected cells (Figure 5.3 upper panel). This is similar to that observed for the Flrt3/FgfR1 (positive control) transfected cells. The prominent band in each lane of the immunoprecipitation is the heavy Ig chain from the immunoprecipitation antibody, mouse anti-FLAG, which appears due the use of a mouse secondary antibody in the Western blot. Cells over-expressing Flrt3 and EphA4 receptor, along with cells over-expressing LRR protein Lingo1 and FgfR1 show no interaction between the over-expressed proteins, as observed by the lack of a band in the immunoprecipitation.

Transfection and expression of each of the proteins was successful, demonstrated by the bands in appropriate lanes of westerns of WCLs (Figure 5.3 middle and lower panels). When expressed alone, Flrt3 (Flrt3/-) cells show no band when probed for FgfR1, demonstrating the specificity of the anti-FLAG western antibody. Cells over-expressing FgfR1 alone (-/FgfR1) show no bands when probed for HA-tagged proteins, demonstrating the specificity of the HA-antibody in the Western blot. The results of these experimental controls are as expected and validate the experiment.

The immunoprecipitation assay has revealed that an interaction exists between Lrrtm3 and FgfR1. Due to the nature of this technique, it is not clear whether this interaction takes place in the native cell, or upon cell lysis. To have an effect on FgfR signalling as Flrt1 and Flrt3 do, Lrrtm3 and FgfR1 must be expressed in the same cell membrane for an interaction to take place.

5.2.2 Localisation of over-expressed Lrrtm3 and FgfR1

Immunoprecipitation has shown that an interaction between Lrrtm3 and FgfR1 exists, but the context of this interaction is undefined. To have any functional relevance, these proteins need to be localised to common membranes within the cell. Immunofluorescence experiments on cultured Cos-7 cells transiently transfected with expression vectors encoding for Lrrtm3-HA and FgfR1 were performed to determine the sub-cellular localisation of Lrrtm3, and if it co-localises with FgfR1 within cellular membranes (Figure 5.4).

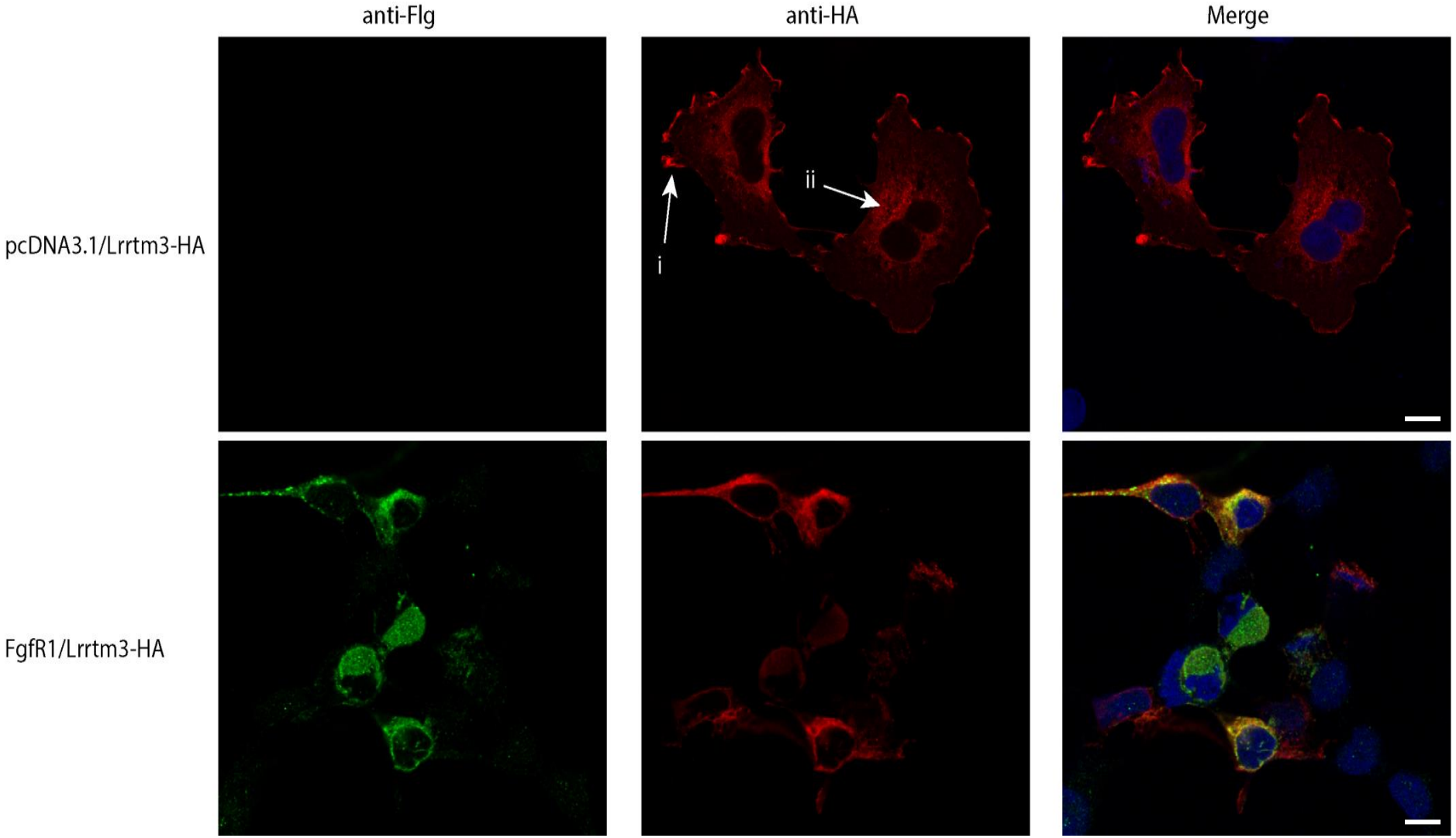

Figure 5.4. Lrrtm3-HA co-localises with FgfR1: Immunofluorescence assay of Cos-7 cells transiently co-transfected with 3'HA-Lrrtm3 and FgfR1 or pcDNA3.1 (vector only control). Cells stained with anti-FgfR1 (Flg antibody, green) and anti-HA (Lrrtm3, red). 'i' shows cell surface membrane localisation. 'ii' shows intracellular membrane staining. Merged images show co-localisation in yellow. Images taken a Leica SP5 Spectral Scanning confocal microscope. 100x magnification. Scale bar is 5 µm.

Expression of Lrrtm3 alone (pcDNA3.1/Lrrtm3-HA) reveals localisation at the cell surface membrane (Figure 5.4 pcDNA3.1/Lrrtm3-HA 'i') and within intracellular membranes close to the nucleus (Figure 5.4 pcDNA3.1/Lrrtm3-HA 'ii'). Cell surface expression of Lrrtm3 was more extensive than that seen previously for FgfR1 (Figure 3.1). Lrrtm3 expression in the cell surface membrane appears concentrated in specific regions including, but not limited to, areas of the cell facilitating cell-cell contacts. Like that observed for cells over-expressing Flrt3, cells over-expressing Lrrtm3 generally occur in small clusters, although lone single cells expressing Lrrtm3 were also observed. Co-expression of Lrrtm3 and FgfR1 showed overlapping and distinct domains of protein expression (Figure 5.4 FgfR1/Lrrtm3-HA, yellow staining). Co-localisation of FgfR1 and Lrrtm3 exists mostly in the vesicles and membranes within the cytoplasm, adjacent to the nucleus. When co-expressed, Lrrtm3 is co-localised with FgfR1 at the extremities of the cell, but not at the cell membrane as observed when expressed alone.

Co-transfecting cells with vectors encoding Lrrtm3 and empty pcDNA3.1 reveals these cells do not exhibit detectable Flg-antibody staining in the exposure time used (Figure 5.4 pcDNA3.1/Lrrtm3-HA). Use of the HA-antibody to detect the over-expressed protein results in detectible signal for both transfection experiments, acting as positive controls for the experiment. The results of these controls validate the experiment.

This experiment has shown that Lrrtm3 and FgfR1 co-localise in the same membranes within the cell, providing an *in vivo* context for the interaction. Co-localisation of Lrrtm3 and FgfR1 in intracellular membranes is similar to that observed for the Flrt1/Flrt3 and FgfR1 interaction, and facilitates a possible regulation of FgfR1 signalling as observed with Flrt1 and Flrt3 [41] (Chapter 3).

5.2.3 Effect of Lrrtm3 over-expression on FgfR1 signalling

Similar to Flrt1 and Flrt3, the majority of Lrrtm3 interaction with FgfR1 co-localisation occurs within intracellular vesicles, which positions Lrrtm3 in the correct location to be able to influence the output of FgfR1. Wheldon *et al.* (2010) showed that over-expression of Flrt1 caused a subtle but consistent increase in ERK phosphorylation when analysed using a time course of Fgf-2 stimulation, while I have shown that Flrt3 over-expression causes a trend towards increase in ERK phosphorylation [41] (Chapter 3). Regulated FgfR1 signalling due to the expression of Lrrtm3 and the mechanism associated with the interaction can be assessed in a similar manner. HEK-293T cells were transiently

co-transfected with Lrrtm3-HA and FgfR1 and stimulating the cells with Fgf-2, with FgfR1 signalling evaluated by measuring pERK levels by Western blot (Figure 5.5).

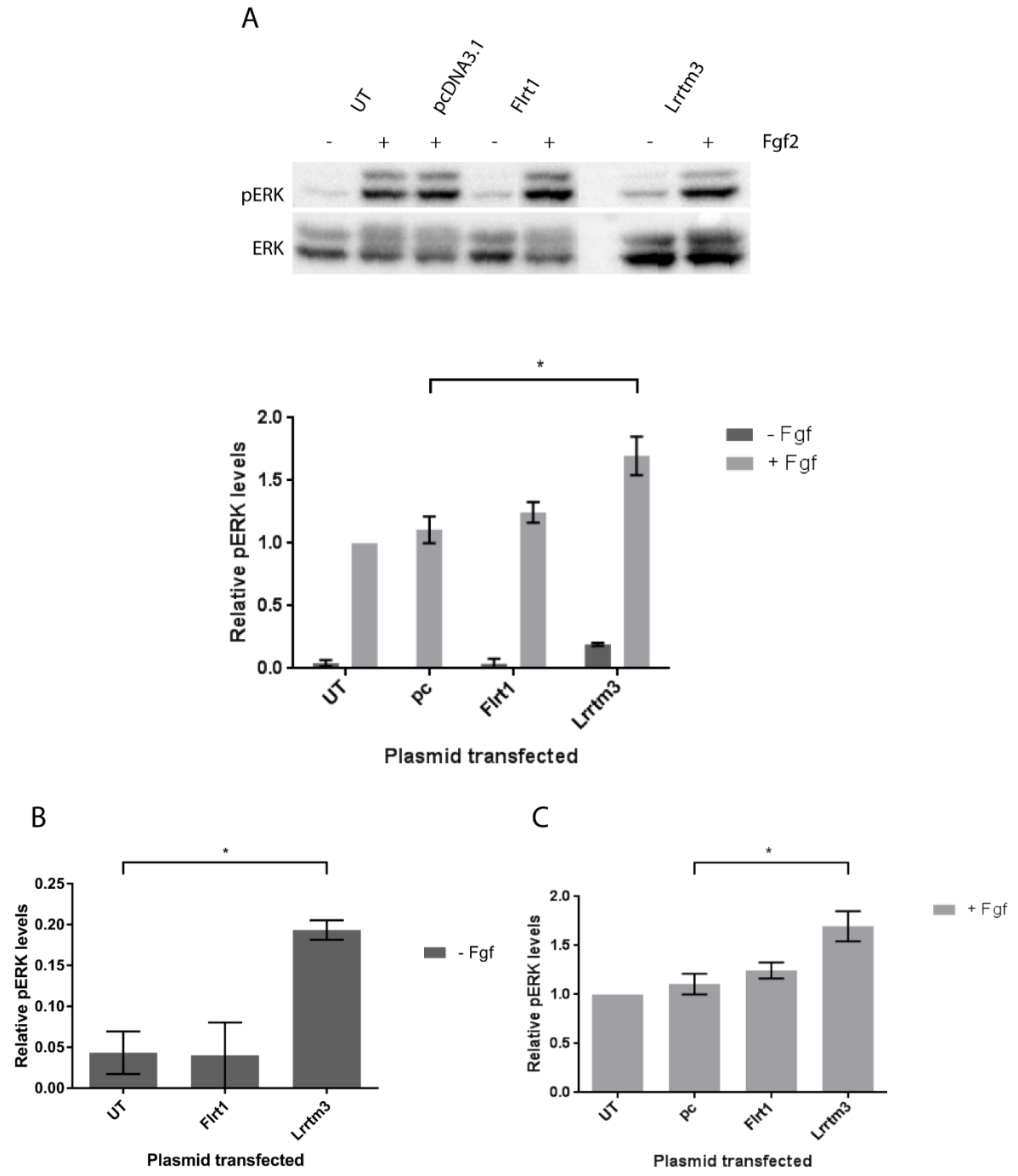

Figure 5.5. Over-expression of Lrrtm3 causes an increase in pERK levels: Western blot of HEK-293T cells transiently transfected with indicated plasmids (UT = untransfected, pc = pcDNA3.1 transfected (vector only control)) for 20 h, then stimulated with Fgf-2 and heparin for 10 min. A) Western blot probed with anti-pERK and anti-ERK (for pERK densitometric normalisation). Representative of 3 independent experiments. ERK phosphorylation levels compared between unstimulated (-Fgf) and Fgf-2 stimulated (+ Fgf) cells relative to untransfected Fgf-2 stimulated cells. B) Quantification of pERK levels in unstimulated cells. C) Quantification of pERK in Fgf-2 stimulated cells. Error bars are S.E.M, n=3. Statistics analysed utilising the Student's t-test, *=p<0.05.

Basal levels of pERK are observed in untransfected cells (UT - Fgf) which is significantly increased (23-fold) upon stimulation with Fgf-2 (UT + Fgf), showing that Fgf-2 stimulation is inducing FgfR activation and subsequent ERK phosphorylation (Figure 5.5). In this experiment, untransfected (UT) and pcDNA3.1-transfected cells (pc) are used as controls for basal pERK levels when untreated and for pERK levels upon Fgf-2 stimulation. The Fgf stimulated pc cells (pc + Fgf) show no difference in pERK levels compared to UT + Fgf cells, indicating that transfection of the expression vector alone does not drastically alter ERK phosphorylation. Cells transfected with Flrt1 show no significant difference in ERK phosphorylation when compared to untransfected cells or cells transfected with empty expression vector pcDNA3.1 (pc - Fgf) ($p>0.05$), whether unstimulated or stimulated with Fgf-2 (Figure 5.5). This is consistent with previous data for over-expression of Flrt1 at this time point [41].

Unstimulated cells over-expressing Lrrtm3 (Lrrtm3 - Fgf) result in a 4.5-fold increase in pERK levels when compared to untransfected cells ($p<0.05$) (Figure 5.5 B). A similar observation is made when comparing to the Flrt1-transfected cells, with a 4.8-fold increase in ERK phosphorylation, which is significant at a 90% confidence level (Figure 5.5 B). Fgf-2 stimulated Lrrtm3 over-expressing cells (Lrrtm3 + Fgf) showed a 1.6-fold increase in the amount of pERK when compared to untransfected HEK-293T cells, and a significant 1.5-fold increase when compared to cells transfected with empty vector ($p<0.05$ for both) (Figure 5.5 C). No difference in ERK phosphorylation between Flrt1 and Lrrtm3 transfected cells is observed at the 95% confidence interval (Figure 5.5 C).

In summary, this experiment shows that not only are pERK levels increased in Lrrtm3 over-expressing cells upon stimulation with Fgf-2, but in the absence of Fgf-2 stimulation, these cells also show increased levels of basal ERK phosphorylation, when compared to Flrt1 at a 90% confidence level.

Similar to my previous data on Flrt3, Lrrtm3 over-expression in cells causes a significant increase in ERK phosphorylation upon Fgf-2 stimulation, possibly caused by the interaction with FgfR1. To confirm that the increase in ERK phosphorylation identified in cells over-expressing Lrrtm3 is dependent on activation of the Fgf receptor, the pan-Fgf receptor inhibitor SU5402 was utilised. Lrrtm3 or empty vector (pcDNA3.1) transiently transfected HEK-293T cells were serum-starved for 60 min with SU5402 (50 μM) where indicated. Cells were then stimulated with Fgf-2 for 10 min and cell lysates analysed for levels of pERK by Western blot (Figure 5.6).

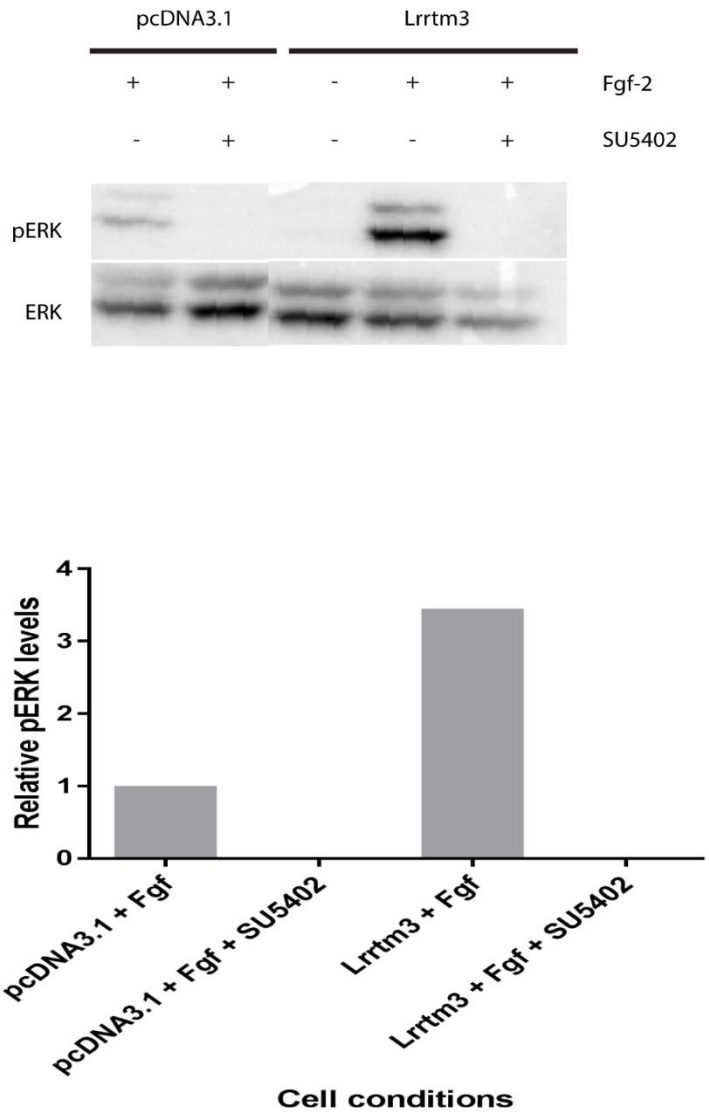

Figure 5.6. Increased pERK levels caused by Lrrtm3 over-expression require FgfR activity: Western blot of HEK-293T cells transiently transfected with Lrrtm3 vector or pcDNA3.1 (vector only control) for 20 h, then stimulated with Fgf-2 and heparin for 10 min (+ Fgf). Appropriate samples were incubated with 50 μM SU5402 during Fgf-2 stimulation (+ Fgf + SU5402). Blot probed with anti-pERK and anti-ERK (for pERK densitometric normalisation). Bar graph represents the normalised quantification of pERK levels between Fgf-2 stimulated cells with and without SU5402 treatment relative to untransfected Fgf-2 stimulated cells without SU5402 treatment. n=1.

Fgf-2 stimulation of pcDNA3.1-transfected cells (pcDNA3.1 + Fgf) results in activation of Fgf receptor and subsequent ERK phosphorylation (Figure 5.6). The inclusion of SU5402 in Fgf-2 stimulated pcDNA3.1-transfected cells (pcDNA3.1 + Fgf + SU5402) results in complete absence of pERK, showing the effectiveness of the inhibitor in blocking activation of the FgfR signalling, and the specificity for Fgf-2-resultant pERK increase to the FgfR. As previously shown, stimulation of Lrrtm3 over-expressing cells with Fgf-2 (Lrrtm3 + Fgf) results in higher levels of pERK than stimulation of pcDNA3.1-transfected cells. In this case, the increase in ERK phosphorylation is greater (3.5-fold increase) than previously shown (1.5-fold increase) for Lrrtm3 over-expressing cells in comparison to

pcDNA3.1-transfected cells. When Lrrtm3 over-expressing Fgf-2 stimulated cells are incubated with SU5402 (Lrrtm3 + Fgf + SU5402), levels of pERK are essentially eliminated. This implies that the increase in pERK in the cells transfected with Lrrtm3 is caused by the signalling activity of FgfR1.

Like Flrt3, I have shown that Lrrtm3 co-localises with FgfR1 within intracellular vesicle membranes. These proteins have been shown to interact, and the result of Lrrtm3 expression causes significant increase in pERK levels upon Fgf-2 stimulation, and a trending increase in basal pERK levels. This increase is directly attributed to increased activity of the FgfR receptors, with use of the pan-FgfR inhibitor resulting in the abolishment of ERK phosphorylation.

5.3 Discussion

Previous studies, including those shown in Chapter 3, have demonstrated that Flrt1 and Flrt3 can co-localise with FgfR1 in intracellular vesicles, interact with FgfR1, and influence the phosphorylation of ERK, the output of FgfR1 [5, 41]. In this chapter, a novel FgfR1/Lrrtm3 protein interaction was identified and investigated to determine if the regulation effects of Flrt1 and 3 on FgfR1 signalling are shared by other single-pass LRR transmembrane proteins. Lrrtm3 was investigated for a role in regulating FgfR signalling due to expression in regions that require FgfR activity. By using immunoprecipitation, Lrrtm3 was shown to interact with FgfR1 when over-expressed (Figure 5.3), facilitated by co-localisation of Lrrtm3 and FgfR1 to common intracellular membranes, first identified in this project using immunolocalisation (Figure 5.4). These results draw similarities with Flrt1 and Flrt3 co-transfected with FgfR1, which showed overlapping expression patterns as described in Chapter 3 and in previous studies [41]. Lrrtm3 shows a similar cellular localisation to Flrt1 and Flrt3, with localisation of the protein shared between intracellular membranes and the cell surface membrane. Upon co-expression with FgfR1, Lrrtm3 localisation appears to be altered, with stronger intracellular expression and subsequently weaker cell membrane expression. The immunolocalisation assay results suggest that Lrrtm3 and FgfR1 are co-localised to a number of different intracellular membranes which are undefined in this study. These intracellular membrane structures most probably include the rough ER and/or Golgi body and other intracellular vesicles. Accumulation in the rough ER and/or Golgi is likely to be due to the large levels of protein over-expression. It is important to note that Lrrtm3 co-localisation in these over-expression assays is similar to that of Flrt1 and 3, which were subsequently shown to co-localise with endogenously expressed FgfR1 and Fgf signalling components, and influence FgfR1 output [41] (Chapter 4).

Over-expression of Flrt1 and Flrt3 in HEK-293T cells results in a subtle increase in pERK levels as a result of FgfR1 activation. Flrt1 over-expression demonstrates a rapid increase of pERK after just 1 min that is sustained at a higher level for at least 30 min [41]. To analyse the effect of Lrrtm3 over-expression on pERK levels we initially attempted this analysis with Lrrtm3 over-expressing cells stimulated with Fgf-2 for 10 min. The 23-fold increase in pERK levels in untransfected cells upon Fgf-2 stimulation indicates that activation of Fgf receptors is occurring as expected in our cells, and it is clear to see that the stimulation is also successful in the Flrt1 and Lrrtm3 over-expressing samples due to the large increase in pERK levels (Figure 5.5) suggesting Flrt1 and Lrrtm3 are not inhibiting FgfR activation. Lrrtm3 over-expressing cells showed a significant 1.5-fold increase in pERK levels after 10 minutes stimulation that was consistent over 3 experiments using a Student's t- test. This increase is larger than that observed for Flrt3 over-expressing cells, and may also differ at different time-points, resulting in the potential of a greater regulation of FgfR1 activation. Furthermore, in unstimulated cells there was increased pERK in cells over-expressing Lrrtm3 that was significant at 90% confidence. It is interesting to note in stimulated and unstimulated cells that pERK levels in Lrrtm3 over-expressing samples show a larger increase in pERK levels compared to Flrt1 over-expressing cells suggesting Lrrtm3 may be more influential in FgfR activation than Flrt1. This could be due to the time-point analysed, as ERK activation by Flrt1 over-expression was not present at this time point in previous studies. No difference in pERK levels between pcDNA3.1 and Flrt1 over-expressing cells was observed, which is inconsistent with Wheldon *et al.* suggesting that there may be a difference in our cells or the experimental system compared to the published system [41].

Over-expression of Lrrtm3 causes an increase in ERK phosphorylation. While ERK is a signalling molecule for many different receptors, the increase in pERK levels observed in Lrrtm3 over-expressing samples was attributed predominantly to activation of the Fgf receptors (Figure 5.6). The Fgf receptor inhibitor was effective in blocking Fgf receptor activation, with levels of pERK in Fgf-2 stimulated, SU5402 treated cells being markedly lower than the level observed in cells not treated with SU5402. When Lrrtm3 over-expressing cells are stimulated with Fgf-2 in the presence of the inhibitor, pERK levels are almost abolished, suggesting the increase in pERK levels is due to the influence that Lrrtm3 has on the activation of the Fgf receptor and not a result of activation of some other signalling receptor or cascade. While the levels of pERK for stimulated Lrrtm3-transfected cells appear higher in this assay compared to Figure 5.5, the difference would likely be resolved by collating three repeats of the experiment, rather than just the one experiment that I have shown. Combined, this data suggests

that Lrrtm3 over-expression results in increased stimulated FgfR activation compared to non-Lrrtm3 over-expressing and Flrt1 over-expressing cells.

5.4 Conclusion

This Chapter has identified a potential novel interaction between LRR protein Lrrtm3 and FgfR1. Initial investigation of this interaction reveals similar FgfR1-signalling regulatory characteristics to that of Flrt1 and Flrt3. Lrrtm3 was shown to bind to FgfR1, and both proteins were shown to co-localise within common membranes within the cell. Over-expression experiments using the HEK-293T cell line with transient transfection of appropriate expression vectors have been previously used to analyse Flrt1 and Flrt3 dependent alteration of Fgf signalling, and this system was utilised to assess the regulator effects of Lrrtm3 on FgfR1 signalling. The system consistently showed increased ERK phosphorylation with Lrrtm3 over-expression, in both the absence and presence of Fgf-2 stimulation, with this increase in pERK levels being directly attributed to a change in activity of FgfR1. While the initial data gathered here infers a role for Lrrtm3 in regulating FgfR signalling, further investigation into the function and mechanism of this interaction are required to elucidate the role of Lrrtm3 in FgfR signalling modulation, and more broadly as a characteristic of LRR proteins to regulate FgfR1 signalling.

6. General Discussion

In this thesis, I investigated the mechanism of Flrt3 function in the regulation of Fgf signalling, including its role in early neural commitment, and whether other single-pass LRR proteins could also regulate Fgf signalling, using Lrrmt3 as an example.

The leucine-rich repeat super family is characterised by repeating motifs containing a high number of leucine residues. Multiple single-pass LRR transmembrane protein families show overlapping expression with FgfR1 during embryonic development, including the Flrt and Lrrtm families, with Flrt1 shown to regulate FgfR1 signalling [41]. This finding raises the possibility of other LRR proteins interacting with and regulating FgfR1 signalling during embryonic development. Expression of Flrt3 is observed at the apical ectodermal ridge, the mid-hind brain boundary, and in the developing somite. Study into the function of Flrt3 has been confined to over-expression systems, as the knockout mouse model of *Flrt3* is embryonic lethal. This project has attempted to identify the function of Flrt3 in embryonic development by studying the interaction with FgfR1 and using a cellular model to study endogenous Flrt3 function. It has also attempted to identify novel LRR protein and FgfR1 interactions, and characterise them.

6.1 Investigation of Flrt3 function

6.1.1 Analysis of Flrt3 localisation and activity using an over-expression system

One of the aims of this project was to investigate the function of Flrt3 expression at regions where Fgf signalling is important in development. This study identified for the first time the co-localisation of Flrt3 and FgfR1 to intracellular vesicular membranes, and at the cell surface membrane. Co-over-expression of Flrt3 and FgfR1 resulted in an FgfR-dependent 1.41-fold average increase in pERK levels in cells stimulated with Fgf-2, although this was shown to not be statistically significant using a Student's t-test. A trend of increased pERK levels in unstimulated cells transfected with Flrt3 compared to Flrt1 was also observed, suggesting Flrt3 increased activation of the MAPK pathway by FgfR1. Investigations into the importance of specific domains of Flrt3 that contribute to this trend failed to reveal required individual domains. Finally, analysis of Flrt3 tyrosine phosphorylation identified several different phosphorylation sites which are dependent on the over-expression of FgfR1.

Co-localisation of Flrt3 and FgfR1 to common cellular membranes is vital for the previously identified interaction to occur within the cell. Co-over-expression of tagged Flrt3 protein and FgfR1 revealed overlapping and distinct regions of expression for each protein. This result draws similarities with the localisation of Flrt1 and FgfR1 previously described in Chapter 3 [41]. Based on these results, the validity of the interaction between over-expressed Flrt3 and FgfR1 in a viable cell context is strengthened, whereas previous to this experiment, it could be argued that the identified interaction between Flrt3 and FgfR1 could occur as a result of cell lysis. The localisation of Flrt3 to the cell surface agrees with a number of previous studies [7, 8]. It has also previously been reported that Flrt3 promotes homotypic cell adhesion *in vitro* and *in vivo*. Observations from this study can neither clearly support nor oppose these findings [10]. While two or more cells over-expressing Flrt3 were observed to be in contact with each other on several occasions, both over-expression in isolated cells and cells separated within a mixed population were observed. The differences with the previous study could be explained by Flrt3 being sequestered to intracellular membranes, if it does play a role in cell-cell adhesion as predicted, or be explained by the uncomprehensive nature of immunofluorescence assays as opposed to using a EGFP co-transfection system, utilised when this was first observed [10].

Investigations carried out on the interaction between Flrt1 and FgfR1 by Wheldon *et al.* (2010) using over-expression in the HEK-293T cell line identified Flrt1 as a novel regulator of FgfR1 signalling activity. This cellular model was adopted to analyse the outcome of the interaction between Flrt3 and FgfR1 on FgfR1 signalling output.

As previously mentioned, reproduction the observations made by Wheldon and colleagues was unsuccessful in my hands; Flrt1 showed no significant increase in ERK phosphorylation upon Fgf-2 cell stimulation. These differences could be attributed to slight variations in the HEK-293T cell line used, or potentially missing details from the protocol. Using the protocol provided in the 2010 paper, a trend was observed of Flrt3 being able to increase FgfR-mediated ERK phosphorylation [41]. Studies have also shown the expression of *Flrt2* in regions reliant on Fgf signalling for embryonic development, and that Flrt2 interacts with extracellular and intracellular domains of FgfR2 [5, 58]. These results strongly suggest a role for Flrt protein family members in the regulation of FgfR signalling during early embryogenesis to facilitate normal embryonic development. The 10-minute time-point chosen to analyse pERK levels resulted in an apparent increase in ERK phosphorylation in cells over-expressing Flrt3 compared to cells over-expressing Flrt1, suggesting that the kinetics of the increasing trend in FgfR1 MAPK signalling activity due to the Flrt3 interaction may be different to that due to the over-expression of Flrt1. A futile phosphorylation cycle between Flrt1 and FgfR1 was observed by Wheldon *et al*., (2010),

by which Flrt1 activates FgfR1, FgfR1 dimerisation and autophosphorylation of intracellular tyrosine residues, resulting in phosphorylation of 3 intracellular Flrt1 tyrosines and attenuation of Flrt1-mediated FgfR signalling enhancement [41]. Three tyrosines residues were identified on the Flrt3 intracellular tail as likely to be phosphorylated, and it is proposed that these are the residues being detected. Extensive investigation of the phosphorylation of Flrt3 was undertaken and revealed that different species of Flrt3 are phosphorylated depending on the expression of FgfR1. Co-expression with FgfR1 results in tyrosine phosphorylation of an approximately 80 kDa species, while expression in the absence of FgfR1 over-expression results in tyrosine phosphorylation of an approximately 98 kDa species. This differs from that observed for Flrt1. As expected, when over-expressed with FgfR1, an approximately 75 kDa Flrt1 species is detected, representing a species with little to no post-translational modification, as observed by Wheldon *et al*. (2010) [41]. Expanding on the findings of Wheldon *et al*. (2010), it was shown that when over-expressed in the absence of FgfR1, Flrt1 lacks phosphorylation of the identified tyrosines, which is different to that of Flrt3. This suggests different roles for Flrt1 and 3, with Flrt3 possibly being phosphorylated by an interaction at the cell membrane to carry out a Flrt3-specific function, such as cell adhesion, with a homotypic cell adhesion phenotype previously observed in Flrt3 over-expressing cells [10]. Further to this, the mode-of-action for Flrt3 may differ from that of Flrt1, as mutation of the top three tyrosine residues predicted to be phosphorylated on the intracellular tail of Flrt3 does not result in constitutively high pERK levels that was observed upon mutation of the equivalent Flrt1 tyrosine residues [41]. This could be explained by the mode-of-action occurring through different adaptor proteins to Flrt1, which could function through the phosphorylation of other currently unknown residues. It had previously been shown that Flrt3 from X*enopus laevis* (XFlrt3) required the fibronectin III domain to interact with FgfR1, allowing FgfR1 signalling modulation [8]. None of the mutations created and tested in this thesis were shown to alter pERK levels, indicating that these individual domains were not required for FgfR1 interaction, contrasting the results observed for XFlrt3. Mutational loss of the transmembrane domain of XFlrt3 had a subtle effect on FgfR1 interaction, and could contribute to the Flrt3/FgfR1 interaction.

Previous studies on Flrt3 have identified its importance in binding to several other proteins to facilitate nerve development and remodelling, as well as cell adhesion and morphogenesis [6, 11, 59, 60]. This study provides support for a role of Flrt proteins as FgfR signalling regulators during early embryonic development. Further experiments as outlined in the Future Directions section are required to provide more evidence for this role.

6.1.2 Identification of the P19 EC cell line to study endogenous *Flrt3* function

To date, functional studies of Flrt3 have been restricted to over-expression systems due to the early embryonic lethality of knockout models [42]. The use of over-expression systems to gain functional information about a protein is a double-edged sword; while they are generally easier to obtain data compared to endogenous systems due to the much higher expression of the target protein, data obtained from these systems may not be an accurate representation of the endogenous function, with the potential for cells to display a mutant phenotype [61]. Over-expression systems can give us an indication of the involvement of the Flrt3 protein in Fgf signalling, but over-expression of a single protein can cause aberrant localisation of that protein, while over-expression of two proteins that interact could cause mis-localisation of one or the other protein. For example, over-expression of Flrt3 could localise FgfR1 to vesicles that it is not normally present in, or to the cell surface membrane, which may give it access to a different signalling environment causing a different output compared to the endogenous protein.

Differentiation of P19 EC cells with retinoic acid toward a neural lineage, a developmental timepoint similar to early neurectoderm formation, resulted in an increase in *Flrt3* expression. This increase was rapid and robust, with an increase in expression observed within 5 hours and sustained beyond 4 days of differentiation, with similar results observed in cells differentiated in aggregates or as a monolayer. Correlating with the increase in mRNA levels was an increase in observed Flrt3 protein levels in RA-differentiated P19 EC cells observed by immunofluorescence. Similar to that of the over-expression studies undertaken in Chapter 3, endogenous Flrt3 was strongly expressed at cell-cell junctions and also localised to intracellular vesicles. Analysis of ERK phosphorylation due to RA differentiation resulted in a 5-fold decrease in pERK, after the 1st day of differentiation compared to random differentiation. Interestingly, over-expression of Flrt3 also resulted in no increase in pERK levels, as assessed by transient transfection, whereas differentiation without RA or Flrt3 over-expression resulted in a 4.7-fold induction of ERK phosphorylation, before returning to basal levels by 48 h. During RA differentiation, expression of *Flrt3* was shown to be induced before *Sox1*, widely regarded to be the first known marker of neural induction, yet over-expression of Flrt3 alone is insufficient to induce *Sox1* expression.

The rapid and robust induction of *Flrt3* upon RA differentiation suggested that the *Flrt3* promoter may be directly regulated by retinoic acid. A DNA element upstream of *Flrt3* is conserved across species but was shown not to play a key role in the regulation of *Flrt3* induction. It may though, play a

role in the inhibition of *Flrt3* expression, or even be a regulatory element for another gene and has no effect on expression of *Flrt3*. A fragment from 4-6 kb upstream of the *Flrt3* start site was shown to respond 2-fold to RA treatment. Closer inspection of this region revealed a γF-hormone response element (HRE) (PuGGTCA, preceded by a 6 bp A/T rich sequence), to which RAR-related orphan receptor α (RORα) can bind as a monomer and activate transcription [13]. While normally the HRE are required in tandem, one element is all that is required to bind RORα. In the absence of RA, the retinoid receptor complexes block activation of RORα. It has previously been shown that the combination of RORα expression and RA treatment increase expression of the target gene, while the presence of RARα prevents RORα-regulated gene expression in the absence of RA. This demonstrates that RARα and RORα compete for the same binding site, and that RARα can repress target gene transcription in the absence of RA. Therefore, a proposed mechanism of *Flrt3* induction would be that RORα and RARα compete for the HRE in the region between the 5' 6 kb upstream from the Flrt3 start site and CE. In the absence of RA, RARα is bound to the HRE and prevents RORα activating Flrt3 transcription. Upon addition of RA to the system, RARα binds RA and releases from the HRE, allowing RORα activation of *Flrt3* transcription, resulting in increased expression of *Flrt3*.

The increase in Flrt3 protein expression as a result of RA differentiation observed in the immunofluorescence assay suggests that the increase in *Flrt3* mRNA directly leads to increased levels of protein. The current Flrt3 antibody does not work for Western blotting, so it would be beneficial to obtain a Flrt3 antibody that is optimised for Western blot to quantitatively measure the increase in protein levels. The introduction of a tag, such as HA or Flag, onto the endogenous Flrt3 protein using CRISPR technology to create a stable P19 cell line could be utilised with well characterised antibodies to confirm the increase in expression. The localisation of endogenous Flrt3 to cell-cell junctions agrees with localisation of the over-expressed protein and facilitates the cell sorting phenotype previously observed in cell expressing higher levels of Flrt3. Intracellular vesicle membrane localisation provides the spatial context to facilitate an interaction with FgfR1 [10]. This data adds to the hypothesis that Flrt3 acts as a homophilic cell adhesion molecule that was based on Flrt3 over-expression, extending the concept to endogenous Flrt3.

The role of the ERK signalling pathway during neural differentiation has been extensively studied, with Fgf signalling being a conserved initiator of neural development in vertebrates [62-66]. The modulation of Fgf signalling is important in neural induction, with an early increase followed by decrease in signalling. RA is shown to play a dual role in neural differentiation; initially increasing MAPK signalling by induction of *Fgf8*, then gradually repressing *Fgf4*, resulting in decreasing MAPK signalling by day 2

of differentiation [67]. This enforces the importance of the timing of signalling events during differentiation giving rise to particular cell fates. Given that P19 EC cells are more differentiated than the 46C ES cells used to identify the changes in Fgf signalling, it is not unforeseen that we did not observe an increase in MAPK signalling as a result of P19 EC differentiation with RA or Flrt3 over-expression [67]. The increase in MAPK signalling via Fgfs observed in the 46C ES cells (pluripotent) may have subsided due to the repression of *Fgf4* prior to reaching the differentiation status of P19 EC cells (multipotent). In regard to the similar behaviour of Flrt3 over-expression and RA differentiation on pERK levels, it does pose an interesting question; if a function of Flrt3 is to increase FgfR1 signalling, why are pERK levels lower in P19 EC cells that express *Flrt3* at high levels (either induced by RA treatment or by transient over-expression)? It is possible that with the down-regulation of *Fgf4* expression, that Flrt3 facilitates FgfR basal signalling activity.

Sox1 expression and localisation data agrees with that of Pevny *et al*. (1998), who observed induction within the initial 96 hours of P19 differentiation with RA, with protein expression localised exclusively to the nucleus; as expected for a transcription factor [50]. This study is the first to identify that increased *Sox1* expression is not observed within the initial 6 h of RA differentiation of P19 EC cells. Despite *Flrt3* induction prior to induction of *Sox1*, expression of Flrt3 alone was shown to be insufficient to induce *Sox1* expression and therefore drive neural differentiation. Other factors must therefore be required to drive *Sox1* expression.

Given the early embryonic lethality by a complex phenotype of *Flrt3*$^{-/-}$ embryos, a viable system to study endogenous Flrt3 function is required. The P19 EC cell line provides this, utilising RA differentiation which drives a rapid and robust induction of Flrt3 through an apparent direct effect. The function of endogenous Flrt3 can continue to be investigated using this identified model, with experiments outlined in the Future Directions that will help elucidate its function.

6.2 Role of single-pass LRR proteins as FgfR signalling modulators

The Lrrtm family of proteins was identified to be similar in structure to that of the Flrt family, with some members also displaying expression in tissues reliant on Fgf signalling for development. For these reasons, the Lrrtm3 protein was selected as a model to determine if a common function of single-pass LRR proteins is modulation of FgfR signalling. Lrrtm3 was found to interact with FgfR1 in pull-down assays, while the two proteins were also shown to co-localise to common cellular membranes. These

data provided a cellular context for modulation to occur. Cells over-expressing Lrrtm3 showed a 1.5-fold increase in ERK phosphorylation upon Fgf-2 stimulation, which is reliant on FgfR signalling activity.

Previous studies focussing on Lrrtm3 and Alzheimer's related proteins β-secretase 1 (BACE1) and amyloid precursor protein (APP) identified Lrrtm3 localisation to early endosomes in a neuroblastoma cell line [68]. Expression is observed elsewhere within the cell, yet remains undefined as the paper focuses only on membranes which show overlapping expression with BACE1 and APP. Data obtained in this thesis identifies Lrrtm3 localisation to intracellular membranes (which remain undefined), potentially akin to that of Lincoln *et al*. This thesis has also identified Lrrtm3 localising to what appears to be the cell surface membrane, extending the known subcellular localisation of Lrrtm3. This study has also added FgfR1 to the list of proteins known to interact with Lrrtm3, joining APP, BACE1, and neurexin [68, 69]. Evidence now shows that the interaction between Lrrtm3 and FgfR1 results in an increase in FgfR1 signalling by the MAPK pathway, supporting a common function that some other single-pass LRR protein may act as FgfR signalling modulators where overlapping expression is observed. This function cannot be applied broadly to all LRR proteins though, as Lern1 has been shown to not interact with FgfR1 despite regions of overlapping expression during embryogenesis (unpublished data not shown).

Proteins from two single-pass LRR protein families that show overlapping expression with FgfR1 during embryogenesis have now been identified to interact with and influence FgfR1 signalling. This supports a proposed role for other single-pass LRR proteins in the regulation of Fgf receptors when co-expressed during development. It also raises the possibility of other single pass signalling receptors being able to interact with and be regulated by various families of LRR transmembrane proteins. Further experiments, including those outlined in the Future Directions, are required to fully characterise these interactions and strengthen this proposal.

6.3 Significance

Genes that are important in embryonic development are often specifically expressed and have important roles in brain development and neuron formation and specification. I have provided evidence of Flrt function in a model of early embryogenesis, linking it to a role in the regulation of Fgf signalling. Flrt has been shown to be functionally important in the dentate gyrus for neuron specification [19]. Interestingly, Fgf signalling has also been shown to be essential for this process [70].

6.4 Future Directions

I have demonstrated that Flrt3 and Lrrtm3, along with previous studies on Flrt1, can interact with and modulate the output from FgfR1 in over-expression studies. I have also identified the P19 early neural specification system as a model to understand the role of endogenous Flrt3 function, and identified alterations in pERK output in this system that could be linked to *Flrt3* induction. Below are various experiments that could be undertaken to further understand the role of Flrt3 and Lrrtm3, combined with how the possible experimental outcomes could be interpreted.

In regard to Flrt proteins and other single-pass LRR transmembrane proteins exhibiting modulation of FgfR1, the following experiments could be undertaken;

- **Experiment A: Time-course for Fgf stimulation of cells over-expressing FgfR1 and Flrt3. Include analysis of other signal cascade pathways such as PI3K, and PLC.**

Using time-points similar to that used by Wheldon *et al.* (2010), the dynamics of the apparent increase in MAPK signalling pathway activation can be investigated. Considering that the FgfRs can also signal via the PI3K/Akt and PLC pathways, with all three pathways shown to be important in neural differentiation, analysis of all signalling pathways that could be affected should be undertaken [71]. The HEK-293T cell line could still be used, stimulating the cells with Fgf-2 and heparin for 10 min following serum starvation, comparing cells transfected with plasmid over-expressing Flrt3 and cells over-expressing empty vector. Cells can be lysed with lysis buffer containing phosphatase inhibitors as outlined in Chapter 2, and soluble cell fractions analysed by Western blot, or whole cells could be analysed by flow cytometry. Antibodies such as phospho-Akt (Ser473), phospho-Akt (Thr308), and Akt from Cell Signalling Technologies (4058, 4056, and 9272 respectively) could be used to assess the PI3K/Akt pathway activation. Antibodies such as phosphor-PLCγ1 (Tyr783) (D6M9S) and PLCγ1 from Cell Signalling Technologies (14008 and 2822 respectively could be used to assess the PLC pathway. Changes in levels of the phosphorylated proteins (ERK, Akt, PLCγ1) in cells over-expressing Flrt3 compared to empty vector could be directly contributed to the expression of Flrt3 and the interaction with FgfR1.

- **Experiment B: Explore the interaction between Flrt2 and FgfR1 for modulation of FgfR signalling.**

Flrt2 expression is observed in the developing sclerotome, which, like tissue expression patterns for *Flrt1* and *Flrt3*, is an area that requires Fgf signalling for correct development. Flrt2 has also been shown to interact with FgfR1 [5]. Despite this interaction being known to occur, no studies investigating the effect the interaction has on FgfR signalling have been carried out. The experiments used to investigate the Flrt3 and FgfR1 interaction in HEK-293T cells in this thesis could be carried out with Flrt2. Experiment A could also be repeated to include Flrt2 to further understand the interaction.

- **Experiment C: Changes in target gene expression due to Flrt3 over-expression.**

Given that Flrt3 shows a trend to increase FgfR1-mediated ERK signalling, and may show effects on PI3K/Akt and PLC signalling pathway activation, there is potential for changes in target gene expression. Nanostring analysis could be undertaken to determine changes in both mRNA and protein expression profiles between cells transfected with plasmid over-expressing Flrt3 and cells transfected with empty vector. This would give functional relevance to the modulation of FgfR1 signalling activity. The HEK-293T cell line could still be used, stimulating the cells with Fgf-2 and heparin for 10 min following serum starvation. Cells would be lysed, with mRNA and protein collected. mRNA would be converted to cDNA for the analysis. Using a custom-designed panel of genes known to be regulated by FgfR1 signalling during development, such as c-Fos and Elk-1, changes between mRNA and protein expression levels could be identified between. Changes in levels of mRNA and protein expression in cells over-expressing Flrt3 compared to cells transfected with empty vector could be directly contributed to the expression of Flrt3 and the interaction with FgfR1. Microarray analysis could also be undertaken to identify novel target genes. This could also be investigated using stable cell lines over-expressing Flrt3 rather than transient transfection, eliminating the inherent variability of transient transfection efficiency. This would facilitate higher reproducibility, therefore more significant results.

- **Experiment D: Further elucidate the Lrrtm/FgfR1 interaction.**

The Lrrtm3/FgfR1 interaction identified in this thesis was found to influence the MAPK signalling via FgfR1. Like the Flrt1 and Flrt3 interaction, the influence of the interaction with FgfR1 on the PI3K/Akt and PLC pathways has not been investigated. Experiment A could be repeated to include Lrrtm3 in place of Flrt3.

To further investigate Flrt3 function in neural differentiation, the following experiments could be undertaken;

- **Experiment E: Determine if Flrt3 expression is vital for RA-mediated neural differentiation.**

Given that *Flrt3* shows a rapid and robust induction during the initial stages of RA-mediated differentiation, with expression increasing even prior to the induction of *Sox1*, the role of Flrt3 in neural differentiation holds many unanswered questions. To determine if the expression of *Flrt3* is vital for neural differentiation, a *Flrt3* knockdown or knockout system could be utilised. shRNA could be designed against *Flrt3* and cloned under an inducible promoter, such as doxycycline, with antibiotic selection. RA mediated neural differentiation of P19s in the presence of doxycycline would need to be assessed to ensure proper differentiation is still viable. This could be achieved by transfecting the empty inducible vector into P19 EC cells, differentiate the cells with RA in the presence of doxycycline, then assess the expression of *Sox1* by qRT-PCR. If comparable to that of differentiation in the absence of doxycycline, the system can be used. The shRNA construct could be transfected into P19 EC cells, with these cells grown under selection pressure of the antibiotic in the media. Single cell clones would be grown and screened by PCR to ensure substantial knockdown of *Flrt3* upon induction. The top 5 clones would be selected and pooled together to form the stable inducible Flrt3 P19EC knockdown cell line. This pooled cell line would be differentiated with RA over a 24 hr time-course, taking samples hourly for the initial 6 h of differentiation, with samples also taken at 12, 18 and 24 h post-differentiation. mRNA would be harvested, with qRT-PCR used to determine differences in *Sox1* expression. Expression of *Flrt3* would be measured as a control for the knockdown. If Flrt3 is vital in neural differentiation, cells shouldn't express *Sox1*. If the *Sox1* expression profile doesn't change compared to WT cells, Flrt3 is not vital in RA neural differentiation. If *Sox1* is not induced, Flrt3 is important in neural differentiation of P19s. If *Sox1* expression induction is delayed, then Flrt3 plays a role in early neural induction, but other factors compensate for its loss after a lag phase. A *Flrt3* knockout P19 EC cell line could also be created using CRISPR with the guide RNA designed against *Flrt3* to address this question.

- **Experiment F: Determine if over-expression of *Flrt3* is sufficient to induce neural differentiation.**

Similar to using a Flrt3 knockdown or knockout system to investigate decreased levels of *Flrt3* expression on neural differentiation, it is also interesting to investigate the effect of increased *Flrt3* expression levels on RA-mediated P19 neural differentiation. This was addressed somewhat in this thesis, although using a stable cell line over-expressing Flrt3 will be more insightful than cells transiently transfect with plasmid over-expressing Flrt3. Using a lentiviral delivery system containing the *Flrt3* ORF,

P19 EC cells would be infected and grown under antibiotic selection pressure. Single cell clones would be screened by qPCR to assess the over-expression of *Flrt3*. The top 5 clones would be chosen and mixed to form the Flrt3 OE P19 cell line. This cell line would be differentiated with and without RA over a 24 hr time-course, taking samples hourly for the initial 6 h of differentiation, with samples also taken at 12, 18 and 24 h post-differentiation. mRNA would be collected, converted to cDNA, and then assessed for *Sox1* expression using qRT-PCR. *Flrt3* expression would be measured to ensure over-expression in the cell line. A WT P19 EC cell line would be used as a control. In this experiment, if *Sox1* expression is induced in the Flrt3 OE cell line without RA, then the increase in Flrt3 expression is sufficient to induce neural differentiation and subsequent *Sox1* expression. If *Sox1* expression is induced faster in the Flrt3 OE cell line with RA induction, then the increased levels of Flrt3 contribute positively to initiate neural differentiation faster than RA alone, or that increased Flrt3 expression can drive *Sox1* expression. If *Sox1* expression is not induced in Flrt3 OE cells without RA, then the increase in Flrt3 expression is not sufficient to drive neural differentiation and subsequent *Sox1* expression. If *Sox1* induction does not change in Flrt3 OE RA differentiated cells compared to WT RA differentiated cells, this indicates that the increase in Flrt3 expression does not influence the rate of neural differentiation compared to RA alone. Finally, if *Sox1* is not induced, or is induced at a later time-point in Flrt3 OE cells differentiated with RA, then the increase in Flrt3 expression can inhibit neural differentiation, and subsequently *Sox1* expression.

- **Experiment G: Determine the transcription factors vital for *Flrt3* induction.**

Using the results of the luciferase assays and the mechanism of *Flrt3* regulation proposed, investigation into the regulation of *Flrt3* induction during RA-differentiation could be furthered. Site-directed mutagenesis of the identified γF-HRE found to reside between the 5' end of the 6 kb promoter sequence and the CE to render it unrecognisable to RARα and RORα would determine if this site is playing a role in the *Flrt3* expression. If this shows no change in luciferase expression, cloning of luciferase vectors containing smaller portions of the 4kb – 6kb region 5' of *Flrt3* could be undertaken to help identify the sequence of DNA partially responsible for the increase in *Flrt3* expression during RA differentiation. Analysis of the sequence found to be responsive to RA for transcription factor binding sites would provide an insight into possible the transcription factors responsible for the response. ChIP analysis could be undertaken to confirm the identity of this transcription factor and the response element. The element could then be mutated to confirm the binding sequence of the transcription factor. shRNA disruption of transcription factor translation could also be used to confirm the identity, although could pose an issue if the transcription factor is required for cell viability. Broader investigation of the surrounding genome to determine the regulatory regions responsible for the large increase in *Flrt3*

expression upon RA-differentiation could also be undertaken using a luciferase approach, followed by a random mutagenesis approach of the DNA sequences.

- **Experiment H: Explore the endogenous function of *Flrt3* on FgfR signalling during differentiation.**

Using the P19 EC WT, Flrt3 KO and OE cell lines differentiated with RA, the effect of Flrt3 expression on FgfR signalling could be assessed. Investigating the MAPK, PI3K/Akt and PLC pathway activation using the antibodies utilised in this thesis for the MAPK pathway, and the antibodies described in Experiment A for the PI3K/Akt and PLC pathways could be undertaken. Changes identified between the WT cell line and the Flrt3 KO and OE cell lines could be confirmed to be through the FgfRs using the FgfR pan-inhibitor SU5402. A concern for this would be that the cells may not be able to differentiate correctly with the use of the inhibitor, therefore it may be vital to create an inducible FgfR1 knockout cell line for each of the Flrt3 KO and OE cells to achieve this.

- **Experiment I: Investigate the possibility of functional redundancy between Flrt3 and Flrt1 during neural differentiation.**

A stable P19 EC cell line where the *Flrt1* ORF replaces the *Flrt3* coding sequence would be created utilising the CRISPR/Cas9 system. This would use a guide RNA targeted against an appropriate sequence early into the *Flrt3* gene that would be transfected into P19 ECs, along with the donor plasmid containing the *Flrt1* ORF with the neomycin resistance gene on the 3' end. Cells would be selected for the insertion by culturing in media containing neomycin. Single cell clones would be cultured, with next generation sequencing used to confirm the insertion of the *Flrt1* ORF at the targeted site. Cells with the correct insertion would then be differentiated with and without RA, with the mRNA harvested, and expression of *Sox1* assessed by qRT-PCR. Expression of *Flrt1* would be assessed as a control to ensure increased *Flrt1* expression upon neural differentiation, and *Flrt3* expression assessed to ensure expression is not observed. The WT P19 EC cell line would be used as a control for the expression of *Flrt1* and *Flrt3*. As a result of this experiment, if *Sox1* expression is induced and neural differentiation occurs in the *Flrt1* knockin cell line, then Flrt3 and Flrt1 are functionally redundant during neural differentiation, indicating only the modulation of FgfR signalling facilitated by interaction between Flrt1 or Flrt3 and FgfR1 required to support neural differentiation. If *Sox1* expression is not induced upon RA differentiation, then Flrt1 and Flrt3 are not functionally redundant in neural differentiation. This therefore potentially identifies a unique function of Flrt3 in relation to Flrt1, in facilitating neural differentiation.

6.5 Conclusion

In this project, the previously identified interaction between Flrt3 and FgfR1 was investigated. Flrt3 was shown to co-localise with FgfR1, while over-expression of Flrt3 resulted in a trend of increased MAPK signalling through the activity of FgfR1. Some of the characteristics of Flrt3 were examined, revealing tyrosine phosphorylation present on the Flrt3 protein independent of Fgf-2 stimulation, while no specific domain was identified as being responsible for the change in MAPK signalling. A system to study the function of endogenous Flrt3 was established, with the P19 EC cell line showing a rapid and robust increase in *Flrt3* expression upon differentiation with RA, which translated to an increase in Flrt3 levels. A minor part of this induction may be encoded in a sequence in the promoter region between 4 kb and 6 kb upstream of the *Flrt3* transcription start site, with the majority of RA-dependent induction located elsewhere. *Flrt3* induction was found to occur prior to that of *Sox1*, although transient Flrt3 over-expression in the absence of RA was not sufficient to induce *Sox1* expression. Interestingly, differentiation of P19 cells with RA or while over-expressing Flrt3 resulted in a decrease in pERK levels compared to P19 cells differentiated randomly. The proposal that a role for single-pass LRR proteins, which show overlapping expression with FgfR1, is in modulating the signalling output of the receptor was explored using Lrrtm3. FgfR1 was found to interact with Lrrtm3 and co-localise to common intracellular membranes. Similar to that of Flrt3, the interaction was found to increase FgfR1 signalling via the MAPK pathway. This data supports a role of single-pass transmembrane LRR proteins as modulators of FgfR activity in the developing embryo in regions where Fgf signalling is vital, and may lead to a further understanding of the causes of improper neural development during embryogenesis.

References

1. Kajava, A.V., *Structural diversity of leucine-rich repeat proteins.* Journal of Molecular Biology, 1998. **277**(3): p. 519-527.
2. Buchanan, S.G. and N.J. Gay, *Structural and functional diversity in the leucine-rich repeat family of proteins.* Prog Biophys Mol Biol, 1996. **65**(1-2): p. 1-44.
3. Kobe, B. and A.V. Kajava, *The leucine-rich repeat as a protein recognition motif.* Curr Opin Struct Biol, 2001. **11**(6): p. 725-32.
4. Hess, D., et al., *Identification of the disulphide bonds in human platelet glycocalicin.* Eur J Biochem, 1991. **199**(2): p. 389-93.
5. Haines, B.P., et al., *Regulated expression of FLRT genes implies a functional role in the regulation of FGF signalling during mouse development.* Dev Biol, 2006. **297**(1): p. 14-25.
6. Ranaivoson, F.M., et al., *Structural and Mechanistic Insights into the Latrophilin3-FLRT3 Complex that Mediates Glutamatergic Synapse Development.* Structure, 2015. **23**(9): p. 1665-77.
7. Robinson, M., et al., *FLRT3 is expressed in sensory neurons after peripheral nerve injury and regulates neurite outgrowth.* Mol Cell Neurosci, 2004. **27**(2): p. 202-14.
8. Bottcher, R.T., et al., *The transmembrane protein XFLRT3 forms a complex with FGF receptors and promotes FGF signalling.* Nat Cell Biol, 2004. **6**(1): p. 38-44.
9. Tsuji, L., et al., *FLRT3, a cell surface molecule containing LRR repeats and a FNIII domain, promotes neurite outgrowth.* Biochem Biophys Res Commun, 2004. **313**(4): p. 1086-91.
10. Karaulanov, E.E., R.T. Bottcher, and C. Niehrs, *A role for fibronectin-leucine-rich transmembrane cell-surface proteins in homotypic cell adhesion.* EMBO Rep, 2006. **7**(3): p. 283-90.
11. Karaulanov, E., et al., *Unc5B interacts with FLRT3 and Rnd1 to modulate cell adhesion in Xenopus embryos.* PLoS One, 2009. **4**(5): p. e5742.
12. Krantz, D.E. and S.L. Zipursky, *Drosophila chaoptin, a member of the leucine-rich repeat family, is a photoreceptor cell-specific adhesion molecule.* EMBO J, 1990. **9**(6): p. 1969-77.
13. Milan, M., et al., *The LRR proteins capricious and Tartan mediate cell interactions during DV boundary formation in the Drosophila wing.* Cell, 2001. **106**(6): p. 785-94.
14. Tanabe, K., et al., *Fibroblast growth factor-inducible-14 is induced in axotomized neurons and promotes neurite outgrowth.* J Neurosci, 2003. **23**(29): p. 9675-86.
15. Yamagishi, S., et al., *FLRT2 and FLRT3 act as repulsive guidance cues for Unc5-positive neurons.* EMBO J, 2011. **30**(14): p. 2920-33.
16. Leonardo, E.D., et al., *Vertebrate homologues of C. elegans UNC-5 are candidate netrin receptors.* Nature, 1997. **386**(6627): p. 833-8.
17. Lelianova, V.G., et al., *Alpha-latrotoxin receptor, latrophilin, is a novel member of the secretin family of G protein-coupled receptors.* J Biol Chem, 1997. **272**(34): p. 21504-8.
18. Arcos-Burgos, M., et al., *A common variant of the latrophilin 3 gene, LPHN3, confers susceptibility to ADHD and predicts effectiveness of stimulant medication.* Mol Psychiatry, 2010. **15**(11): p. 1053-66.
19. O'Sullivan, M.L., et al., *FLRT proteins are endogenous latrophilin ligands and regulate excitatory synapse development.* Neuron, 2012. **73**(5): p. 903-10.
20. Lesch, K.P., et al., *Dances with black widow spiders: Dysregulation of glutamate signalling enters centre stage in ADHD.* Eur Neuropsychopharmacol, 2012.
21. Bansal, R., et al., *Expression of FGF receptors 1, 2, 3 in the embryonic and postnatal mouse brain compared with Pdgfralpha, Olig2 and Plp/dm20: implications for oligodendrocyte development.* Dev Neurosci, 2003. **25**(2-4): p. 83-95.

22. Yamaguchi, T.P., et al., *fgfr-1 is required for embryonic growth and mesodermal patterning during mouse gastrulation.* Genes Dev, 1994. **8**(24): p. 3032-44.
23. Guillemot, F. and C. Zimmer, *From cradle to grave: the multiple roles of fibroblast growth factors in neural development.* Neuron, 2011. **71**(4): p. 574-88.
24. Dorey, K. and E. Amaya, *FGF signalling: diverse roles during early vertebrate embryogenesis.* Development, 2010. **137**(22): p. 3731-42.
25. Turner, N. and R. Grose, *Fibroblast growth factor signalling: from development to cancer.* Nat Rev Cancer, 2010. **10**(2): p. 116-29.
26. Eswarakumar, V.P., I. Lax, and J. Schlessinger, *Cellular signaling by fibroblast growth factor receptors.* Cytokine Growth Factor Rev, 2005. **16**(2): p. 139-49.
27. Ozaki, K., et al., *Efficient suppression of FGF-2-induced ERK activation by the cooperative interaction among mammalian Sprouty isoforms.* J Cell Sci, 2005. **118**(Pt 24): p. 5861-71.
28. Mason, J.M., et al., *Tyrosine phosphorylation of Sprouty proteins regulates their ability to inhibit growth factor signaling: a dual feedback loop.* Mol Biol Cell, 2004. **15**(5): p. 2176-88.
29. Hanafusa, H., et al., *Sprouty1 and Sprouty2 provide a control mechanism for the Ras/MAPK signalling pathway.* Nat Cell Biol, 2002. **4**(11): p. 850-8.
30. Yu, K. and D.M. Ornitz, *FGF signaling regulates mesenchymal differentiation and skeletal patterning along the limb bud proximodistal axis.* Development, 2008. **135**(3): p. 483-91.
31. Niswander, L., et al., *FGF-4 replaces the apical ectodermal ridge and directs outgrowth and patterning of the limb.* Cell, 1993. **75**(3): p. 579-87.
32. Sun, X., F.V. Mariani, and G.R. Martin, *Functions of FGF signalling from the apical ectodermal ridge in limb development.* Nature, 2002. **418**(6897): p. 501-8.
33. Chi, C.L., et al., *The isthmic organizer signal FGF8 is required for cell survival in the prospective midbrain and cerebellum.* Development, 2003. **130**(12): p. 2633-44.
34. Blak, A.A., et al., *Expression of Fgf receptors 1, 2, and 3 in the developing mid- and hindbrain of the mouse.* Dev Dyn, 2005. **233**(3): p. 1023-30.
35. Nakamura, H., T. Sato, and A. Suzuki-Hirano, *Isthmus organizer for mesencephalon and metencephalon.* Dev Growth Differ, 2008. **50 Suppl 1**: p. S113-8.
36. Orr-Urtreger, A., et al., *Developmental expression of two murine fibroblast growth factor receptors, flg and bek.* Development, 1991. **113**(4): p. 1419-34.
37. Deng, C.X., et al., *Murine FGFR-1 is required for early postimplantation growth and axial organization.* Genes Dev, 1994. **8**(24): p. 3045-57.
38. Mi, S., et al., *LINGO-1 is a component of the Nogo-66 receptor/p75 signaling complex.* Nat Neurosci, 2004. **7**(3): p. 221-8.
39. Fournier, A.E., T. GrandPre, and S.M. Strittmatter, *Identification of a receptor mediating Nogo-66 inhibition of axonal regeneration.* Nature, 2001. **409**(6818): p. 341-6.
40. Wang, K.C., et al., *Oligodendrocyte-myelin glycoprotein is a Nogo receptor ligand that inhibits neurite outgrowth.* Nature, 2002. **417**(6892): p. 941-4.
41. Wheldon, L.M., et al., *Critical role of FLRT1 phosphorylation in the interdependent regulation of FLRT1 function and FGF receptor signalling.* PLoS One, 2010. **5**(4): p. e10264.
42. Egea, J., et al., *Genetic ablation of FLRT3 reveals a novel morphogenetic function for the anterior visceral endoderm in suppressing mesoderm differentiation.* Genes Dev, 2008. **22**(23): p. 3349-62.
43. Blom. N., G., S., and Brunak, S., *Sequence- and structure-based prediction of eukaryotic protein phosphorylation sites.* Journal of Molecular Biology, 1999. **294**(5): p. 1351-1362.
44. Jones-Villeneuve, E.M., et al., *Retinoic acid induces embryonal carcinoma cells to differentiate into neurons and glial cells.* J Cell Biol, 1982. **94**(2): p. 253-62.
45. Jasmin, et al., *Chemical induction of cardiac differentiation in p19 embryonal carcinoma stem cells.* Stem Cells Dev, 2010. **19**(3): p. 403-12.
46. So, E.N. and D.L. Crowe, *Characterization of a retinoic acid responsive element in the human ets-1 promoter.* IUBMB Life, 2000. **50**(6): p. 365-70.

47. Stehlin-Gaon, C., et al., *All-trans retinoic acid is a ligand for the orphan nuclear receptor ROR beta.* Nat Struct Biol, 2003. **10**(10): p. 820-5.
48. Jetten, A.M., S. Kurebayashi, and E. Ueda, *The ROR nuclear orphan receptor subfamily: critical regulators of multiple biological processes.* Prog Nucleic Acid Res Mol Biol, 2001. **69**: p. 205-47.
49. Soprano, D.R., B.W. Teets, and K.J. Soprano, *Role of retinoic acid in the differentiation of embryonal carcinoma and embryonic stem cells.* Vitam Horm, 2007. **75**: p. 69-95.
50. Pevny, L.H., et al., *A role for SOX1 in neural determination.* Development, 1998. **125**(10): p. 1967-78.
51. Lauren, J., et al., *A novel gene family encoding leucine-rich repeat transmembrane proteins differentially expressed in the nervous system.* Genomics, 2003. **81**(4): p. 411-21.
52. Linhoff, M.W., et al., *An unbiased expression screen for synaptogenic proteins identifies the LRRTM protein family as synaptic organizers.* Neuron, 2009. **61**(5): p. 734-49.
53. Haines, B.P. and P.W. Rigby, *Developmentally regulated expression of the LRRTM gene family during mid-gestation mouse embryogenesis.* Gene Expr Patterns, 2007. **7**(1-2): p. 23-9.
54. Smith, J.D., et al., *Alpha T-catenin (CTNNA3): a gene in the hand is worth two in the nest.* Cell Mol Life Sci, 2011. **68**(15): p. 2493-8.
55. Voikar, V., et al., *LRRTM1-deficient mice show a rare phenotype of avoiding small enclosures--a tentative mouse model for claustrophobia-like behaviour.* Behav Brain Res, 2013. **238**: p. 69-78.
56. Sousa, I., et al., *Polymorphisms in leucine-rich repeat genes are associated with autism spectrum disorder susceptibility in populations of European ancestry.* Mol Autism, 2010. **1**(1): p. 7.
57. Mudo, G., et al., *The FGF-2/FGFRs neurotrophic system promotes neurogenesis in the adult brain.* J Neural Transm, 2009. **116**(8): p. 995-1005.
58. Wei, K., et al., *Mouse FLRT2 interacts with the extracellular and intracellular regions of FGFR2.* J Dent Res, 2011. **90**(10): p. 1234-9.
59. Chen, X., et al., *A protocadherin-cadherin-FLRT3 complex controls cell adhesion and morphogenesis.* PLoS One, 2009. **4**(12): p. e8411.
60. Leyva-Diaz, E., et al., *FLRT3 is a Robo1-interacting protein that determines Netrin-1 attraction in developing axons.* Curr Biol, 2014. **24**(5): p. 494-508.
61. Prelich, G., *Gene overexpression: uses, mechanisms, and interpretation.* Genetics, 2012. **190**(3): p. 841-54.
62. Bertrand, V., et al., *Neural tissue in ascidian embryos is induced by FGF9/16/20, acting via a combination of maternal GATA and Ets transcription factors.* Cell, 2003. **115**(5): p. 615-27.
63. Delaune, E., P. Lemaire, and L. Kodjabachian, *Neural induction in Xenopus requires early FGF signalling in addition to BMP inhibition.* Development, 2005. **132**(2): p. 299-310.
64. Launay, C., et al., *A truncated FGF receptor blocks neural induction by endogenous Xenopus inducers.* Development, 1996. **122**(3): p. 869-80.
65. Streit, A., et al., *Initiation of neural induction by FGF signalling before gastrulation.* Nature, 2000. **406**(6791): p. 74-8.
66. Wilson, S.I., et al., *An early requirement for FGF signalling in the acquisition of neural cell fate in the chick embryo.* Curr Biol, 2000. **10**(8): p. 421-9.
67. Stavridis, M.P., B.J. Collins, and K.G. Storey, *Retinoic acid orchestrates fibroblast growth factor signalling to drive embryonic stem cell differentiation.* Development, 2010. **137**(6): p. 881-90.
68. Lincoln, S., et al., *LRRTM3 interacts with APP and BACE1 and has variants associating with late-onset Alzheimer's disease (LOAD).* PLoS One, 2013. **8**(6): p. e64164.
69. Um, J.W., et al., *LRRTM3 Regulates Excitatory Synapse Development through Alternative Splicing and Neurexin Binding.* Cell Rep, 2016. **14**(4): p. 808-22.

70. Galvez-Contreras, A.Y., et al., *Role of fibroblast growth factor receptors in astrocytic stem cells.* Curr Signal Transduct Ther, 2012. **7**(1): p. 81-86.
71. Stavridis, M.P., et al., *A discrete period of FGF-induced Erk1/2 signalling is required for vertebrate neural specification.* Development, 2007. **134**(16): p. 2889-94.